Drought-stress-inducible synthetic promoters in rice (*Oryza sativa*)

A Thesis Presented for the

Master of Science

Degree

The University of Tennessee, Knoxville

Paolo Montano Tagaloguin

May 2021

Acknowledgments

I want to thank Dr. Neal Stewart for accepting me as his graduate student and for the opportunity to work in his laboratory. I appreciate his support and invaluable insights into conceiving this project. My special thanks to the other members of my thesis committee, Dr. Reginald Millwood, Dr. Feng Chen, and Dr. Tessa Burch-Smith, for their advice and support.

I also acknowledge Dr. Yongil Yang for assisting and supporting me in this project. Special thanks to Dr. Stephen Rigoulot and Holly Brabazon for helping me with the fluorescence-inducing laser projector (FILP). My appreciation for Yuanhua Shao for providing me the *Agrobacterium*-lines for transformation. I also want to thank Magen Poindexter for her assistance in the genomic DNA extraction and polymerase chain reaction (PCR). My gratitude to the rest of the members of the Stewart laboratory for the support and encouragement.

I express my gratefulness to the US Foreign Fulbright Program, the University of Tennessee-Knoxville Plant Sciences Department, and the Philippine Commission on Higher Education (CHED) for the opportunity to pursue my master's degree.

My deepest thanks to my family and friends in the Philippines for their moral support. Most significantly, my praises to God almighty for the provision and guidance throughout this journey.

Abstract

Drought can potentially affect the global rice supply. Recent climate modeling studies projected a more frequent and intense drought scenario, especially in top producing and exporting countries worldwide. Several drought-tolerant genes had been identified in recent years, and transgenic approaches had been employed to develop drought-tolerant rice. However, the constitutive expression of some drought-tolerant genes resulted in undesirable phenotypes and metabolic burden. The use of an inducible synthetic promoter is advantageous in preventing the possible pleiotropic effects from constitutively expressing a drought-tolerant gene. In this study, rationally designed synthetic promoters based on poplar (*Populus trichocarpa*) *cis*-motifs were tested for drought-stress inducible activity in rice. Three constructs (SD18-1, SD9-2, and negative control) were stably transformed in rice (*Oryza sativa* L. ssp. Japonica cv. 'Taipei 309') through *Agrobacterium*-mediated transformation. The two constructs SD18-1 and SD9-2 (synthetic promoter from drought-stress-inducible promoters), consisted of heptameric repeats of *cis*-motifs (motifs 18-1 and 9-2). The heptamerized *cis*-motifs were fused upstream of a core promoter, which consisted of the -46 35S promoter with the TMV Ω 5' UTR leader sequence for transcriptional initiation, to express a green fluorescent *TurboGFP* gene. The negative control construct (herein referred to as Neg) contained the core promoter fused to the *TurboGFP* gene but had no heptameric repeats of any *cis*-motif. Synthetic promoter response to drought and salt-stress treatments was tested in two-month-old T1 transgenic rice in greenhouse conditions. Synthetic promoter activity was reported by acquiring the normalized green fluorescence values of the first three young and fully expanded leaves of the main tiller of the transgenic rice at 502 nm emission using 465 nm excitation through fluorescence spectroscopy. Drought-stress treatment was done by water-cessation for 15 days. The green fluorescence values were taken

before and after 7-, 10-, and 15-days of treatment. Here, transgenic rice harboring SD18-1 and SD9-2 synthetic promoter constructs had statistically significant green fluorescence than the mock and the WT control ($p<0.05$) only after 15 days drought-stress treatment. The Neg transgenic rice had no statistically different green fluorescence intensity than the WT control ($p>0.05$) after 7-, 10-, and 15- days of drought-stress treatment. To determine the specificity of drought-stress inducible-response of the synthetic promoters in rice, SD18-1, SD9-2, and Neg transgenic rice were subjected to salt-stress treatment. Salt-stress treatment was done by applying 250 mM NaCl solution directly to the potting-mix for five days. The green fluorescence values were taken before and after 1-, 3-, and 5- days of treatment. Salt-stressed SD18-1, SD9-2, and Neg transgenic rice had statistically significant green fluorescence intensity than the mock control ($p<0.05$) after one and five days of salt-stress treatment. However, the green fluorescence intensities of the SD18-1, SD9-2, and Neg transgenic rice were statistically similar to the WT control ($p>0.05$). From the results, the transgenic rice harboring the SD18-1 and SD9-2 synthetic promoters only showed an inducible response to drought-stress treatment. The statistically no significant green fluorescence from the Neg transgenic rice versus the WT after the drought- and salt-stress treatments also showed that the core promoter was not driving *TurboGFP* gene expression in rice. Lastly, the rationally-designed synthetic promoters based on poplar *cis*-motifs demonstrating drought-stress inducible response in rice indicated that the SD18-1 and SD9-2 *cis*-motifs are likely highly conserved in both the dicot and monocot plant systems. Overall, this study showed two relatively short synthetic promoters with drought-stress-specific inducible response in rice.

Table of Contents

List of Tables

List of Figures

CHAPTER 1

Literature review

1.1 Abstract

Transgenic approaches to engineer drought-tolerant rice (*Oryza sativa*) rely on appropriate promoter choice. Several genes have been introduced to confer drought-tolerance in rice, mostly relying on cauliflower mosaic virus (CaMV) 35S promoter. However, constitutive expression of drought-tolerance genes can cause pleiotropic effects to the crop. Thus, the use of an inducible promoter may be advantageous in expressing drought-tolerant genes. Inducible synthetic promoters were developed recently, but not extensively in rice. Exploring synthetic promoter development is vital in stacking multiple genes to engineer the "21st-century" rice.

1.2 Introduction

Rice is an important crop worldwide[1]. However, extreme drought poses risks to the global rice supply[2-5]. Transgenic approaches may contribute significantly to enhance the crop's drought-tolerance[6]. Nevertheless, precise transgene expression relies on the regulation of an appropriate genetic switch known as promoter[7]. Promoters are upstream DNA sequences driving gene expression through DNA recognition sequences that interact with the basic transcription machinery[8, 9]. These promoters can be constitutive, spatiotemporal, or inducible[10, 11]. Constitutive promoters drive gene expression across all tissues and throughout the life cycle of the plant[7, 12]. Spatiotemporal promoters restrict gene expression in particular tissues or developmental stages of the plant[8, 13]. Inducible promoters direct gene expression in response to a particular stimulus[14-16]. Thus, promoter choice is essential in any transgenic approach based on a desired gene expression pattern. Synthetic biology recently sparked synthetic promoter development[10, 11]. Synthetic promoters are generally composed of a core-promoter region and multiple repeats and combinations of *cis*-motifs or transcription factor binding elements[17]. Synthetic promoters are envisaged to control ectopic gene expression and reduce the complexity of natural promoters'

expression patterns[10, 17, 18]. Here, I review the impacts of drought on rice and the current state of synthetic promoter development to enhance the crop's tolerance to drought.

1.3 Drought is a complex phenomenon

1.3.1 Drought definition

Drought is a complex natural phenomenon [3] involving the interaction of hydrologic (precipitation), atmospheric (temperature, vapor pressure), and bio-geophysical processes (evapotranspiration, solar radiation). This interaction results in a sustained water-deficit[19], causing severe hydrological imbalance[2].

However, there is no universally accepted criterion for what constitutes drought[20], which is evident in various definitions, metrics, and indices tailored to a particular research community's needs. For instance, an extended period without rainfall in a region characterized by seasonal or year-round precipitation regime represents meteorological drought[21]. A below-average water level in streamflow, reservoir, and groundwater involves hydrological drought [22]. A water-deficit in the topmost layer, root-zone, or the unsaturated-zone of the soil that impacts crops represents agricultural drought[2, 22].

Regardless of these perceived differences, there is a strong linkage among drought types[23]. This linkage is known as drought propagation, where one type translates to another type. Meteorological drought essentially initiates the other two drought types.

As meteorological drought progresses, it propagates to a hydrological drought[24]. In turn, the sustained lack of precipitation (meteorological drought) and poor irrigation due to low water levels in reservoirs or streams (hydrological drought) can manifest into an agricultural drought[22]. This idea of drought propagation puts the definition for each type into one general idea - that drought is a prolonged absence of rainfall affecting the soil moisture and the amount of water in

runoffs and reservoirs. As drought propagation ends in agricultural drought, it implies severe negative impacts on crops, especially in areas depending on the traditional rainfed agriculture[25].

1.3.2 Drought socioeconomic impacts

Various drought events were recorded in the past ten years worldwide: 2010-2018 in Southwestern North America[26], 2017-2018 in Northern China[27], 2015 and 2018 in Eastern Europe[28-30], 2015-2016 in Africa, 2015 in Brazil (EM-DAT: The Emergency Events Database 2017 https://www.emdat.be), 2011-2014 in California[31], 2012 in the US Central Great Plains[32], 2010-2011 in the Horn of Africa[25], and 2009-2011 in southwestern China[33].

These previous droughts had grave socioeconomic impacts, especially in the agricultural sector. For example, China lost 98.9 million hectares of crops in the 2009-2011 drought[33]. The total economic loss for the said drought amounted to 1.1 billion USD. During the 2014 California drought, the total economic loss summed up to 2.2 billion USD, 1.8 million USD of which accounted for crop loss in the said period[34]. In an assessment report of the National Oceanic and Atmospheric Administration (NOAA) - Drought Task Force in 2013, the US Central Great Plains drought in 2012 resulted in 12.0 billion USD estimated economic loss[32, 35]. Corn yield also declined by 26%. The agribusiness sector in Brazil lost 5 billion USD due to drought in 2015 (Assessment Report from the NOAA Drought Task Force Narrative Team 2013, https://cpo.noaa.gov). The 2015-2016 drought in South Africa led to 690 thousand USD agricultural loss in 2015 alone[36]. According to the Emergency Events Database, an international disaster database established by the World Health Organization and the Belgian Government, Africa's drought from 2015-2016 has an estimated 2 million USD economic loss.

1.3.3 Drought estimation

The projected increase in drought intensity, duration, and frequency in the 21st century [37, 38] could amplify these current agroeconomic losses. Recent climatic studies attribute worsening drought conditions to human-induced global warming [19, 22, 37, 38], although disruption in the global hydrologic cycle naturally causes extreme drought and precipitation events in particular regions globally[2]. Primarily, the El Niño Southern Oscillation (ENSO) causes episodic drought. Southeast Asia, Australia, Indonesia, some parts of Africa, northeast Brazil, and Central America are highly likely to experience drought during the El Niño events[2, 20]. Meanwhile, Peru, Ecuador, and the naturally wet areas during El Niño are dryer throughout the La Niña event[2].With the combined effects of global warming due to increased greenhouse gas (GHG: carbon dioxide CO_2, methane CH_4, nitrous oxide N_2O, and fluorinated gases) emissions, "dry regions" receive limited precipitation, whereas wet regions receive excessive rain than the natural effect of ENSO or other hydrological imbalance alone[2].

Depicting future drought characteristics utilizes various 21st-century GHG emission scenarios called relative concentration pathways (RCPs; RCP 2.5, 4.0, 6.0, 8.0). These four RCPs scenarios are categorized based on the perceived 21st-century GHG concentrations (expressed in ppm CO_2-eq concentration), the corresponding increase in global temperature relative to the pre-industrial conditions (1850-1900 CE), and the equivalent radiative forcing (RF) relative to 1750 CE. RCP 2.6 scenario represents low carbon emission, increased reliance on renewable energy, and a strong global effort to mitigate climate change. In this scenario, the average global temperature will increase by 0.3°C to 1.7°C in 2100. The RCP 2.6 scenario accords with the 2015 Paris Agreement to limit the global temperature rise to well below 2.0°C. Meanwhile, RCP 8.5 depicts high fossil-fuel use, limited use of renewable energy, and

fragmented global cooperation to mitigate climate change. The RCP 8.5 describes a "business-as-usual" or "worst-case" scenario where global temperature will rise between 2.6°C to 4.8°C. The RCP 4.5 and 6.0 are intermediate pathways where the global temperature increases to 1.8°C and 2.2°C, respectively. These RCP scenarios are then used as inputs to analyze global climate change impacts using the multiple climatic models integrated into the Coupled Model Intercomparison Project (CMIP). The CMIP subsequently forecasts spatiotemporal changes in precipitation patterns, atmospheric temperature, soil moisture, and evapotranspiration. The forecasted climatic conditions will now be fed into various indices to measure, monitor, and predict the occurrence, intensity, and frequency of drought in the 21st century.

There are three most commonly used indices to characterize drought. A negative value indicates drought for all three indices, while a positive value indicates a wet spell. The Palmer Drought Severity Index (PDSI) has been in use for 55 years to quantify long-term drought for a particular location and time[39]. It uses temperature and precipitation data to estimate relative dryness. However, PDSI provides inconsistent results across diverse climatological regions, making spatial comparison difficult, if not meaningless[40]. The self-calibrating PDSI (sc-PDSI) introduced by Wells et al. (2004) addresses this problem by replacing the empirical constants in the original computation of the index with a more dynamically calculated values (International Panel on Climate Change (IPCC). Climate Change 2014: Synthesis Report). Using the sc-PDSI allows spatial comparison that is not possible with the original PDSI. Another caveat to using PDSI is that it has a fixed timescale, limiting drought identification across a wide range of temporal scales[41, 42]. The Standardized Precipitation Index (SPI) addresses this limitation of the PDSI. SPI can monitor short-term drought (agricultural drought) and long-term drought (hydrological and meteorological drought) because it can quantify drought at various timescales

using the precipitation data only[24]. Its simplicity and low-data requirement explains its wide acceptability in drought-monitoring and analysis. This index's primary constraint is that it excludes evapotranspiration, limiting its usefulness for some applications and research questions[20]. The Standardized Precipitation Evapotranspiration Index (SPEI) takes advantage of the SPI's multi-scalar and robust statistical feature while including evapotranspiration data in characterizing drought[20, 42]. SPEI takes into account the effects of temperature, evapotranspiration, soil water holding capacity, and wind speed along with precipitation data in drought assessment[42]. Because SPEI is multivariable, it is comparable to the sc-PDSI. However, because SPEI is also multi-scalar, it remains more advantageous than the sc-PDSI. Overall, SPEI is superior to the other two indices because it can better reflect the impact of drought, especially in agriculture [43].

1.4 Drought impacts to rice production

1.4.1 Top rice producers and exporters will experience extreme 21st century drought

China ranked first on global milled rice production in 2018/2019, followed by India and other Southeast Asian countries (Indonesia, Bangladesh, Vietnam, Thailand, Myanmar, and the Philippines). Japan and Brazil then trailed as the ninth and tenth top global rice-producers, respectively. These countries are consistently the leading rice producers in the last 20 years (United States Department of Agriculture (USDA). Leading countries based on the production of milled rice in 2018/2019 (in million metric tons) 2020, www.statista.com). On the other hand, India has the highest exported rice in 2018/2019 (Food and Agriculture Organization (FAO). Production of rice, paddy: top 10 producers (1994-2018) 2020, www.fao.org). China fell short to sixth place in exporting rice while Thailand, Vietnam, Pakistan, and the United States ranked

second to the fifth, respectively. The other leading global rice-exporters are Myanmar, Cambodia, Brazil, and Uruguay.

SPEI values were estimated using multi-model ensembles to characterize the 21st-century drought under the different warming (RCP) scenarios. These drought projections consistently show an increasing drought frequency, intensity, and severity in the next 80 years, most especially in these top rice producing and exporting countries. 21st-century drought can potentially threaten food security, especially on populations that depend on rice as a staple commodity.

Yao et al. [41] projected the 21st-century drought in China using 28 global climate models (GCMs) under the RCP 4.5 and the RCP 8.5 scenarios [41]. The arid and the semi-arid western and northwestern China are more likely to experience drought under RCP 4.5. However, northeastern and southeastern China will experience an increase in precipitation under the same RCP 4.5 and RCP 8.5 scenarios. These predictions are consistent with the same study by Guo et al. [43]. Northern, northwestern, and southwestern China are drier under RCP 4.5, while China's southeastern part is highly likely to get wetter at the end of the 21st century [43]. However, at RCP 8.5, all regions in China will get drier[41]. China may experience moderate to severe drought at the end of the 21st century under the RCP 8.5 scenario. Drought frequency will also increase by 60% to 70%, which could last for 96 months to 240 months under the RCP 4.5 and RCP 8.5 scenarios, respectively.

Similar drought projections were observed in India. There will be an increased drought occurrence, severity, duration, and affected-areas[44]. Under the RCP 8.5 scenario, drought frequency increased two to three times each decade. Furthermore, the area affected by drought was identified to increase to 150%.

In Bangladesh, SPEI calculations for the 21st-century drought predict higher frequency and severity in shorter timescales[45]. A more frequent and shorter drought pattern can permanently damage an ecosystem[46]. Schwalm et al.[46] studied drought recovery time, which describes how long an ecosystem can revert to its pre-drought functional condition. The tropics and the high northern latitudes have the longest drought recovery time. The time between droughts may be shorter as the droughts become more frequent. This frequent drought pattern will put ecosystems in a chronic state of incomplete recovery from the previous drought. Downward SPEI trend in Bangladesh until the end of the 21st century implies future extreme drought. While there will be a shift in wet to dry regime over the northeast of Bangladesh, the rest of the country will experience severe drought.

In the Indochina region (ICR; Cambodia, Laos, Myanmar, Malaysia, Thailand, and Vietnam), severe drought hazards will increase in both the RCP 4.5 and the RCP 8.5 scenarios[47]. Cambodia and Thailand were identified as drought-prone countries in the 21st century. The ICR already experiences 10 to 16 droughts during the 30 years of the baseline period (1976-2005). This drought frequency will rise all over ICR except Cambodia and Thailand. Drought lasts for 5 to 10 months in the baseline period. Yet, this can go up to 60 months, especially in Cambodia and Thailand.

Leading rice producers in the US are mainly in the southeast region (Arkansas, Louisiana, Mississippi). Texas, Missouri, and California are also among the top rice producers. Mitra et al.[48] estimated 21st-century drought in the southeast of the USA. The study covered Texas, Oklahoma, Arkansas, Louisiana, Tennessee, Mississippi, Alabama, Georgia, Florida, North Carolina, and South Carolina[48]. SPI and SPEI were used to estimate drought under the RCP 4.5 and RCP 8.5 scenarios. Using the SPI, which relies on precipitation data alone, Texas

will be dry while the rest of the states will have higher precipitation during the winter and spring season in both the RCP 4.5 and RCP 8.5 scenarios. Meanwhile, SPEI drought estimation, which considers temperature and potential evaporation data, predicts drying all over the states during the winter and spring seasons in both the RCP scenarios. Summer and fall season observe a similar trend for both the SPI and SPEI estimations but with more intense drying. This increase in drought severity and frequency during the summer season which corresponds to the growing season may result in lower soil moisture that can impact crop production. Williams et al.[26] compared the 2000-2018 megadrought in Southwestern North America (SWNA; western America and Northern Mexico) with other megadroughts in the last 1200 years. Historical droughts were reconstructed using tree-ring data and hydrological models. Megadrought periods were determined as prolonged drought events with at least a 19-year low soil moisture condition. Four historical SWNA megadroughts were identified in the reconstruction: the late 800s, the mid-1100s, the 1200s, and the late 1500s. The comparison demonstrates that the 2000-2018 megadrought is the second driest 19-year period in the last 1200 years, next to the megadrought that occurred in 1575-1593 CE (common era; CE).

On a global scale, Martin[49] projected future pluvial and drought events using the SPI. The hotspots for worsening drought are the Americas, Central America, the Caribbean, and the Amazon[49]. Meanwhile, North America and Europe will experience worsening pluvial events. Using the SPEI, Naumann et al.[4] predicted increasing drought magnitude and duration in most of Africa (except equatorial Africa), the Caribbean, southern Europe, Australia, and West Asia under 3^{o}C global warming[4]. The drought lengths can go up to 18 months under the same warming scenario. Drought will also occur five to ten times more for most of Africa, the Caribbean, Central America, Central and West Asia, Oceania, and north-west China. Cook et

al.[38] used more robust GCMs under the most recent sixth phase of the CMIP (CMIP6)[38]. Western North America, Central America, Europe, the Mediterranean, the Amazon, China, Australia, and Southeast Asia will experience robust drying and an increase in extreme drought occurrence.

There are still uncertainties in these 21st-century drought projections[47]. Such ambiguities may come from i) the models used to simulate future climate[19, 50-52], ii) the RCP scenarios[53, 54], or iii) the climate's random internal variability[55]. Nevertheless, these drought simulations provide scientists and policy-makers insights into the future drought scenarios that can negatively affect rice and other important crops.

1.4.2 Drought-induced responses in rice cause substantial yield loss

Severe drought conditions put risks to the global rice supply[3-5]. Rice is mostly grown in paddies for weed management[56, 57], and continuous flooding is unnecessary for increased yield[58, 59]. However, in extreme drought scenarios, the prolonged absence of precipitation and insufficient water supply can result in a soil-moisture deficit[2]. The lack of soil-moisture can negatively impact rice and other essential crops.

Drought effects on rice were studied at the molecular, biochemical, physiological and morphological levels. Molecularly, drought alters gene expression in plants. Under drought-stress, rice encodes the genes for transcription-factors and defense-related proteins against dehydration[60-62].

The gene for the WRKY53 transcription factor is elevated during drought-stress[63]. In *Arabidopsis thaliana* (*A. thaliana*), *AtWRKY53* is responsible for senescence-induced cell death[64]. The AREB1, AREB2, and ABF2 transcription factors belonging to the ABRE-binding (AREB) proteins are also upregulated by drought-stress[65]. The three ABRE transcription factors function cooperatively in abscisic acid (ABA) signaling as a drought-stress response. The

OsGRAS23 gene is induced by drought, salt, and jasmonic acid treatments in rice[66]. It encodes a drought-stress responsive GRAS transcription factor involved in the induction of stress-responsive genes. The *OsbZIP46* gene is highly expressed under drought, heat, hydrogen peroxide, and ABA treatments[67]. The *OsbZIP46* gene encodes for a transcription factor belonging to the bZIP transcription factors in rice. The stress-related genes activated by the OsbZIP46 are entirely different from those induced by the AREB transcription factors. The *OsMYB2* gene expression is upregulated by drought, salt, and cold stresses[68]. It encodes a stress-responsive MYB-transcription factor. The transcription factors produced under drought-stress are mainly involved in signal transduction and transcriptional regulation[63].

Biochemically, drought-stress results in the accumulation of osmoprotectants[60, 61, 69]. These osmoprotectants are proline, polyamines, antioxidants, and sugars. When there is water-deficit in plant cells due to drought, plants accumulate inorganic and organic solutes in the cytosol resulting in lower osmotic potential to maintain cell turgor[61]. This process is known as osmotic adjustment. The release of osmoprotectants improves water uptake from the drying soil[61]. Physiologically, drought results in reduced photosynthesis, stomatal conductance, transpiration, water-use efficiency, photosystem II activity, membrane stability, and carbon isotope discrimination[60, 61, 63, 69, 70]. ABA accumulation was also observed as a drought-stress response. Morphologically, drought causes reduced stomatal density, germination, plant height, plant biomass, number of tillers, and leaf area[60, 61, 69].

Rao et al. (2019) investigated the influence of drought-stress on pollen traits and physiology at the flowering stage of two rice genotypes[71]. Under greenhouse conditions, drought reduced net photosynthetic rate and decreased maximal photochemical efficiency of photosystem II in the two rice genotypes. Drought-stress also significantly reduced pollen members on stigma,

anther dehiscence rate, pollen germination rate, pollen viability, and anther starch contents. As a result, yield and yield components (grain/panicles, 1000-grain weight, effective panicles, and seed set percentage) were substantially reduced. Meanwhile, drought-stress elevated levels of antioxidants malondialdehyde (MDH), superoxidase (SOD), peroxidase (POD), and catalase (CAT)[61, 71]. Activities of the said antioxidants can effectively diminish reactive oxygen species (ROS), reducing the negative impacts of drought.

In another study, drought-stress impacts at the flowering stage on rice physiological traits, grain yield, and quality were investigated[72]. Field experiments were conducted on two rice cultivars under two water treatments: traditional flooding and drought-stress at the flowering stage. Similar to Rao et al. (2019), photosynthetic rate (Pn), transpiration rate (Tr), and stomatal conductance (Gs) decreased under drought-stress in field conditions. Typically, physiological traits revert to normal levels after two days of rehydration. However, the activity of physiological traits (Pn, Tr, and Gs) further decreased after 20 days of rehydration. Although drought-stress did not affect protein content, amylose content, and overall nutritional quality of rice under drought-stress, rice quality is significantly affected. Drought-stress increased chalkiness and chalky kernel levels at 74.0-76.0% and 53.0-67.0%, respectively—drought-stress in rice resulted in low grain quality[58, 72-74].

In a meta-analysis study, the effect of drought on agronomic traits was also investigated[75]. Drought-stress resulted in decreased rice yield and biomass at 25.4% and 25.2%, respectively. Furthermore, yield loss is highest when drought occurred during rice's flowering stage than when drought occurred during its vegetative phase[61, 72, 75]. Leng and Hall (2019) estimated potential drought-induced yield loss in rice, wheat, corn, and soybean[3]. Crop-country specific SPI and census yield information in 1961-2016 were used to project yield losses due to

drought. Rice has the highest yield loss risk than any of the three crops. Historical drought-induced yield loss in rice is approximately 60%. By the end of the 21st-century, drought-induced yield loss in rice can increase to 79%. This projection means an estimated yield loss risk of 19% in rice. Meanwhile, wheat, corn, and soybean yield-loss risk are 12.0 %, 7%, and 16%, respectively.

Overall, an integrated understanding of the molecular, biochemical, and physiological responses of rice to drought stress can be used as a basis for 1) studying or discovering genes, proteins, or other biochemical or physiological pathways that can be modified or regulated to engineer drought tolerance in rice, 2) selecting rice varieties for conventional breeding, resulting in a drought-tolerant rice hybrid, and 3) improving rice management practices in the farm. For example, the upregulated genes under drought stress can be introduced via transgene approaches under constitutive or inducible expression to study their potential for conferring drought-tolerance characteristics in rice. Since proline is an osmoprotectant that accumulates in rice as a drought-stress response, investigating varieties with high proline content may facilitate germplasm selection for conventional breeding, leading to a hybrid rice variety with a drought-tolerance trait. Since rice panicle and spikelet morphogenesis are critical factors in rice grain development, an appropriate water management strategy is essential to ensure that the rice does not undergo stress from water deficit during the rice flowering stage. Adaptive measures should be in place to guarantee sustainable rice production in the 21st century.

1.5 Transgenic approaches to produce drought tolerant rice

1.5.1 Drought tolerance genes were identified and introduced in rice

Drought tolerance is a multigenic trait. Several genes were recently introduced for overexpression in rice. These genes function in a variety of ways: i) enhance root growth and

development[6, 76], ii) encodes for transcription factor that responds to drought[77, 78], iii) sugar signaling[79], iv) improve reactive oxygen scavenging (ROS)[80], v) enhance stomatal closure[80], and vii) improve ABA-sensitivity[16].

Rice *Root Architecture Associated 1* (*OsRAA1*) gene is involved in extensive root development[6, 76]. Transgenic lines showed increased tolerance to drought-stress than the wild-type, had higher proline and abscisic acid accumulation, and had lower lipid peroxidation. Under drought conditions, transgenic rice lines had more tillers, higher spikelet fertility, and developed larger grains, hence, an observed 20.0-40.0% higher grain yield than the wild type. Here, the overexpression of *OsRAA1* was demonstrated that extensive root growth and development allowed more efficient uptake and improved access to moisture at greater soil depth[6, 81].

Rice *OsMYB6,* an MYB family gene, is a transcription factor that responds to drought and salt-stress[6, 77]. Overexpression of *OsMYB6* had no negative phenotypic effect to the transgenic rice under normal conditions. Transgenic lines had higher tolerance to drought and salt-stress than the wild type, had higher proline content, increased SOD and CAT activities, and lower relative electrolyte leakage (REL) and malondialdehyde (MDA) content. SOD and CAT are antioxidants that serve as osmoprotectants while REL and MDA are closely related with the degree of cell membrane damage under abiotic stress[60, 61, 69, 77].

The gene *OsMT6* was derived from rice and was recently used to confer drought-tolerance in *A. thaliana* [79]. It encodes for a monosaccharide transporter protein that is critical to cell-to-cell and long-distance sugar distribution throughout the plant. In this study, physiological analyses showed that transgenic *A. thaliana* had increased membrane stability, lower water loss rate, higher relative water content, and higher total soluble sugar than the parental genotype[79, 82].

OsPUB67 is a gene that encodes for E-3 Ubiquitin ligase and is significantly induced by drought, salt, cold, jasmonic acid, and ABA[80]. Overexpression of the *OsPUB67* enhanced stomatal closure activity and improved ROS activity.

Overexpression of *OsPYL10* gene that encodes for an ABA-receptor PYL (pyrabactin resistance-like) protein was also explored in rice[16]. At vegetative drought-stress, transgenic rice lines had higher grain yield (40.0-58.0%). At reproductive stage drought-stress, one of the three transgenic rice lines had twice as much grain yield than the wild-type. Similar with other studies, transgenic rice lines had higher membrane stability index, relative water content, and chlorophyll content whereas MDA and peroxide accumulation was low. This study demonstrated that overexpression of *OsPYL10* gene conferred ABA-hypersensitivity of rice thereby improving its drought tolerance.

1.5.2 Constitutive expression of some drought-stress tolerance genes can cause negative effects

Overexpression of some drought tolerance genes driven under a constitutive promoter such as *35S* from CaMV (*Cauliflower mosaic virus*), *ZmUbi1* from maize (*Zea mays*), *PvUbi1* and *PvUbi2* from switchgrass (*Panicum virgatum*), or *OsAct1* from rice have been shown to lead to undesirable phenotypes, metabolic burden, epigenetic silencing, or off-target effects[9, 14-16, 83]. Constitutive expression of drought-tolerance genes in transgenic rice led to floret sterility, reduced shoot length, smaller flag-leaf area, as well as fewer panicle and tillers, which could potentially manifest decreased rice yield[12]. For example, constitutive overexpression of *OsTZF5* driven by *ZmUbi1* promoter resulted in drought-tolerant transgenic rice but with lower biomass, reduced seed setting, and underdeveloped panicles than the wild-type variety[15]. In contrast, overexpression of the same *OsTZF5* gene driven by drought-stress inducible *OsNAC6* promoter generated transgenic rice with normal phenotype with significantly higher yield than the wild-type genotype

under drought-condition[15]. Constitutive overexpression of *OsRAA1* under the *ZmUbi1* promoter resulted in drought-tolerant transgenic rice exhibiting floret sterility (abnormal filament length, white and shrunken anthers)[76]. Whereas, overexpression of the same gene under the control of the drought-inducible promoter *pHAK1* generated drought-tolerant transgenic rice with normal floret phenotypes, regardless of drought conditions[6]. The use of an inducible promoter, therefore, is advantageous in generating crops that accumulate transgene products only under stressed conditions.

1.5.3 Synthetic promoters as gene switch for drought-tolerant genes in rice

Recent studies for drought-tolerance transgene expression in rice reported use of drought-inducible native promoters of the following genes: *OsHAK1* [84], *OsNAC6* [15], *OsRhoGAP2* [85], *Osr40c1* [86], *OsNAC14* [81], *OsHox24* [87], *Rab21* [87], and *OsLEA3*-1 [87]. Nevertheless, induction condition, specificity, expression level, and size are the major constraints to native promoter activity [17]. Native promoters are generally longer (>1000 bp) and some have a weak expression profile than some constitutive viral promoters like the CaMV 35S, which are unbiquitously used in plant biotechnology (Figure 1 A). Such limitations prompted the engineering of smaller, robust, and versatile synthetic promoters, which are generally composed of a core-promoter region and multiple repeats and combinations of *cis*-motifs or transcription factor binding elements [18] (Figure 1 B-C). Designing drought-stress inducible synthetic promoters is a promising field but only a few have been published in rice thus far. The latest report developed inducible synthetic promoters *Ap*, *Dp*, and *ANDp* in combination with functional genes *CAARK1* (cytosolic abscisic acid (ABA) receptor kinase 1), and *RCAR11* (regulatory components of ABA receptor 11), resulting in drought-tolerant *Arabidopsis thaliana* [88]. In rice, the latest literature on stress-inducible promoters was reported in 2011 and 2015. Chen et al. (2015) designed an ABA-responsive complex (ABRC)

based synthetic promoter (*3xABRC21*) to control late embryogenesis abundant protein HVA1 expression [89]. Transgenic rice lines (*3xABRC21*:*HVA1*) demonstrated stress tolerance to ABA, salt, dehydration, and cold without compensating for rice yield. Ganguly et al. (2011) utilized four-tandem repeats of the ABA-responsive element (*4xABRE*) and two-tandem repeats of the ABA-responsive complex (*2xABRC*) linked to *gusA* gene, in comparison with a stress-inducible native promoter *Rab16A* [90]. Results indicated that *4XABRE* and *2xABRE* have higher GUS expression (142 pmol $h^{-1}\mu g^{-1}$ and 161 pmol $h^{-1}\mu g^{-1}$, respectively) than the native *Rab16A* promoter (100 pmol $h^{-1}\mu g^{-1}$) after the application of 100 µM ABA to 21-day-old T_2 transgenic plants [90]. Further literature search revealed that the most recent work on synthetic promoters in rice is limited to tissue-specific promoters [13, 91].

1.6 Conclusion

Drought is projected to be more frequent and highly intense in the future which may potentially affect global rice supply. Transgenic approaches can be exploited to generate drought-tolerant rice. However, gene expression relies on the control of appropriate promoter. Constitutive expression of some drought-tolerance genes may be detrimental to the crop. Alternatively, the use of inducible promoters may be exploited. Designing synthetic promoters for drought inducibility should further be explored in rice (Figure 2). Since effect of drought to yield loss is highest at the flowering stage in rice, synthetic promoters that can be temporally expressed at this stage may also be done. Engineering for 21st century rice would involve various genes that confer traits for drought-tolerance, increased-yield, and advanced nutrition. This can be achieved by multiple stacking of genes. Using the same promoter may result in homology-dependent gene-silencing. Developing a battery of short, highly-inducible, synthetic promoters may be necessary to run the gene circuit.

References

1. Ye, X. et al. Engineering the provitamin A (β-carotene) biosynthetic pathway into (carotenoid-free) rice endosperm. *Science* **287**, 303-305 (2000).
2. Trenberth, K.E. et al. Global warming and changes in drought. *Nature Climate Change* **4**, 17-22 (2014).
3. Leng, G. & Hall, J. Crop yield sensitivity of global major agricultural countries to droughts and the projected changes in the future. *Science of the Total Environment* **654**, 811-821 (2019).
4. Naumann, G. et al. Global changes in drought conditions under different levels of warming. *Geophysical Research Letters* **45**, 3285-3296 (2018).
5. Wang, Y. et al. Mitigating rice production risks from drought through improving irrigation infrastructure and management in China. *Australian Journal of Agricultural and Resource Economics* **62**, 161-176 (2018).
6. Chen, G. et al. Driving the expression of *RAA1* with a drought-responsive promoter enhances root growth in rice, its accumulation of potassium and its tolerance to moisture stress. *Environmental and Experimental Botany* **147**, 147-156 (2018).
7. Jiang, P. et al. Characterization of a strong and constitutive promoter from the Arabidopsis serine carboxypeptidase-like gene *AtSCPL30* as a potential tool for crop transgenic breeding. *BMC Biotechnology* **18**, 1-13 (2018).
8. Dutt, M. et al. Temporal and spatial control of gene expression in horticultural crops. *Horticulture Research* **1**, 1-17 (2014).

9. Xue, M. et al. Isolation and characterization of a green-tissue promoter from common wild rice (*Oryza rufipogon Griff.)*. *International Journal of Molecular Sciences* **19**, 1-13 (2018).

10. Liu, W. & Stewart, C.N. Plant synthetic promoters and transcription factors. *Current Opinion in Biotechnology* **37**, 36-44 (2016).

11. Hernandez-Garcia, C.M. & Finer, J.J. Identification and validation of promoters and *cis*-acting regulatory elements. *Plant Science* **217-218**, 109-119 (2014).

12. Bhattacharjee, A. et al. Over-expression of *OsHOX24* confers enhanced susceptibility to abiotic stresses in transgenic rice via modulating stress-responsive gene expression. *Frontiers in Plant Science* **8**, 1-11 (2017).

13. Wang, R. et al. Novel green tissue-specific synthetic promoters and *cis*-regulatory elements in rice. *Scientific Reports* **5**, 1-11 (2015).

14. Singh, P. et al. Development of efficient protocol for rice transformation overexpressing MAP kinase and their effect on root phenotypic traits. *Protoplasma* **256**, 997-1011 (2019).

15. Selvaraj, M.G. et al. Expression of the *CCCH*-tandem zinc finger protein gene *OsTZF5* under a stress-inducible promoter mitigates the effect of drought stress on rice grain yield under field conditions. *Plant Biotechnology Journal* **18**, 1711-1721 (2020).

16. Verma, R.K. et al. Overexpression of ABA receptor *PYL10* gene confers drought and cold tolerance to indica rice. *Frontiers in Plant Science* **10**, 1-16 (2019).

17. Ali, S. & Kim, W.C. A fruitful decade using synthetic promoters in the improvement of transgenic plants. *Frontiers in Plant Science* **10**, 1-14 (2019).

18. Bilas, R. et al. *Cis*-regulatory elements used to control gene expression in plants. *Plant Cell, Tissue and Organ Culture (PCTOC)* **127**, 269-287 (2016).

19. Lu, J. et al. Uncertainty and hotspots in 21st century projections of agricultural drought from CMIP5 models. *Scientific Reports* **9**, 1-12 (2019).

20. Ault, T.R. On the essentials of drought in a changing climate. *Science* **368**, 256-260 (2020).

21. Wilhite, D.A. & Glantz, M.H. Understanding the drought phenomenon: the role of definitions. *Water International* **10**, 111-120 (1985).

22. Van Loon, A.F. et al. Drought in the anthropocene. *Nature Geoscience* **9**, 89-91 (2016).

23. Eltahir, E.A.B. & Yeh, P.J.F. On the asymmetric response of aquifer water level to floods and droughts in Illinois. *Water Resources Research* **35**, 1199-1217 (1999).

24. Huang, S. et al. The propagation from meteorological to hydrological drought and its potential influence factors. *Journal of Hydrology* **547**, 184-195 (2017).

25. Dutra, E. et al. The 2010–2011 drought in the Horn of Africa in ECMWF reanalysis and seasonal forecast products. *International Journal of Climatology* **33**, 1720-1729 (2013).

26. Williams, A.P. et al. Large contribution from anthropogenic warming to an emerging North American megadrought. *Science* **368**, 314-318 (2020).

27. Wang, L. et al. The 2017–2018 winter drought in North China and its causes. *Atmosphere* **10**, 1-10 (2019).

28. Ionita, M. et al. The European 2015 drought from a climatological perspective. *Hydrology and Earth System Sciences* **21**, 1397-1419 (2017).

29. Laaha, G. et al. The European 2015 drought from a hydrological perspective. *Hydrology and Earth System Sciences* **21**, 3001-3024 (2017).

30. Brunner, M.I. & Tallaksen, L.M. Proneness of European catchments to multiyear streamflow droughts. *Water Resources Research* **55**, 8881-8894 (2019).

31. Seager, R. et al. Causes of the 2011–14 California drought. *Journal of Climate* **28**, 6997-7024 (2015).

32. Hoerling, M. et al. Causes and predictability of the 2012 Great Plains drought. *Bulletin of the American Meteorological Society* **95**, 269-282 (2014).

33. Sun, C. & Yang, S. Persistent severe drought in southern China during winter–spring 2011: Large-scale circulation patterns and possible impacting factors. *Journal of Geophysical Research: Atmospheres* **117**, 1-18 (2012).

34. Howitt, R. et al. Economic analysis of the 2014 drought for California agriculture. (Center for Watershed Sciences University of California, Davis, CA, 2014).

35. Hoerling, M. et al. An interpretation of the origins of the 2012 central great plains drought. *Assessment Report from the NOAA Drought Task Force Narrative Team* (2013).

36. Bahta, Y.T. et al. Communal farmers' perception of drought in South Africa: Policy implication for drought risk reduction. *International Journal of Disaster Risk Reduction* **20**, 39-50 (2016).

37. Tokarska, K.B. et al. Past warming trend constrains future warming in CMIP6 models. *Science Advances* **6**, 1-13 (2020).

38. Cook, B. et al. Twenty-first century drought projections in the CMIP6 forcing scenarios. *Earth's Future* **8** (2020).

39. Palmer, W.C. Meteorological drought, Vol. 30. (US Department of Commerce, Weather Bureau, 1965).

40. Wells, N. et al. A self-calibrating Palmer Drought Severity Index. *Journal of Climate* **17**, 2335-2351 (2004).

41. Yao, N. et al. Projections of drought characteristics in China based on a standardized precipitation and evapotranspiration index and multiple GCMs. *Science of The Total Environment* **704**, 1-18 (2020).

42. Vicente-Serrano, S.M. et al. A multiscalar drought index sensitive to global warming: the Standardized Precipitation Evapotranspiration Index. *Journal of Climate* **23**, 1696-1718 (2010).

43. Guo, X. et al. Drought trend analysis based on the standardized precipitation–evapotranspiration index using NASA's earth exchange global daily downscaled projections, high spatial resolution coupled model intercomparison project phase 5 projections, and assessment of potential impacts on China's crop yield in the 21st century. *Water* **11**, 2455 (2019).

44. Bisht, D.S. et al. Drought characterization over India under projected climate scenario. *International Journal of Climatology* **39**, 1889-1911 (2019).

45. Khan, J.U. et al. Future changes in meteorological drought characteristics over Bangladesh projected by the CMIP5 multi-model ensemble. *Climatic Change* **162**, 667-685 (2020).

46. Schwalm, C.R. et al. Global patterns of drought recovery. *Nature* **548**, 202-205 (2017).

47. Chhin, R. et al. Drought projection in the Indochina Region based on the optimal ensemble subset of CMIP5 models. *Climatic Change* **162**, 687-705 (2020).

48. Mitra, S. et al. Probabilistic assessment of projected climatological drought characteristics over the Southeast USA. *Climatic Change* **147**, 601-615 (2018).

49. Martin, E.R. Future projections of global pluvial and drought event characteristics. *Geophysical Research Letters* **45**, 11913-11920 (2018).

50. Herrera-Estrada, J.E. & Sheffield, J. Uncertainties in future projections of summer droughts and heat waves over the contiguous United States. *Journal of Climate* **30**, 6225-6246 (2017).

51. Prudhomme, C. et al. Hydrological droughts in the 21st century, hotspots and uncertainties from a global multimodel ensemble experiment. *Proceedings of the National Academy of Sciences* **111**, 3262-3267 (2014).

52. Zhao, T. & Dai, A. Uncertainties in historical changes and future projections of drought. Part II: model-simulated historical and future drought changes. *Climatic Change* **144**, 535-548 (2017).

53. Ashrafi, S. et al. Uncertainties in runoff projection and hydrological drought assessment over Gharesu basin under CMIP5 RCP scenarios. *Journal of Water and Climate Change* **11**, 145-163 (2020).

54. Shi, L. et al. Quantifying future drought change and associated uncertainty in southeastern Australia with multiple potential evapotranspiration models. *Journal of Hydrology* **590**, 1-13 (2020).

55. Deser, C. et al. Projecting North American climate over the next 50 years: Uncertainty due to internal variability. *Journal of Climate* **27**, 2271-2296 (2014).

56. Caton, B.P. et al. Canopy development of direct-seeded rice and some important grass and sedge weeds in response to water management. *Agricultural and Forest Meteorology* **111**, 39-53 (2002).

57. Bhager, R. et al. Effect of water, tillage and herbicide on ecology of weed communities in intensive wet-seeded rice system. *Crop Protection* **18**, 293-303 (1999).

58. Kumar, A. et al. Effects of water deficit stress on agronomic and physiological responses of rice and greenhouse gas emission from rice soil under elevated atmospheric CO2. *Science of The Total Environment* **650**, 2032-2050 (2019).

59. Lampayan, R.M. et al. Adoption and economics of alternate wetting and drying water management for irrigated lowland rice. *Field Crops Research* **170**, 95-108 (2015).

60. Pandey, V. & Shukla, A. Acclimation and tolerance strategies of rice under drought stress. *Rice Science* **22**, 147-161 (2015).

61. Korres, N.E. et al. Temperature and drought impacts on rice production: an agronomic perspective regarding short- and long-term adaptation measures. *Water Resources and Rural Development* **9**, 12-27 (2017).

62. Shinozaki, K. et al. Regulatory network of gene expression in the drought and cold stress responses. *Current Opinion in Plant Biology* **6**, 410-417 (2003).

63. Khan, M. et al. Detection of biochemical and molecular changes in *Oryza sativa* L during drought stress. *Biocatalysis and Agricultural Biotechnology* **19**, 1-8 (2019).

64. Zentgraf, U. et al. The complex regulation of *WRKY53* during leaf senescence of *Arabidopsis thaliana*. *European Journal of Cell Biology* **89**, 133-137 (2010).

65. Yoshida, T. et al. AREB1, AREB2, and ABF3 are master transcription factors that cooperatively regulate ABRE-dependent ABA signaling involved in drought stress tolerance and require ABA for full activation. *The Plant Journal* **61**, 672-685 (2010).

66. Xu, K. et al. OsGRAS23, a rice GRAS transcription factor gene, is involved in drought stress response through regulating expression of stress-responsive genes. *BMC Plant Biology* **15**, 1-13 (2015).

67. Tang, N. et al. Constitutive activation of transcription factor OsbZIP46 improves drought tolerance in rice. *Plant Physiology* **158**, 1755-1768 (2012).

68. Yang, A. et al. A R2R3-type MYB gene, *OsMYB2*, is involved in salt, cold, and dehydration tolerance in rice. *Journal of Experimental Botany* **63**, 2541-2556 (2012).

69. Anupama, A. et al. Morphological, transcriptomic and proteomic responses of contrasting rice genotypes towards drought stress. *Environmental and Experimental Botany* **166**, 1-14 (2019).

70. Sahoo, S. et al. Physiological introspection into differential drought tolerance in rice cultivars of North East India. *Acta Physiologiae Plantarum* **41**, 1-15 (2019).

71. Rao, G. et al. Low soil temperature and drought stress conditions at flowering stage affect physiology and pollen traits of rice. *Journal of Integrative Agriculture* **18**, 1859-1870 (2019).

72. Yang, X. et al. The different influences of drought stress at the flowering stage on rice physiological traits, grain yield, and quality. *Scientific Reports* **9**, 1-12 (2019).

73. Zhang, Y. et al. The effects of dry cultivation on grain-filling and chalky grains of upland rice and paddy rice. *Food and Energy Security* **9**, 1-19 (2020).

74. Chen, J. et al. Effects of short-term high temperature on grain quality and starch granules of rice (*Oryza sativa* L.) at post-anthesis stage. *Protoplasma* **254**, 935-943 (2017).

75. Zhang, J. et al. Effect of drought on agronomic traits of rice and wheat: a meta-analysis. *International Journal of Environmental Research and Public Health* **15**, 1-14 (2018).

76. Ge, L. et al. Overexpression of *OsRAA1* causes pleiotropic phenotypes in transgenic rice plants, including altered leaf, flower, and root development and root response to gravity. *Plant Physiology* **135**, 1502-1513 (2004).

77. Tang, Y. et al. Overexpression of a *MYB* family gene, *OsMYB6*, increases drought and salinity stress tolerance in transgenic rice. *Frontiers in Plant Science* **10**, 1-12 (2019).

78. Latha, G.M. et al. Genetic engineering of indica rice with *AtDREB1A* gene for enhanced abiotic stress tolerance. *Plant Cell, Tissue and Organ Culture (PCTOC)* **136**, 173-188 (2019).

79. Monfared, H.H. et al. Overexpression of a rice monosaccharide transporter gene (*OsMST6*) confers enhanced tolerance to drought and salinity stress in *Arabidopsis thaliana*. *Plant Molecular Biology Reporter* **38**, 151-164 (2020).

80. Qin, Q. et al. A U-box E3 ubiquitin ligase *OsPUB67* is positively involved in drought tolerance in rice. *Plant Molecular Biology* **102**, 89-107 (2020).

81. Shim, J.S. et al. Overexpression of *OsNAC14* improves drought tolerance in rice. *Frontiers in Plant Science* **9**, 1-14 (2018).

82. Yamada, K. et al. Functional analysis of an *Arabidopsis thaliana* abiotic stress-inducible facilitated diffusion transporter for monosaccharides. *The Journal of Biological Chemistry* **285**, 1138-1146 (2010).

83. Xu, W. et al. A profilin gene promoter from switchgrass (*Panicum virgatum* L.) directs strong and specific transgene expression to vascular bundles in rice. *Plant Cell Reports* **37**, 587-597 (2018).

84. Chen, G. et al. Functional characterization of *OsHAK1* promoter in response to osmotic/drought stress by deletion analysis in transgenic rice. *Plant Growth Regulation* **88**, 241-251 (2019).

85. Huang, J. et al. *OsRhoGAP2* promoter drives inflorescence-preferential expression and confers responses to abiotic stresses in transgenic Arabidopsis. *Acta Physiologiae Plantarum* **41**, 1-11 (2019).

86. De Silva, W.S.I. et al. *In silico* analysis of *osr40c1* promoter sequence isolated from indica variety Pokkali. *Rice Science* **24**, 228-234 (2017).

87. Teng, H. et al. Responsiveness comparison of three stress inducible promoters in transgenic rice. *Acta Physiologiae Plantarum* **40**, 1-10 (2018).

88. Ge, H. et al. The expression of *CARK1* or *RCAR11* driven by synthetic promoters increases drought tolerance in *Arabidopsis thaliana*. *International Journal of Molecular Sciences* **19**, 1-13 (2018).

89. Chen, Y.S. et al. A late embryogenesis abundant protein HVA1 regulated by an inducible promoter enhances root growth and abiotic stress tolerance in rice without yield penalty. *Plant Biotechnology Journal* **13**, 105-116 (2015).

90. Ganguly, M. et al. Inducibility of three salinity/abscisic acid-regulated promoters in transgenic rice with *gusA* reporter gene. *Plant Cell Reports* **30**, 1617-1625 (2011).

91. Bai, J. et al. Comprehensive construction strategy of bidirectional green tissue-specific synthetic promoters. *Plant Biotechnology Journal* **18**, 668-678 (2020).

CHAPTER 2

Rationally designed synthetic promoters from poplar *cis*-regulatory elements are drought-stress inducible in transgenic rice (*Oryza sativa*)

2.1 Abstract

Utilizing stress-inducible promoters is advantageous in developing drought-tolerant rice to address potential metabolic burden and undesirable phenotypes from constitutive expression. Here, rationally-designed synthetic promoters SD18-1 and SD9-2 were stably transformed into rice and the T1 generation of transgenic rice was characterized for their drought and salt-stress responses. The SD18-1 and SD9-2 synthetic promoters included heptameric repeats of *cis*-regulatory elements discovered from native poplar promoters. These repeated elements putatively play a role in water deficit stress-response in poplar. The repeated elements were fused upstream of a core promoter which consisted of the -46 35S promoter with the TMV Ω 5' UTR leader sequence for transcriptional initiation to express a *TurboGFP* reporter gene. Synthetic promoter responses via GFP synthesis were measured by fluorescence spectroscopy of green fluorescence at 502 nm emission with 465 nm excitation before and after 7-, 10-, and 15-days of drought-stress treatment and after 1-, 3-, and 5- days of salt-stress treatment. The drought stress treatment consisted of water-cessation for 15 days. Drought-stressed transgenic rice containing SD18-1 and SD9-2 synthetic promoters had higher green fluorescence compared to the mock and WT control after 15 days of treatment ($P<0.05$). The salt-stress treatment consisted of applying 250 mM NaCl solution to potted plants for five days. SD18-1 and SD9-2 synthetic promoters in salt-stress treated transgenics had higher green fluorescence than the mock control ($P<0.05$) after the first and fifth day of salt-stress treatment but show similarity to the WT control ($P>0.05$). The rationally designed SD18-1 and SD9-2 synthetic promoters based on poplar *cis*-regulatory elements were induced by drought stress in rice.

2.2 Introduction

Rice (*Oryza sativa*) is an important crop and staple food worldwide [1]. Its production in 2018-2019 was recorded at 495.90 Mt showing a modest margin with the total rice consumption in the same period at 490.27 Mt (USDA 2020). The main areas of rice cultivation are China, India, South East Asia, USA, and Brazil. Climate models projected a five- to ten-fold increase in drought frequency and intensity in these rice-producing areas if global temperature increases by 3^{o}C higher than the pre-industrial conditions [2, 3]. Furthermore, drought-induced yield-loss risk was forecasted to be greater in rice compared with soybean, wheat, and maize [4]. Drought-stress in rice causes sterile florets [5], a slower grain-filling rate [6], reduced grain-size [7], lower grain-weight [8], and ultimately lower grain yield [9]. Undeniably, extreme drought conditions pose threats to global rice production. One approach to increase drought tolerance in rice is through genetic engineering.

Several genes were recently shown to confer drought-tolerance to rice [10-17]. However, overexpression of most of the drought-tolerant genes under a constitutive promoter led to undesirable phenotypes [18], metabolic burden [19], epigenetic silencing [20], or off-target effects [21] . In transgenic rice, constitutive overexpression of the drought-tolerance genes led to sterile florets [22], reduced shoot and root length [12], smaller flag-leaf area, fewer tillers and panicles, lower biomass [15], underdeveloped panicles, reduced seed-setting, and decreased yield compared to wild-type (WT). Contrastingly, when transgenes were placed under the control of drought-inducible promoters, the off-target effects were ameliorated, which resulted in drought-tolerant rice with higher yield than the WT genotypes under drought conditions [10, 15]. Hence, the use of inducible promoters is advantageous in expressing drought-tolerance genes only when drought-stress

ensues. Promoters of some drought-responsive native genes were recently reported to be drought-inducible in rice [23-26]. However, promoter activity is constrained by its relatively large size (500 – 2000 bp), induction condition, specificity, and expression level [27]. Such limitations prompted the engineering of smaller, robust, and versatile synthetic promoters, which are generally composed of a core-promoter region and multiple repeats and combinations of *cis*-motifs or transcription factor binding elements [28].

Development of drought-inducible synthetic promoters was explored recently, yet only a few have been identified in rice thus far. The most recent was in 2018 which developed drought-inducible synthetic promoters driving the expression of a known functional gene in *A. thaliana* [29]. In rice, the latest studies were reported in 2011 and 2015 using multiple repeats of abscisic acid (ABA)-responsive complexes (ABRC) and ABA responsive elements (ABRE) [30, 31]. The transgenic rice lines demonstrated stress tolerance to drought, as well as ABA, salt, and cold without affecting rice yield [30]. Expression levels are also higher in synthetic promoters than a known drought-inducible native promoter [31]. The most recent research on synthetic promoters in rice are confined to tissue-specific promoters [32, 33]. These observations spurred interest for drought-inducible synthetic promoters for transgenic rice applications.

Two synthetic promoters were designed with heptamerized *cis*-motifs, fused to a common core promoter sequence downstream, to express a green fluorescent protein (GFP) gene. Two osmotic stress inducible motifs were identified by *de novo* motif detecting software. These synthetic promoters were introduced in rice via *Agrobacterium*-mediated transformation to verify stress inducibility. In this study, I hypothesized that the rationally-designed synthetic promoters, based on poplar *cis*-regulatory elements, will induce *TurboGFP* expression in rice

under drought- and salt-stress conditions. The objectives of the study were to: 1) compare the green fluorescence of drought- and salt-stressed with the non-stressed transgenic rice, and 2) compare the green fluorescence of drought- and salt-stressed transgenic rice with the drought-stressed wild-type (WT) rice. Here, we envisage a suite of synthetic promoters with high specificity, immediate inducibility, and high expression of functional genes in developing drought-tolerant rice.

2.3 Materials and Methods

2.3.1 Rice plants

Rice (*O. sativa* L. ssp. Japonica cv. 'Taipei 309') seeds were sourced from the United States Department of Agriculture - Agricultural Research Service (USDA-ARS). Transgenic and wild-type (WT) rice were grown in 1:1 ProMix BK25 potting medium (Premier Tech, Quakertown, PA) and Turface MVP potting medium (Profile, Buffalo Grove, IL) mixture. Putative rice transformants (T0) were hardened in the growth chamber under standard growing conditions (16/8-h photoperiod, 25-29°C) (Percival Scientific, Perry, IA) for two weeks before transferring to the greenhouse. Transgenic T1and wild-type (WT) rice plantlets were also initially grown for hardening in the growth chamber under standard growing conditions (16/8-h photoperiod, 25-29 °C; Percival Scientific, Perry, IA) for two weeks before transferring to the greenhouse. Transgenic and WT rice were maintained in the greenhouse (16/8-h photoperiod, 28-30 °C; 11 x 11 cm pots submerged in 6 cm deep water).

2.3.2 Bioinformatic analysis for selection of stress-responsive motif

The selection of drought-stress responsive *cis*-motifs were described in the previous study[34]. Profiling of all promoter sequences for bioinformatic analyses were performed using

BioMart[35] integrated in Phytozome v12.1.6 (www.phytozyme.org). The poplar (*Populus trichocarpa*) v 3.0 genome annotation[36] were used in collecting the two kilobase upstream sequences flanking the ATG start codon. The promoter sequences were then subjected to command line application of MEME Suite (v5.0.5), MotifSampler (v3.2.2), and Weeder (v 2.0). Up to 20 bases long DNA motifs were predicted to design reliable core sequences for the downstream experiments. The DNA motifs were then submitted to the plant *cis*-acting regulatory DNA elements database (PLACE; https://www.dna.affrc.go.jp/PLACE/) with default analysis parameters, to identify cis-elements over the DNA motifs.

2.3.3 Construction of plasmids with fluorescent reporter genes

Synthetic promoter construct generation was described in the previous study[34]. The Goldengate cloning technique was performed to generate a binary backbone plasmid containing two different gene constructs: i) a gene construct for synthetic promoter cloning site comprising BsaI restriction site, CaMV 35S core domain (-42 to -1 bp), and TMV 5' UTR (Ω) leader, fused with *TurboGFP*, and ii) a gene construct consisting of 2× CaMV 35S short promoter driving *TurboRFP* expression[34, 37]. Two complementary single stranded oligonucleotides containing heptameric repeats of a DNA motif plus 5′ overhangs of BsaI digestion sites were reannealed on the backbone plasmid to generate the synthetic promoter fragments. A pair of complementary strands was combined then incubated for 2 min at 95°C, followed by 65°C for 5 min, and then was cooled down gradually to 4°C using a thermal cycler. The annealed double strands were cloned into a BsaI-digested final destination vector. Sanger sequencing analysis was utilized to verify all gene construct DNA sequences and ligation conditions (UT Genomics Core, Knoxville, TN)[34].

2.3.4 Agrobacterium-mediated transformation

The synthetic promoter constructs (Table 1, Figure 3) were designed and transformed to *Agrobacterium tumefaciens* EHA105, as previously described[34]. *Agrobacterium*-mediated transformation was performed on embryogenic calli, as previously described[38].

Embryogenic calli were induced from the surface-sterilized seeds on 2N6-C medium for 25-30 days, with subculturing every 14 days[38]. Rice seeds were de-hulled and surface-sterilized in 70% ethanol for five minutes, then 5% sodium hypochlorite (NaOCl) solution for 45 minutes with constant shaking at 140 rpm. The seeds were then rinsed five times with sterile de-ionized (DI) water for three minutes and blot-dried in sterile filter paper. The sterile seeds were placed onto solid callus induction medium (2N6-C) and incubated in the dark at 28 ^{o}C for two weeks. The callus induction medium (2N6-C) was prepared by dissolving 4 g Chu N6 basal salt medium, 1 mL of 2mg/mL 2,4-D; 1 ml 1000x Cu/Mo/Co (25 mg $CuSO_4.5H_2O$, 250 mg $NaMoO_4.2H_2O$, 25 mg $CoCI_2.6H_2O$); 1 mL 0.8 mg/mL potassium iodide (KI); 1 mL 1000x Chu N6 vitamin solution; 100 mg myoinositol; 300 mg casein hydrolysate; 2.8 g proline; 30 g sucrose, pH=5.6, and 4 g Gelrite up to 1 L with DI water, as described[38]. After two weeks, the scutellum of each seed was removed and the primary callus was sub-cultured onto solid 2N6-C in the dark at 28^{o}C for two weeks to obtain the embryogenic calli.

The primary *A. tumefaciens* culture was prepared from a single colony grown onto 3 mL yeast extract broth (YEB with 50 mg/L kanamycin and 50 mg/L rifampicin) overnight at 28^{o}C with constant shaking at 150 rpm. Secondary culture was prepared by pipetting 100 µL of the primary culture onto 50 mL YEP broth (with 50 mg/L kanamycin and 50 mg/L rifampicin), then incubated overnight at 28^{o}C with constant shaking at 150 rpm. The secondary culture was

induced with 100 µM acetosyringone (AS) for two hours to induce *vir* genes, then centrifuged at 3250 x g to pellet. The pelleted *Agrobacterium* was resuspended in 2N6-AS medium to OD_{600} = 0.5. The 2N6-AS medium was prepared by dissolving 4 g Chu N6 basal salt medium, 1 mL of 2mg/mL 2,4-D; 1 ml 1000x Cu/Mo/Co (25 mg $CuSO_4.5H_2O$, 250 mg $NaMoO_4.2H_2O$, 25 mg $CoCI_2.6H_2O$); 1 mL 0.8 mg/mL potassium iodide (KI); 1 mL 1000x Chu N6 vitamin solution; 100 mg myoinositol; 300 mg casein hydrolysate; 2.8 g proline; 30 g sucrose, 200 µM AS, pH=5.6, up to 1L with DI water, as described[38]. Embryogenic rice calli culture were submerged in the 2N6-AS/*Agrobacterium* suspension for five minutes. The suspension was decanted, and the calli were blot-dried in sterile filter paper for five minutes. The calli were transferred onto sterile filter paper placed on top of 2N6-AS solid medium (prepared as described with 2 g/L Gelrite). Co-cultivation in the dark was done at 25°C for three days. After co-cultivation, the calli were washed five times in sterile water and finally in Timentin® water (sterile water with 150 mg/L Timentin®). The calli were grown in 2N6-S selection medium (2N6 medium as described but supplemented with 35 mg/L hygromycin +150 mg/L Timentin®) in the dark at 28°C for one month. Subculture was done every two weeks. Calli surviving the selection were moved to Murashige and Skoog (MS)[39] regeneration medium for 30 days with subculturing every two weeks. The MS regeneration medium was prepared by dissolving 4.44 g MS with vitamins (M404), 500 mg casein hydrolysate, 20 g sorbitol, 30 g sucrose, with 2 mg/L kinetin, 0.05 mg/L NAA, and 2 g Gelrite up to 1 L of DI water[38]. Sterile MS regeneration medium was supplemented with 35 mg/L hygromycin. Regenerated shoots were grown in 1/2 MS rooting medium for two weeks for root induction and complete regeneration. The ½ MS rooting medium was prepared by dissolving 2.22 g MS with vitamins (M404), 15 g sucrose, pH=5.6, and 2 g

Gelrite up to 1L with DI water, as described[38]. Regenerated plantlets were transferred onto the potting-mix and hardened for two weeks in the growth chamber (16/8-h photoperiod, 25-29 °C; Percival Scientific, Perry, IA) before moving to the greenhouse (16/8-h photoperiod, 28-30 °C; 11 x 11 cm pots submerged in 6 cm deep water).

2.3.5 Confirmation of putative transgenics

Constitutive expression of TurboRFP was visually-confirmed in one-month-old putative transgenic rice (T0) under normal growth conditions using the fluorescence-inducing laser projector (FILP)[40]. TurboRFP fluorescent images were acquired using the 525 nm excitation laser (1.4 W) and 575/40 nm emission filter with 300 ms exposure. To visualize potential background green fluorescence under normal growth conditions, TurboGFP fluorescent images were also acquired in transgenic rice without stress treatment using the 465 nm excitation laser (1.4 W) and 525/50 emission filter with 300 ms exposure. FILP images were processed using the ImageJ analysis software (version 1.53a).

Molecular analysis of putative transgenic rice (T0) was performed. Genomic DNA was extracted from two-month-old putative transgenic rice events as described by Kang and Yang (2004)[41] with modification. Leaf-tissues were rapidly frozen in liquid nitrogen and homogenized by TissueLyser II (Qiagen, Hilden, Germany). The samples were centrifuged quickly and added with 400 µL DNA extraction buffer (200 mM Tris-HCl pH 7.5, 250 mM NaCl, 25 mM EDTA pH 8.0, 3.5% SDS), vortexed briefly, and incubated at 65ºC for 30 minutes. The samples were centrifuged at 17000 x g for five minutes and 300 µL of the supernatant was transferred to a new tube. Equal volume of chloroform:isoamyl alcohol (24:1) was added, vortexed briefly, and centrifuged at 17000 x g for ten minutes. The upper phase solution (300 µL) was transferred onto

a new tube. Equal volume of isopropanol was added and incubated at room temperature for five minutes. This was followed by centrifugation at 17000 x g for 10 minutes. The supernatant was removed and 300 µL of 70% ice-cold ethanol was added to the pellet. Centrifugation was done at 17000 RCF for five minutes and the 70% ethanol was completely removed and air-dried for 10 minutes. The pellet was dissolved in 50 µL sterile water.

Genomic DNA (100 ng) was pipetted to DreamTaq Green PCR master mix (Thermo Scientific) including 200 nM of *TurboGFP* and *OsAct1* forward and reverse primers (Table 2). Rice *Actin1* (*OsAct1*) gene was used as positive control for DNA loading.

PCRs were performed as 1 cycle of 95°C for 5 min, 35 cycles repeating a chain of 95°C for 30 sec, 60°C for 30 sec, and 72°C for 30 sec, and final extension at 72°C for 10 min. The PCR products were subjected to gel-electrophoresis at 50 V for 40 min.

2.3.6 Abiotic stress treatment

The T1 seeds of each independent event were collected from their respective self-pollinated, primary rice transformants (T0). The T1 seeds were de-hulled then surface-sterilized in 5% sodium hypochlorite solution (NaOCl). The surface-sterilized T1 seeds were germinated on ½ MS medium with 35 mg/L hygromycin, placed in the dark for three days then transferred under light illumination for 4-5 days. The T1 seedlings for each of the transgenic events were then scored for hygromycin-resistance (Hyg^R) and susceptibility (Hyg^S). The ratio of hygromycin-resistant to hygromycin-susceptible seedlings (Hyg^R: Hyg^S) was evaluated for the goodness of fit to the Mendelian 3:1 segregation ratio using the chi-square test (χ^2). The 14-day old hygromycin-resistant T1 seedlings were transferred and further grown into 1:1 ProMix BK25

(Premier Tech, Quakertown, PA) and Turface MVP (Profile, Buffalo Grove, IL) potting mixture for further growth in the greenhouse.

Drought and salt-stress treatments were carried out in two-month-old WT and transgenic rice in the greenhouse. The transgenic rice lines and events used for the drought- and salt-stress treatments were selected based on i) the primary (T0) transgenic events, which were PCR-positive for the *TurboGFP* gene, ii) available T1 seeds at the start of the experiment, and iii) the Hyg^R: Hyg^S goodness of fit to the Mendelian 3:1 segregation ratio of each transgenic event determined by χ^2 test (Table 3).

The transgenic rice harboring the SD18-1 (events 1 and 3) and SD9-2 (events 2, 4, 6, and 7) constructs were tested for their synthetic promoter response in the drought- and salt-stress experiments. A transgenic rice referred to as Neg (events 2, 4, and 5) was used as a control. The Neg transgenic rice contained the construct that did not consist of a synthetic promoter sequence, but only the -46 35S promoter with the TMV 5' Ω UTR leader sequence (negative for synthetic promoter construct).

Drought-stress treatment was done by withholding water until complete-leaf rolling was observed. Mock control consisted of pots submerged in 6 cm deep deionized (DI) water.

Potting-mix moisture was measured on a scale of 1-10 (moisture scale levels 1-3 = dry, 4-7 = normal, 8-10 = wet) using an analog soil moisture meter (MS04, Sonkir, Hanoi, Vietnam), at various time intervals (day 0, 2, 5, 7, 10, 12, and 15), until complete leaf rolling was observed in drought-stress treated rice (day 15). One potting-mix moisture measurement per transgenic event (SD18-1 events 1 and 5; SD9-2 events 2, 4, 6, and 7; Neg events 2 and 4) and WT control was performed (n=9 total observations each for mock control and drought-stress treatment per time

point). The transgenic and WT rice were grown in a 11 cm square pot (Griffin Greenhouse Supplies, Inc., Tewksbury, MA). Day 0 was the last day the plants under drought-stress treatment submerged in 6 cm deep water.

Salt-stress treatment was done by drenching 250 mL of salt solution (250 mM NaCl) into the potting-mix. After adding the salt solution into the potting mix, the transgenic plant pots under salt-stress treatment remained submerged in the salt solution collected in the containment tray of the said pots. One day after the initial salt solution application, the salt solution in the containment trays from the previous day's application was replaced with a fresh 250 mM salt solution directly into the potting mix. The described salt solution application was done for five consecutive days (from day 0 until day 4). Salt solution application was halted on day 5 of the salt-stress experiment. Mock control plant pots were submerged in 6 cm deep DI water.

Potting-mix electrical conductivity (EC) measurement was performed daily in 11 cm deep square pot using a soil EC meter (HI98331 Soil Test™ Direct Soil EC Tester by Hanna Instruments). On day 0, EC was measured before applying salt solution into the potting-mix. Day one to day five EC measurements were obtained one day after applying the salt solution. Three independent pot measurements per transgenic event (SD18-1 events 1 and 5; SD9-2 events 2, 4, 6, and 7; Neg events 2 and 4) and WT control were performed (n = 27 total potting-mix EC measurement per mock control and salt-stress treatment per time point).

2.3.7 Fluorescence spectroscopy

Fluorescence excitation and emission measurements were done using a Fluorolog-3 spectrofluorometer (HORIBA Scientific, version 3.8.0.60). Red fluorescence spectra were acquired using 540 nm excitation and 550-580 nm emission range. Red fluorescence values were

recorded at 572 nm emission on day 0 of drought- and salt-stress treatment. Green fluorescence spectra were acquired using 465 nm excitation and 480-520 nm emission range. Green fluorescence values were recorded at 502 nm. Green fluorescence values were measured before (on day 0) and after drought- and salt-stress treatment. For drought-stress synthetic promoter response, green fluorescence was measured after the 7^{th}, 10^{th}, and 15^{th} days of treatment. For salt-stress synthetic promoter response, green fluorescence was measured after 1^{st}, 3^{rd}, and 5^{th} days of treatment. Fluorescence spectroscopy measurements were carried out in 3 transgenic plants per event per mock control and treatment group for each time point, each plant consisted of independent measurements of the 3 youngest leaves from the main tiller. Fluorescence spectroscopy data were normalized using the WT rice fluorescence values, as described[42].

2.3.8 Standoff detection

Standoff detection was performed after 15 days of drought-stress and 5 days of salt-stress treatment using FILP[40]. Red fluorescent images were acquired using the 525 nm excitation laser (1.4 W) and 575/40 nm emission filter with 300 ms exposure. Green fluorescent images were acquired using the 465 nm excitation laser (1.4 W) and 525/50 emission filter with 300 ms exposure. Assembly of the FILP images was done using the ImageJ analysis software (version 1.53a).

2.3.9 Statistical analysis

For Hyg^R:Hyg^s goodness of fit to the Mendelian 3:1 segregation ratio, Chi-square test was performed in SAS ($P<0.05$). Statistical analyses for fluorescence, and potting-mix moisture and EC measurements were also performed using the SAS statistical software and results were analyzed using mixed model analysis of variance (mmaov) at $P<0.05$ (SAS 9.4, Cary, N.C.,

U.S.A.). *Post-hoc* analysis was done using Fisher's least significant difference (LSD) to determine significant differences among means when results are statistically significant (P<0.05). A completely randomized experimental design was used throughout the experiments.

2.4 Results

2.4.1 Agrobacterium-mediated transformation

The twelve synthetic promoter constructs were transformed into rice through *Agrobacterium*-mediated transformation. Visual confirmation through FILP stand-off detection shows RFP expression across all representative putative transgenic (T0) rice (Figures 4-6).

Molecular confirmation by PCR shows the presence of *gfp* gene amplicon across all transgenic events except in SD9-2 event 5, SD18-3 event 4, and Neg event 1 (Figures 7-9).

The transgenic rice harboring the SD18-1 (events 1 and 5), SD9-2 (events 2, 4, 6, and 7), and Neg (events 2, 4, and 5) synthetic promoter constructs were used for drought- and salt-stress treatments. The said transgenic events for each of the transgenic line demonstrated Hyg^R: Hyg^S ratio similar to the Mendelian 3:1 segregation ratio (Table 3).

2.4.2 Drought-stress treatment

2.4.2.1 Red fluorescence intensity in transgenic rice

All transgenic events had significantly high red fluorescence mean value than the WT (n=6, P<0.05), except for the transgenic Neg event 5. The Neg transgenic rice event 5 was not used for the succeeding experiments (Figure 10). Three biological replicates were randomly assigned for mock and drought-stress treatment for each of the transgenic events being tested. Red fluorescence mean values were similar between mock and drought-stress treated rice for each transgenic event (n=3, P >0.05; Table 3).

2.4.2.2 Potting-mix moisture data and drought-stress phenotype in rice

Potting-mix moisture data per time-point were measured on a scale of 1-10 and classified as dry (1-3), normal (4-7), and wet (8-10) (Figure 11). Mean potting-mix moisture scale for drought-stress treated rice were classified normal after the second and fifth days of drought-stress treatment. Mean potting-mix moisture scale for drought-stress treated rice were classified dry after the seventh until the fifteenth day of drought-stress treatment. WT and most of the transgenic rice had no significant leaf rolling on day seven and day ten, but leaf rolling was observed on day 15 (Figures 12-14). Leaf-rolling was observed to start on day 10 for the transgenic SD9-2 events 2 and 4. The drought-stress treatment was stopped on day 15 to avoid significant plant damage.

2.4.2.3 Drought-stress synthetic inducible promoter activity in rice

The mean green fluorescence value was significantly higher in drought-stress treated versus mock control across all transgenic rice after 15-days of drought-stress treatment (n=3, $P<0.05$; Figures 15-17). Green fluorescence was significantly higher for the transgenics containing the SD18-1 and SD9-2 constructs (except SD18-1 event 5 and SD9-2 event 6) when compared to the WT. Transgenics containing the Neg construct had no significant difference in green fluorescence with the WT (Figure 16). Highest green fluorescence intensity was observed in SD9-2 event 2 (38128.00 ± 1308.14 CPS) and SD9-2 event 7 (37039.00 ± 1933.33 CPS) transgenics.

Synthetic promoter activity was investigated across various time points of decreasing potting mix moisture in drought-stress treated rice (Figures 18-20). Green fluorescence was significantly higher in drought-stress treated transgenics than the mock control only when

significant leaf-rolling was observed in drought-stress treated transgenic rice. Drought-stress treated SD9-2 events 2 and 4 had higher green fluorescence starting on day 10 of the drought-stress treatment. The rest of the drought-stress treated transgenic events had higher green fluorescence than the mock control on day 15.

Stand-off detection using FILP showed intense green fluorescence in drought-stress treated transgenics, most especially for SD9-2 transgenic events (Figures 21-23).

2.4.3 Salt-stress treatment

2.4.3.1 Red fluorescence intensity in stable transgenic rice

All transgenic events had significantly higher red fluorescence than the WT (n=6, P <0.05), except for the Neg transgenic rice event five (Figure 24). The transgenic Neg event 5 had no significant difference from the WT red fluorescence values, and was not used for the subsequent experiments. Similar red fluorescence values were observed between the replicates assigned for salt-stress treatment and mock control for each of the transgenic events (P >0.05; Table 5).

2.4.3.2 Potting-mix electrical conductivity (EC) and salt-stress phenotype in rice

Soil EC values were significantly higher in the salt-stress treated pots (soil EC=2.58 ± 0.04 dS/m) than in the mock control (soil EC=0.80 ± 0.04 dS/m) 24 hours after application of 250 mM salt solution (Figure 25). Soil EC measured >4.00 dS/m and plateaued starting on the second day of salt stress treatment. WT and transgenic rice started to show phenotypes of salt-stress on the third day of salt-stress treatment (Figure 26-28). Significant leaf-tip burning was apparent most especially in the older leaves on the fifth day of salt-stress treatment. Salt-stress

treatment was stopped on the fifth day to avoid significant damage to the WT and transgenics (Figures 26-28).

2.4.3.3 Salt-stress inducible synthetic promoter activity in rice

Salt-stress treated transgenics had significantly higher green fluorescence intensity than the mock control after five days of drenching 250 mM salt solution into the soil (Figures 29-31). However, green fluorescence of all the salt-stress treated transgenics, except transgenic SD9-2 events 2 and 4, were similar to the WT. Green fluorescence intensity was the highest in SD9-2 event 2 (33820.00 ± 997.37 CPS) and SD9-2 event 4 (31427.00 ± 562.43).

Synthetic promoter responses to salt stress were also investigated at various time points of salt-stress treatment (0-, 1-, 3-, and 5 days). All SD18-1 and SD9-2 transgenic events under salt-stress had significantly higher green fluorescence on day one (n=3, $P<0.05$; Figures 32-34). Mock and salt-stressed transgenics had similar green fluorescence on day three of salt-stress treatment (n=3, $P>0.05$). Difference in green fluorescence was again observed on day 5 of salt-stress treatment. To further confirm the synthetic promoter activity on day one of salt stress treatment, green fluorescence of each transgenics was compared from the WT (Figures 35-37). green fluorescence values of the transgenics were similar to the WT.

Standoff detection using FILP did not show intense green fluorescence in the salt-stress treated rice than the mock control after five days of salt-stress treatment (Figures 38-40).

2.5 Discussion

This study demonstrated on the basis of fluorescence spectroscopy and FILP, two relatively short synthetic promoters SD18-1 and SD9-2 composed of heptamerized, 7-8 bp long dicot-based *cis*-motifs, exhibiting drought-stress-specific inducible response in rice.

The inducible response of the SD18-1 and SD9-2 synthetic promoters to drought stress in transgenic rice showed similar activity in stable transgenic *A. thaliana*[34]. In the previous study, fluorescence spectroscopy data for green fluorescence in transgenic SD18-1 and SD9-2 *Arabidopsis* after water cessation for ten days reached maximum mean values of approximately 140,000 CPS and 180,000 CPS, respectively[34]. In this present study, the maximum mean values for the green fluorescence after 15 days of drought stress treatment in rice, as compared to the previous study in *Arabidopsis*[34], seemed lower at approximately 37,000 CPS in SD18-1 and 43,000 CPS in SD9-2 transgenic rice. I took the ratios for the maximum reported green fluorescence values of the treatment and the mock control in SD18-1 and SD9-2 transgenic rice and the transgenic *Arabidopsis* to obtain a thorough comparison of changes in green fluorescence intensities after drought-stress treatment. Surprisingly, both the SD18-1 and SD9-2 transgenic rice and *Arabidopsis* showed similar treatment: mock green fluorescence ratios after imposing drought stress. The treatment: mock green fluorescence ratios after drought stress treatment were 1.22 (140,000 CPS: 115,000 CPS) in SD18-1 and 1.50 (180,000 CPS: 120, 000 CPS) in SD9-2 transgenic *Arabidopsis*[34]. In this present study, the treatment: mock green fluorescence ratios after drought stress treatment were 1.32 (37,000 CPS: 28,000 CPS) and 1.54 (43,000 CPS: 28,000 CPS) in SD18-1 and SD9-2 transgenic rice, respectively. This present study further showed that both the SD18-1 and SD9-2 synthetic promoters did not show inducible response to salt-stress treatment in rice, similar to *Arabidopsis* as previously described[34]. This is not the first instance where a set of designed synthetic promoters showed similar activities in both dicot and monocot plants. A synthetic promoter RP1-MP1 was derived from *Rice Tungro Bacilliform Virus* (RTBV) and *Mirabilis Mosaic Virus* (MMV)[43]. Compared to the *CaMV35S* promoter, the

RP1-MP1 synthetic promoter constitutively expressing the *gus* reporter gene exhibited significantly 1.87-fold and 1.97-fold increase in transgenic tobacco (*Nicotiana tabacum* cv. 'Xanthi') and transgenic rice, respectively[43]. Two CmYLCV9.11 and CmYLCV4 synthetic promoters were derived from *Cestrum yellow leaf curling virus* (CmYLCV) and shown to drive efficient GUS activity in tobacco and maize transient expression assays[44]. However, in a rationally designed constitutive synthetic promoter "MinSyn" based on plant-infecting pathogen *cis*-motifs (*CaMV35S*, *A. tumefaciens* nopaline synthase (*AtuNOS*) and *Mirabilis Mosaic Virus* (MMV)[45], the MinSyn synthetic promoter exhibited lower activity in the monocot barley (*Hordeum vulgare*) compared to the dicots *Arabidopsis*, tobacco, and *Brassica rapa*[45]. The synthetic promoters described in the previous studies which were compared between monocot and dicot plant systems were designed based on *cis*-motifs or promoter parts of plant viral pathogens[43-45]. To the best of my knowledge, this is the first synthetic promoter rationally-designed from a dicot poplar *cis*-motif, to exhibit similar synthetic promoter activity in a monocot plant model. The similarities in the synthetic promoter responses in both rice and *Arabidopsis* indicate that the SD18-1 and SD92 *cis*-motifs are likely highly conserved regions in the DNA in monocot and dicot plant systems.

The rice genome had multiple, publicly available omics data which were annotated with high quality[46, 47]. The synthetic promoter design pipeline as previously described[34], can be a valuable tool in mining *cis*-motifs to further optimize the development of various synthetic promoters targeted for utility in rice biotechnology.

Most of the synthetic promoters recently developed in rice consisted of constitutive or tissue-specific properties. The synthetic promoters BiGSSP2, BiGSSP3, BiGSSP6, BiGSSP7 as previously described[32] showed bidirectional expression patterns, expressing *GFP* and *GUS* reporter genes in two reverse directions, specifically in the leaf, sheath, panicle, and stem tissues in transgenic rice[32]. The synthetic promoters GSSP1, GSSP3, GSSP5, GSSP6, GSSP7, and GEAT also exhibited constitutive expression in transgenic rice green-tissues[33]. In 2011 and 2014, inducible synthetic promoters 3xABRC321[48], 4xABRE[31], and 2xABRC[31] were developed from a well-conserved ABA response element (ABRE)[49] and ABA response complex (ABRC)[50]. The 3xABRC321[48], 4xABRE[31], and 2xABRC[31] synthetic promoters were induced by various abiotic stresses such as osmotic-, cold-, salt-, and ABA-stress in transgenic rice[31, 48]. However, a precisely defined stress-specific response[26, 28] of an inducible synthetic promoter is more desirable to ensure a tightly regulated inducible expression of a drought-tolerance gene. A set of drought-stress inducible promoters were also recently developed but were only studied in *Arabidopsis*[29, 51, 52], and tobacco[53]. The described SD18-1 and SD9-2 synthetic promoters in this present study are, by far, the most recently reported drought-stress inducible synthetic promoters in rice.

In this present study, the SD18-1 and SD9-2 synthetic promoters consisted of seven copies of the eight bp and seven bp long *cis*-motifs, respectively. Hence, the synthetic promoter SD18-1 had a 56 bp while SD9-2 had a 49 bp long synthetic *cis*-regulatory sequence. Compared to the *cis*-element sequences of the other drought-stress inducible synthetic promoters developed in rice, the SD18-1 and SD9-2 synthetic promoters described in this study, had relatively shorter synthetic *cis*-element sequences. For example, the 3xABRC321[48], 4xABRE[31], and 2xABRC[31],

which consisted of only 2-4 copies of *cis*-motifs, the synthetic promoter lengths were 168 bp, 93 bp, and 59 bp long, respectively. The longer lengths of the synthetic promoter sequences of the three drought-inducible synthetic promoters 3xABRC321[48], 4xABRE[31], and 2xABRC[31] were due to the flanking sequences among each copy of their respective multimerized *cis*-motifs[31, 48]. Motif copy number and the spacing between each motif are important factors to be considered once the desired *cis*-motifs were identified to optimize synthetic promoter architecture and activity[51]. Although the motif copy number is often correlated to synthetic promoter strength,[54] multiple copies of *cis*-motifs might not necessarily enhance the synthetic promoter activity[55]. A threshold of *cis*-motif copy number should be determined for each synthetic promoter being designed. The endogenous transcription factors may be depleted due to excessive transcription factor binding sites brought about by the multiple copies of similar *cis*-motif [55]. Most importantly, once the threshold number of *cis*-motifs were identified, assembly of the synthetic promoter architecture would require optimum spacing among motifs for the hierarchal binding of their corresponding transcription factors[51, 54]. Since this present study utilized heptameric repeats of the SD18-1 and SD9-2 *cis*-motifs without spacing between motifs, the length of flanking sequences among multimerized *cis*-motifs may be further explored.

Overall, this study is significant in developing drought-tolerant rice that primarily relied on a few and a similar set of virus-derived or plant-derived (native) promoter systems. In this present study, 1) I reported a set of relatively short synthetic promoters that can be relevant in rice biotechnology; 2) I described the drought-stress-specific response of the synthetic promoters in rice, addressing the lack of available drought-stress inducible promoters in rice; and lastly 3) I demonstrated the utility of the rationally-designed dicot-based synthetic promoters in rice.

2.6 Conclusions

This study demonstrated the response of the rationally designed synthetic promoters, from poplar *cis*-regulatory elements, to drought and salt-stress treatment. Here, I report the synthetic promoter activity measured by green fluorescence spectroscopy in stable transgenic rice after drought and salt-stress treatment. The stable transgenic rice containing SD18-1 and SD9-2 synthetic promoters are induced only by drought-stress. The results show the universal application to both monocot and dicot system of the rationally designed SD18-1 and SD9-2 synthetic promoters.

References

1. Ye, X. et al. Engineering the provitamin A (β-carotene) biosynthetic pathway into (carotenoid-free) rice endosperm. *Science* **287**, 303-305 (2000).
2. Naumann, G. et al. Global changes in drought conditions under different levels of warming. *Geophysical Research Letters* **45**, 3285-3296 (2018).
3. Trenberth, K.E. et al. Global warming and changes in drought. *Nature Climate Change* **4**, 17-22 (2014).
4. Leng, G. & Hall, J. Crop yield sensitivity of global major agricultural countries to droughts and the projected changes in the future. *Science of the Total Environment* **654**, 811-821 (2019).
5. Sheoran, I.S. & Saini, H.S. Drought-induced male sterility in rice: changes in carbohydrate levels and enzyme activities associated with the inhibition of starch accumulation in pollen. *Sexual Plant Reproduction* **9**, 161-169 (1996).
6. Yang, X. et al. The different influences of drought stress at the flowering stage on rice physiological traits, grain yield, and quality. *Scientific Reports* **9**, 1-12 (2019).
7. Acuña, T.L.B. et al. Genotype×environment interactions for grain yield of upland rice backcross lines in diverse hydrological environments. *Field Crops Research* **108**, 117-125 (2008).
8. Lilley, J.M. & Fukai, S. Effect of timing and severity of water deficit on four diverse rice cultivars III. Phenological development, crop growth and grain yield. *Field Crops Research* **37**, 225-234 (1994).

9. Lafitte, H.R. et al. Whole plant responses, key processes, and adaptation to drought stress: the case of rice. *Journal of Experimental Botany* **58**, 169-175 (2006).

10. Chen, G. et al. Driving the expression of *RAA1* with a drought-responsive promoter enhances root growth in rice, its accumulation of potassium and its tolerance to moisture stress. *Environmental and Experimental Botany* **147**, 147-156 (2018).

11. Tang, Y. et al. Overexpression of a *MYB* family gene, *OsMYB6*, increases drought and salinity stress tolerance in transgenic rice. *Frontiers in Plant Science* **10**, 1-12 (2019).

12. Bhattacharjee, A. et al. Over-expression of *OsHOX24* confers enhanced susceptibility to abiotic stresses in transgenic rice via modulating stress-responsive gene expression. *Frontiers in Plant Science* **8**, 1-11 (2017).

13. Qin, Q. et al. A U-box E3 ubiquitin ligase *OsPUB67* is positively involved in drought tolerance in rice. *Plant Molecular Biology* **102**, 89-107 (2020).

14. Sengupta, S. et al. An actin-depolymerizing factor from the halophyte smooth cordgrass, *Spartina alterniflora* (*SaADF2*), is superior to its rice homolog (*OsADF2*) in conferring drought and salt tolerance when constitutively overexpressed in rice. *Plant Biotechnology Journal* **17**, 188-205 (2019).

15. Selvaraj, M.G. et al. Expression of the *CCCH*-tandem zinc finger protein gene *OsTZF5* under a stress-inducible promoter mitigates the effect of drought stress on rice grain yield under field conditions. *Plant Biotechnology Journal* **18**, 1711-1721 (2020).

16. Verma, R.K. et al. Overexpression of ABA receptor *PYL10* gene confers drought and cold tolerance to indica rice. *Frontiers in Plant Science* **10**, 1-16 (2019).

17. Shim, J.S. et al. Overexpression of *OsNAC14* improves drought tolerance in rice. *Frontiers in Plant Science* **9**, 1-14 (2018).

18. Ito, Y. et al. Functional analysis of rice DREB1/CBF-type transcription factors involved in cold-responsive gene expression in transgenic rice. *Plant and Cell Physiology* **47**, 141-153 (2006).

19. Karlowski, W.M. & Hirsch, A.M. The over-expression of an alfalfa *RING-H2* gene induces pleiotropic effects on plant growth and development. *Plant Molecular Biology* **52**, 121-133 (2003).

20. Schubert, D. et al. Silencing in *Arabidopsis* T-DNA transformants: the predominant role of a gene-specific RNA sensing mechanism versus position effects. *The Plant Cell* **16**, 2561-2572 (2004).

21. Anand, A. et al. Stable transgene expression and random gene silencing in wheat. *Plant Biotechnology Journal* **1**, 241-251 (2003).

22. Ge, L. et al. Overexpression of *OsRAA1* causes pleiotropic phenotypes in transgenic rice plants, including altered leaf, flower, and root development and root response to gravity. *Plant Physiology* **135**, 1502-1513 (2004).

23. Chen, G. et al. Functional characterization of *OsHAK1* promoter in response to osmotic/drought stress by deletion analysis in transgenic rice. *Plant Growth Regulation* **88**, 241-251 (2019).

24. Huang, J. et al. *OsRhoGAP2* promoter drives inflorescence-preferential expression and confers responses to abiotic stresses in transgenic Arabidopsis. *Acta Physiologiae Plantarum* **41**, 1-11 (2019).

25. De Silva, W.S.I. et al. *In silico* analysis of *osr40c1* promoter sequence isolated from indica variety Pokkali. *Rice Science* **24**, 228-234 (2017).

26. Teng, H. et al. Responsiveness comparison of three stress inducible promoters in transgenic rice. *Acta Physiologiae Plantarum* **40**, 1-10 (2018).

27. Liu, W. et al. Advanced genetic tools for plant biotechnology. *Nature Reviews Genetics* **14**, 781-793 (2013).

28. Bilas, R. et al. *Cis*-regulatory elements used to control gene expression in plants. *Plant Cell, Tissue and Organ Culture (PCTOC)* **127**, 269-287 (2016).

29. Ge, H. et al. The expression of *CARK1* or *RCAR11* driven by synthetic promoters increases drought tolerance in *Arabidopsis thaliana*. *International Journal of Molecular Sciences* **19**, 1-13 (2018).

30. Chen, Y.S. et al. A late embryogenesis abundant protein HVA1 regulated by an inducible promoter enhances root growth and abiotic stress tolerance in rice without yield penalty. *Plant Biotechnology Journal* **13**, 105-116 (2015).

31. Ganguly, M. et al. Inducibility of three salinity/abscisic acid-regulated promoters in transgenic rice with *gusA* reporter gene. *Plant Cell Reports* **30**, 1617-1625 (2011).

32. Bai, J. et al. Comprehensive construction strategy of bidirectional green tissue-specific synthetic promoters. *Plant Biotechnology Journal* **18**, 668-678 (2020).

33. Wang, R. et al. Novel green tissue-specific synthetic promoters and *cis*-regulatory elements in rice. *Scientific Reports* **5**, 1-11 (2015).

34. Yang, Y. et al. Rational design and testing of abiotic stress-inducible synthetic promoters from poplar cis-regulatory elements. *Plant Biotechnology Journal*, 1-16 (2021).

35. Smedley, D. et al. The BioMart community portal: an innovative alternative to large, centralized data repositories. *Nucleic Acids Research* **43**, 589-598 (2015).

36. Tuskan, G.A. et al. The genome of black cottonwood, *Populus trichocarpa* (Torr. & Gray). *Science* **313**, 1596-1604 (2006).

37. Engler, C. et al. A golden gate modular cloning toolbox for plants. *ACS synthetic biology* **3**, 839-843 (2014).

38. Wu, C. & Sui, Y. Efficient and fast production of transgenic rice plants by agrobacterium-mediated transformation. *Transgenic Plants*, 95-103 (2019).

39. Murashige, T. & Skoog, F. A revised medium for rapid growth and bio assays with tobacco tissue cultures. *Physiologia plantarum* **15**, 473-497 (1962).

40. Rigoulot, S.B. et al. Imaging of multiple fluorescent proteins in canopies enables synthetic biology in plants. *Plant Biotechnology Journal* **19**, 830-843 (2020).

41. Kang, T.-J. & Yang, M.-S. Rapid and reliable extraction of genomic DNA from various wild-type and transgenic plants. *BMC Biotechnology* **4**, 1-12 (2004).

42. Millwood, R.J. et al. Instrumentation and methodology for quantifying GFP fluorescence in intact plant organs. *BioTechniques* **34**, 638-643 (2003).

43. Gupta, D. et al. Development of efficient synthetic promoters derived from pararetrovirus suitable for translational research. *Planta* **253**, 1-15 (2021).

44. Sahoo, D.K. et al. Comparative analysis of synthetic DNA promoters for high-level gene expression in plants. *Planta* **240**, 855-875 (2014).

45. Cai, Y.-M. et al. Rational design of minimal synthetic promoters for plants. *Nucleic Acids Research* **48**, 11845-11856 (2020).

46. Zhang, Z. et al. RiceWiki: a wiki-based database for community curation of rice genes. *Nucleic Acids Research* **42**, 1222-1228 (2014).

47. Sang, J. et al. IC4R-2.0: rice genome reannotation using massive RNA-seq data. *Genomics, Proteomics & Bioinformatics* **18**, 161-172 (2020).

48. Chen, Y.-S. et al. A late embryogenesis abundant protein HVA1 regulated by an inducible promoter enhances root growth and abiotic stress tolerance in rice without yield penalty. *Plant Biotechnology Journal* **13**, 105-116 (2015).

49. Shen, Q. et al. Hormone response complex in a novel abscisic acid and cycloheximide-inducible barley gene. *Journal of Biological Chemistry* **268**, 23652-23660 (1993).

50. Shen, Q. et al. Modular nature of abscisic acid (ABA) response complexes: composite promoter units that are necessary and sufficient for ABA induction of gene expression in barley. *The Plant Cell* **8**, 1107-1119 (1996).

51. Jameel, A. et al. Tinkering *cis* motifs jigsaw puzzle led to root-specific drought-inducible novel synthetic promoters. *International Journal of Molecular Sciences* **21**, 1-22 (2020).

52. Hou, L. et al. Construction of stress responsive synthetic promoters and analysis of their activity in transgenic *Arabidopsis thaliana*. *Plant Molecular Biology Reporter* **30**, 1496-1506 (2012).

53. Na, J.-K. & Metzger, J.D. Chimeric promoter mediates guard cell-specific gene expression in tobacco under water deficit. *Biotechnology Letters* **36**, 1893-1899 (2014).

54. Liu, W. & Stewart, C.N. Plant synthetic promoters and transcription factors. *Current Opinion in Biotechnology* **37**, 36-44 (2016).

55. Hernandez-Garcia, C.M. & Finer, J.J. Identification and validation of promoters and *cis*-acting regulatory elements. *Plant Science* **217-218**, 109-119 (2014).

Appendix

Table 1 List of synthetic promoters used in *Agrobacterium*-mediated transformation of Taipei 309 rice. SD (synthetic promoter from drought-stress-inducible promoters) motifs[34]. The synthetic *cis*-regulatory elements were composed of seven (7) or eight (8) base pairs repeated seven times.

Synthetic Promoter ID	***cis*-element sequence**	**no. of base pairs**	**heptamerized *cis*-element sequence**
SD18-1	GCTCATAT	8	GCTCATATGCTCATATGCTCATATGCTCATATGCTCATATGCTCATATGCTCATAT
SD9-2	CGCGCAA	7	CGCGCAACGCGCAACGCGCAACGCGCAACGCGCAACGCGCAACGCGCAA
Neg	without synthetic promoter; control	0	only contains the -46 35S promoter with the TMV 5' Ω UTR leader sequence for transcriptional initiation

Table 2 List of primer sequences used for qRT-PCR and PCR amplification. for=forward, rev=reverse.

Primer ID	Sequence
TurboGFP_genotyping_for	GGATCTGGATCTGAGTCTGATGAGTCT
TurboGFP_genotyping_rev	CCTTGAAATCTCCGATCACTCTTCCAG
Act1_for	ATCCTTGTATGCTAGCGGTCGA
Act1_rev	ATCCAACCGGAGGATAGCATG

Table 3 Chi-square test for goodness of fit to Mendelian 3:1 segregation of hygromycin-resistant (Hyg^R) and hygromycin-susceptible (Hyg^S) T1 rice seeds. T1 rice seeds were germinated in ½ MS medium with 35 mg/L hygromycin. Hyg^R: Hyg^s segregation of transgenic rice were tested for goodness of fit to the Mendelian 3:1 segregation ratio through Chi-square (χ^2) test carried out in SAS. Asterisk represent significant difference (P<0.05). n.s. non-significant. Hygromycin-resistant T1 seedlings demonstrating n.s. difference to Mendelian 3:1 segregation ratio were used for the drought- and salt-stress experiments.

			Observed		Expected (3:1)			
Transgenic	**Event**	**No. of seeds plated**	**Hyg^R**	**Hyg^S**	**Hyg^R**	**Hyg^S**	**χ^2**	**Significance**
SD18-1	E1	33	26	7	24.75	8.25	0.25	n.s.
SD18-1	E2	33	12	21	24.75	8.25	26.27	*
SD18-1	E5	33	25	8	24.75	8.25	0.01	n.s.
SD9-2	E2	34	25	9	25.50	8.50	0.04	n.s.
SD9-2	E4	35	27	8	26.25	8.75	0.09	n.s.
SD9-2	E6	33	21	12	24.75	8.25	2.27	n.s.
SD9-2	E7	33	25	8	24.75	8.25	0.01	n.s.
SD9-3	E1	34	19	15	25.50	8.50	6.63	*
Neg	E2	34	28	6	25.50	8.50	0.98	n.s.
Neg	E4	32	24	8	24.00	8.00	1.61	n.s.
Neg	E5	35	24	11	26.25	8.75	0.77	n.s.

Table 4 Red fluorescence values in counts per second (CPS) between mock and treatment groups taken before imposing drought-stress. Values are the mean ± standard error (SE) (n = 3 transgenic plants per event, each plant consisted of independent measurements of the 3 youngest leaves from the main tiller). *significant difference in red fluorescence (CPS) between the mock and treatment groups determined by mixed model analysis of variance ($P<0.05$). n.s. = no significant difference in red fluorescence (CPS) between the mock and treatment.

Transgenic event	Red fluorescence (CPS)				
	Treatment	± SE	Mock	± SE	Significance
SD18-1 event 1	57417.00	12347.00	45297.00	12209.00	n.s.
SD18-1 event 5	57597.00	12224.00	55295.00	12451.00	n.s.
SD9-2 event 2	38061.00	2386.13	40977.00	2752.84	n.s.
SD9-2 event 4	38708.00	3906.38	63376.00	3783.20	*
SD9-2 event 6	34417.00	2238.94	32946.00	2081.15	n.s.
SD9-2 event 7	58320.00	3128.87	58750.00	3547.81	n.s.
Neg event 2	51094.00	4799.55	35874.00	4735.61	n.s.
Neg event 4	29507.00	3034.70	25731.00	3131.24	n.s.
Neg event 5	12971.00	488.33	10142.00	430.67	*
WT	8337.12	144.63	6673.33	136.81	*

Table 5 Red fluorescence values in counts per second (CPS) between mock and treatment groups taken before imposing salt-stress. Values are the mean ± standard error SE (n = 3 transgenic plants per event, each plant consisted of independent measurements of the 3 youngest leaves from the main tiller). *significant difference in red fluorescence (CPS) between the mock and treatment groups determined by mixed model analysis of variance (P<0.05). n.s. = no significant difference in red fluorescence (CPS) between the mock and treatment.

Transgenic event	Red fluorescence (CPS)				
	Salt stress	± SE	Mock	± SE	Significance
SD18-1 event 1	46957.00	10659.00	48509.00	10270	n.s.
SD18-1 event 5	42448.00	8606.21	52206.00	7330.7	n.s.
SD9-2 event 2	37772.00	2079.78	42224.00	2325.27	n.s.
SD9-2 event 4	40180.00	8205.68	59947.00	8106.81	n.s.
SD9-2 event 6	40253.00	5193.72	32946.00	4924.1	n.s.
SD9-2 event 7	67566.00	5694.06	61883.00	5489.47	n.s.
Neg event 2	27361.00	4685.77	36110.00	4706.49	n.s.
Neg event 4	37601.00	4714.92	25696.00	4670.76	n.s.
Neg event 5	13836.00	1494.74	10142.00	1483.23	n.s.
WT	7906.81	145.33	6673.33	137.02	*

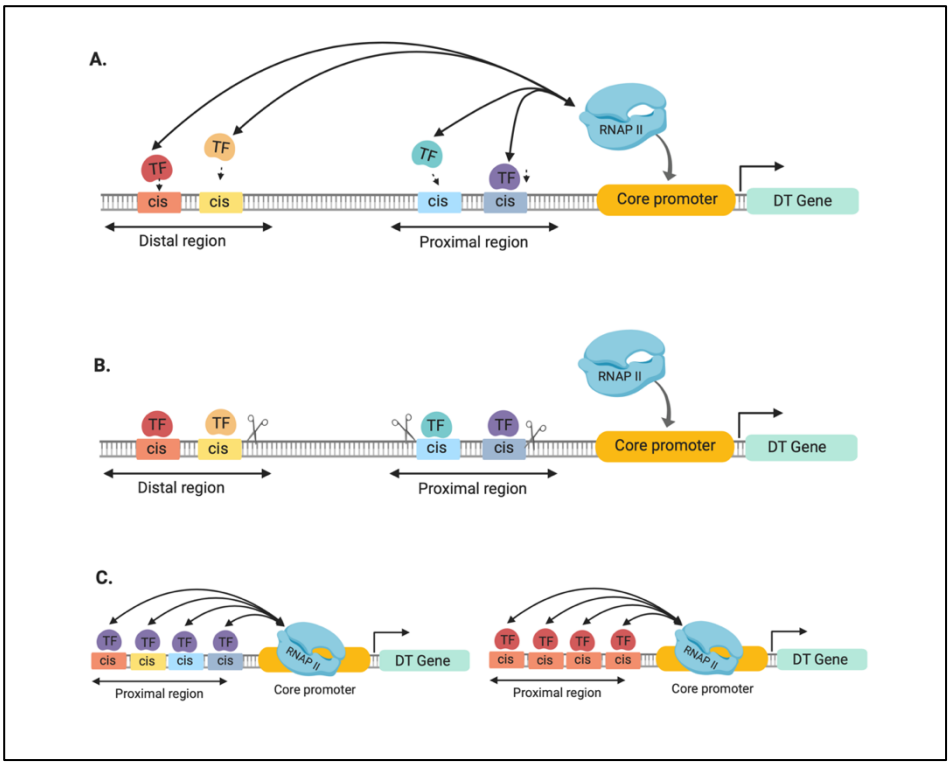

Figure 1 Schematic diagram comparing native and synthetic promoters. A. 500 bp to 2000 bp-long native promoters. Complex expression profile determined by binding of different transcription factors (TF) in *cis*-elements in the proximal and distal region. B. Designing short synthetic promoters by removing the spaces between *cis*-elements in the proximal and distal region. C. Building synthetic promoters for binding of specific transcription factors. Several (left) or similar (right) *cis*-motifs were fused with a core promoter. DT gene = drought tolerant gene (figure adapted from[54, 55];created with BioRender.com).

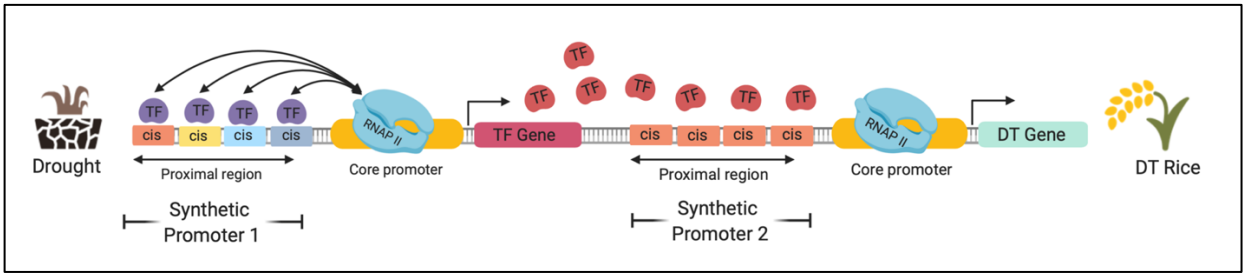

Figure 2 Stacking of multiple genes driven by different synthetic promoters to create drought-tolerant (DT) rice. In the onset of drought, specific TFs (indigo) bind to synthetic promoter 1 expressing a TF-coding gene. Subsequently, desired TFs (red) are produced and bind to synthetic promoter 2 expressing a drought-tolerant gene. (figure created with BioRender.com)

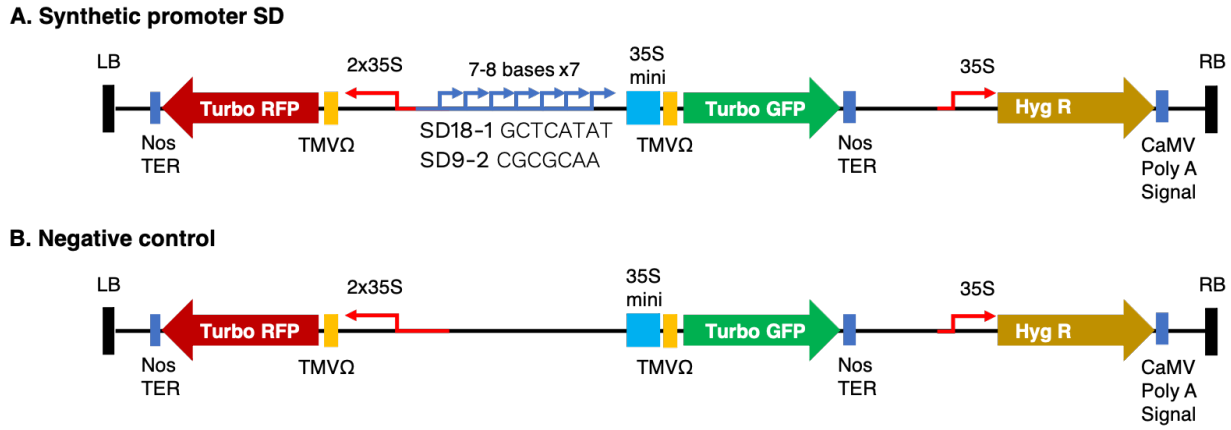

Figure 3 Synthetic promoter constructs. Binary vectors contained a series of synthetic promoters (SD-series) fused to Turbo GFP. The core promoter sequence for synthetic promoters was the -46 35S promoter with the TMV Ω 5' UTR leader sequence for transcriptional initiation. Vectors also contained a 35S::RFP reporter cassette that served as an internal positive control. The synthetic *cis*-regulatory elements were composed of either 8 (SD18-1) or 7 base pairs (SD9-2) repeated 7 times. The negative (Neg) control construct (B) does not contain any *cis*-regulatory element[34] (figure adapted from[34]).

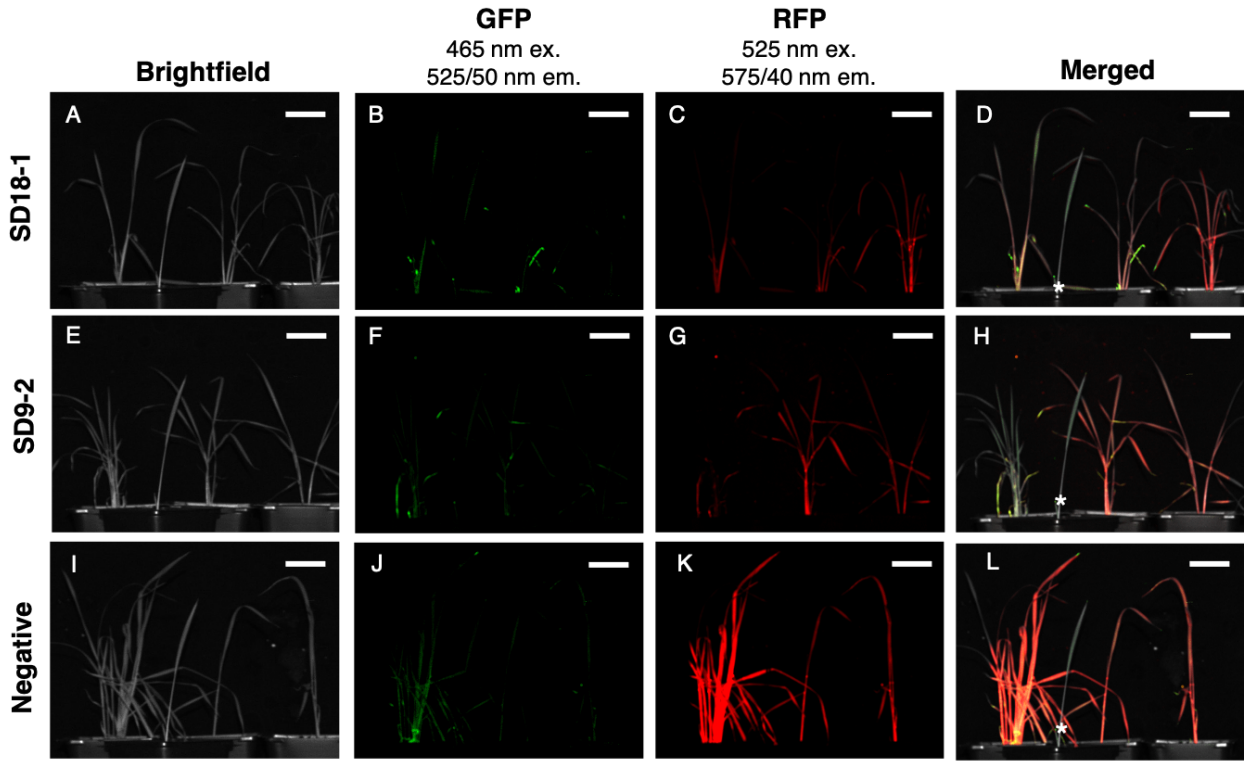

Figure 4 Fluorescence inducing laser projector images for visual confirmation of putative transgenic rice (T0) harboring the SD18-1 (A-D), SD9-2 (E-H), and Neg (I-L) constructs. The images were taken in putative transgenic T0 rice without stress imposition. The same WT was used for all images and is denoted in the merged image using a white asterisk. The WT cannot be observed in the GFP and RFP columns. The plants not indicated with an asterisk in each panel per row represent independent transgenic event per construct. Intense red fluorescence is observed in the transgenic events per construct. A background green fluorescence can be observed in some transgenic events of each construct. Laser power for both the 465 nm and 525 nm lasers was 1.4 W. Images were acquired using a camera exposure time of 300 ms from a distance of 3 meters. Scale bars represent 5 cm.

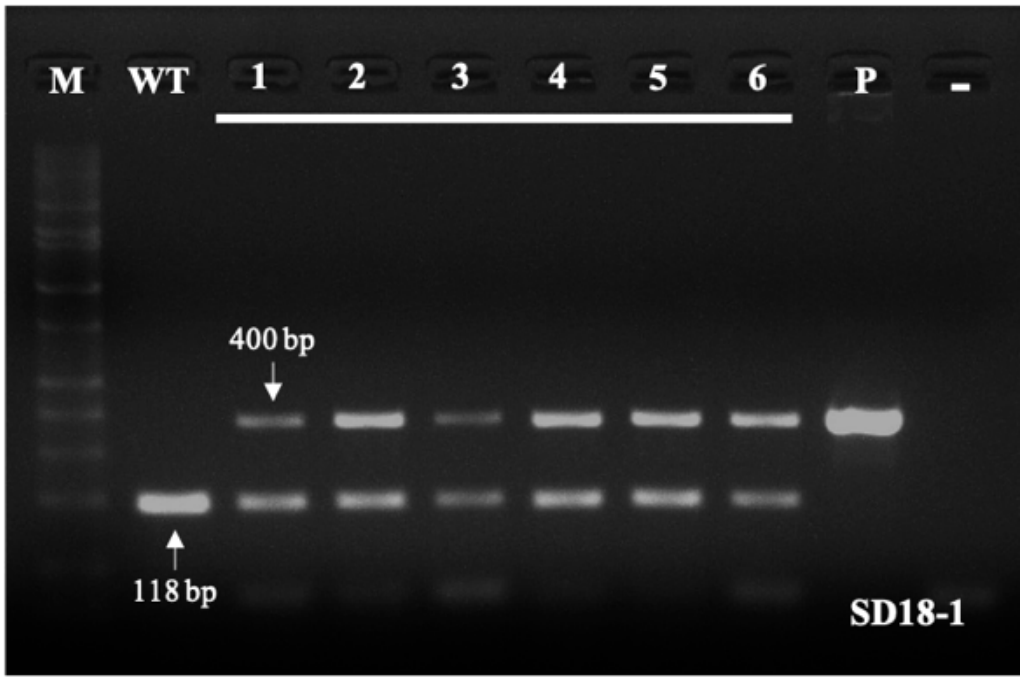

Figure 5 Confirmation by genomic PCR for Taipei 309 rice harboring the SD18-1construct. Genomic DNA was isolated from wild-type (WT) and putative transgenic rice plants. Genomic DNA sample was used for PCR in the presence of *TurboGFP* (400 bp), and *OsAct1* (118 bp)-specific primers. M marker; - blank; WT wild-type; P positive control (Pest#12 plasmid harboring *TurboGFP* gene). The numbers for each lane represent an independent transgenic event.

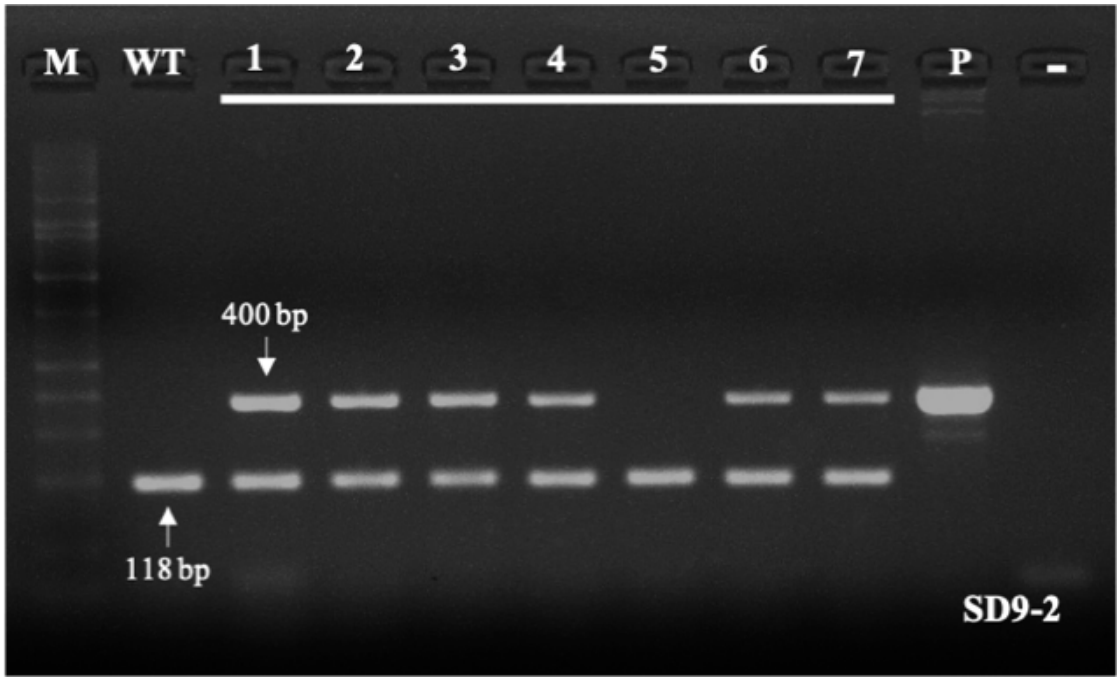

Figure 6 Confirmation by genomic PCR for Taipei 309 rice harboring the SD9-2 construct. Genomic DNA was isolated from wild-type (WT) and putative transgenic rice plants. Genomic DNA sample was used for PCR in the presence of *TurboGFP* (400 bp), and *OsAct1* (118 bp) specific primers. M marker; - blank; WT wild-type; P positive control (Pest#12 plasmid harboring *TurboGFP* gene). The numbers for each lane represent an independent transgenic event.

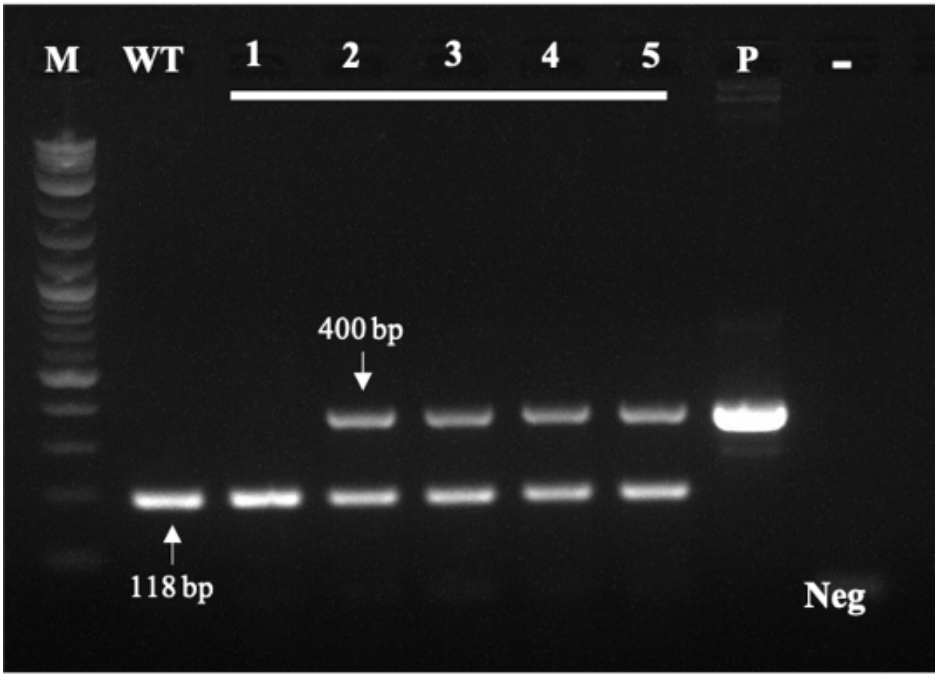

Figure 7 Confirmation by genomic PCR for Taipei 309 rice harboring the Neg. Genomic DNA was isolated from wild-type (WT) and putative transgenic rice plants. Genomic DNA sample was used for PCR in the presence of *TurboGFP* (400 bp), and *OsAct1* (118 bp) specific primers. M marker; - blank; WT wild-type; P positive control (Pest#12 plasmid harboring *TurboGFP* gene). The numbers for each lane represent an independent transgenic event.

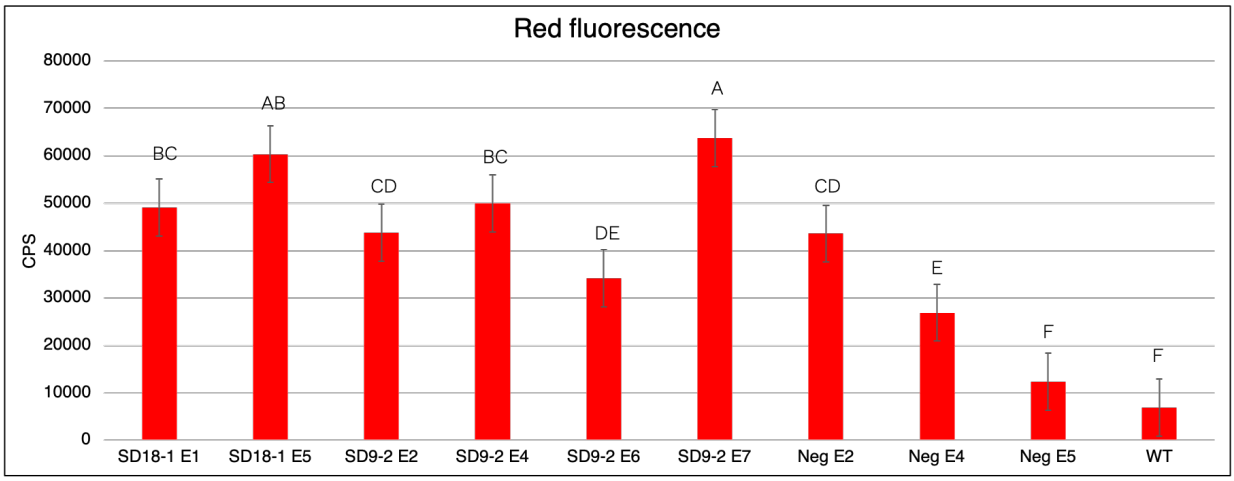

Figure 8 Red fluorescence values in counts per second (CPS) of each of the SD18-1, SD9-2, and Neg transgenic events tested for the drought-stress experiment. Red fluorescence intensity values were measured at 572 nm under a fixed excitation wavelength of 540 nm before drought-stress treatment. Values are the mean ± standard error (SE) (n = 6 transgenic plants per event, each plant consisted of independent measurements of the 3 youngest leaves from the main tiller). From the 6 transgenic plants of each transgenic event, three transgenic plants were randomly assigned to either the drought-stress treatment and mock control groups (Table 3). Different letters above error bars represent significant differences among red fluorescence means determined by mixed-model analysis of variance (Fisher's LSD $P<0.05$). Event 5 of the transgenic rice harboring the Neg construct (Neg E5), having similar letter grouping with the wild-type (WT), was not included in subsequent analyses.

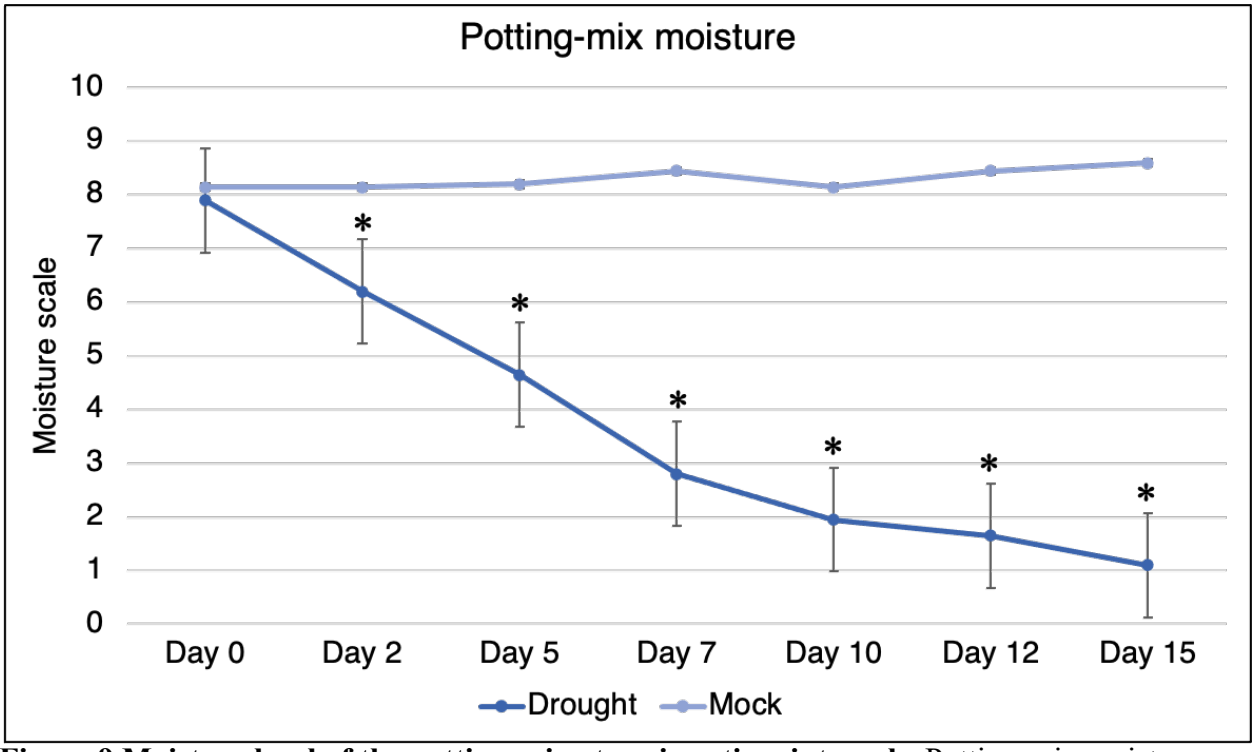

Figure 9 Moisture level of the potting-mix at various time intervals. Potting-mix moisture was measured in a scale of 1-10 using an analog soil moisture meter at various time intervals until complete leaf rolling was observed in drought-stress treated rice (day 15). Moisture scale levels 1-3 = dry, 4-7 = normal, 8-10 = wet. Values are the mean ± standard error (SE). One potting-mix moisture measurement was performed in 11 cm deep square pot per transgenic event (SD18-1 events 1 and 5; SD9-2 events 2, 4, 6, and 7; Neg events 2 and 4) and WT control. n = 9 total potting-mix moisture measurement for mock control and drought-stress treatment each time point. Day 0 was the last day the plants under drought-stress treatment submerged in 6 cm deep water. Mock control consisted of plant pots submerged in 6 cm deep de-ionized (DI) water. The asterisks represent significant difference between mock and drought-stress treatment soil moisture scale values for each time point, according to mixed model analysis of variance (P<0.05).

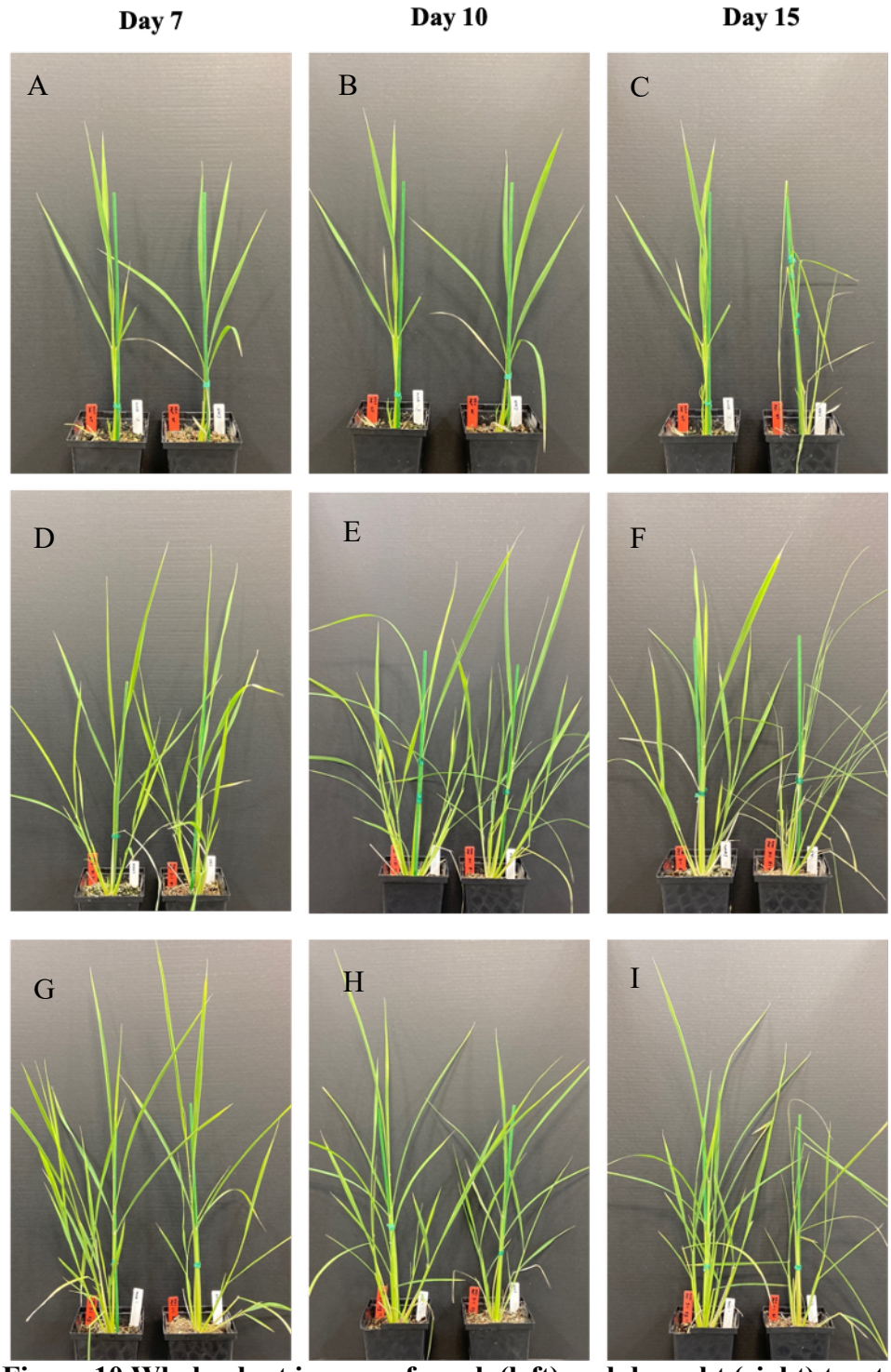

Figure 10 Whole plant images of mock (left) and drought (right) treated rice after 7-, 10-, and 15 days of water cessation. Mock control group were submerged in 6 cm deep deionized water. Wild-type (WT) (A-C) and transgenic rice SD18-1 event 1 (D-F) and SD18-1 event 5 (G-I). Significant leaf-rolling was observed in drought-stress treated rice after 15 days.

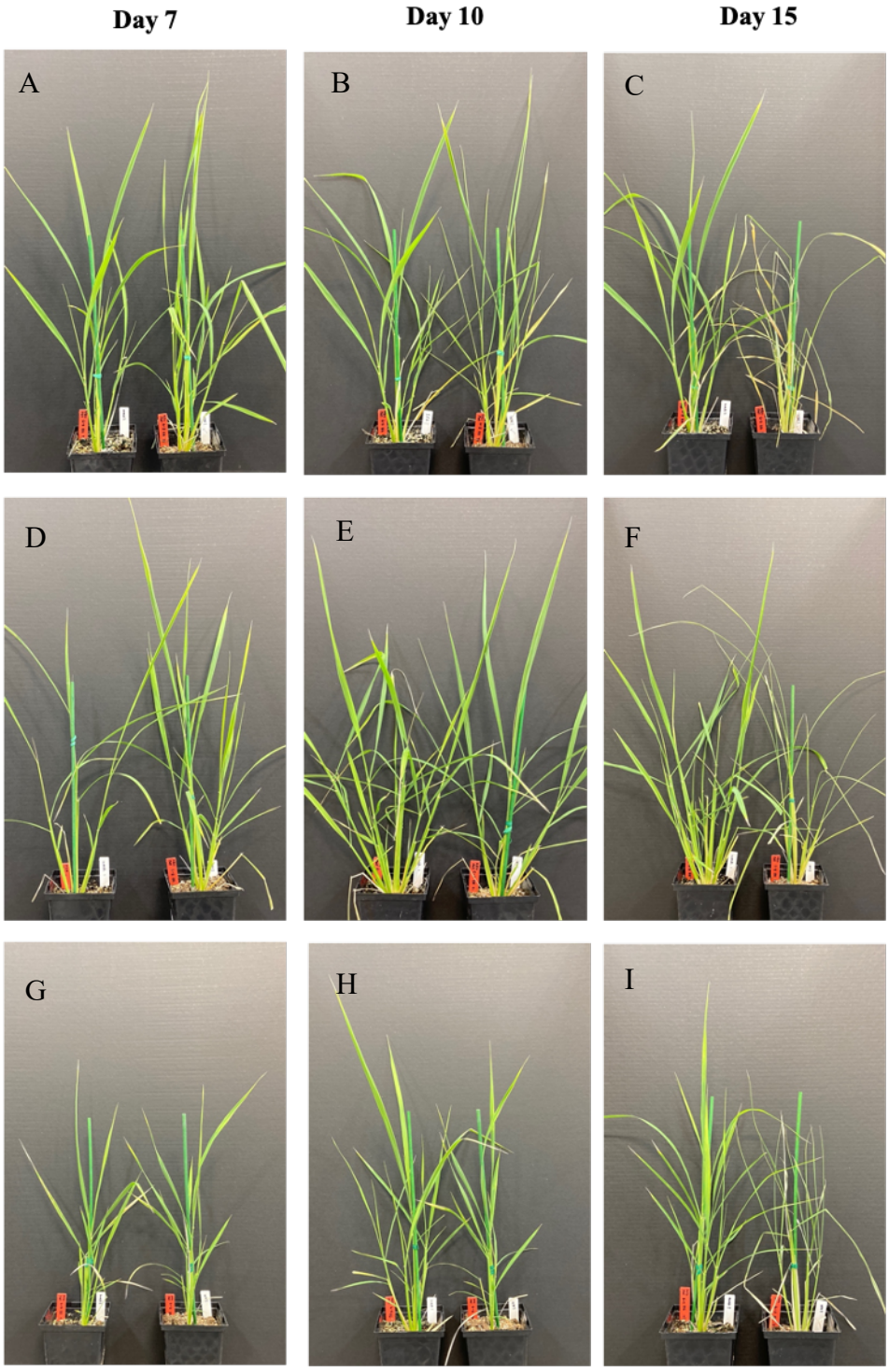

Figure 11 Whole plant images of mock (left) and drought (right) treated rice after 7-, 10-, and 15 days of water cessation. Mock control group were submerged in 6 cm deep deionized water. Transgenic rice SD9-2 event 2 (A-C), SD9-2 event 4 (D-F), and SD9-2 event 6 (G-I). Significant leaf-rolling was observed in drought-stress treated rice after 15 days.

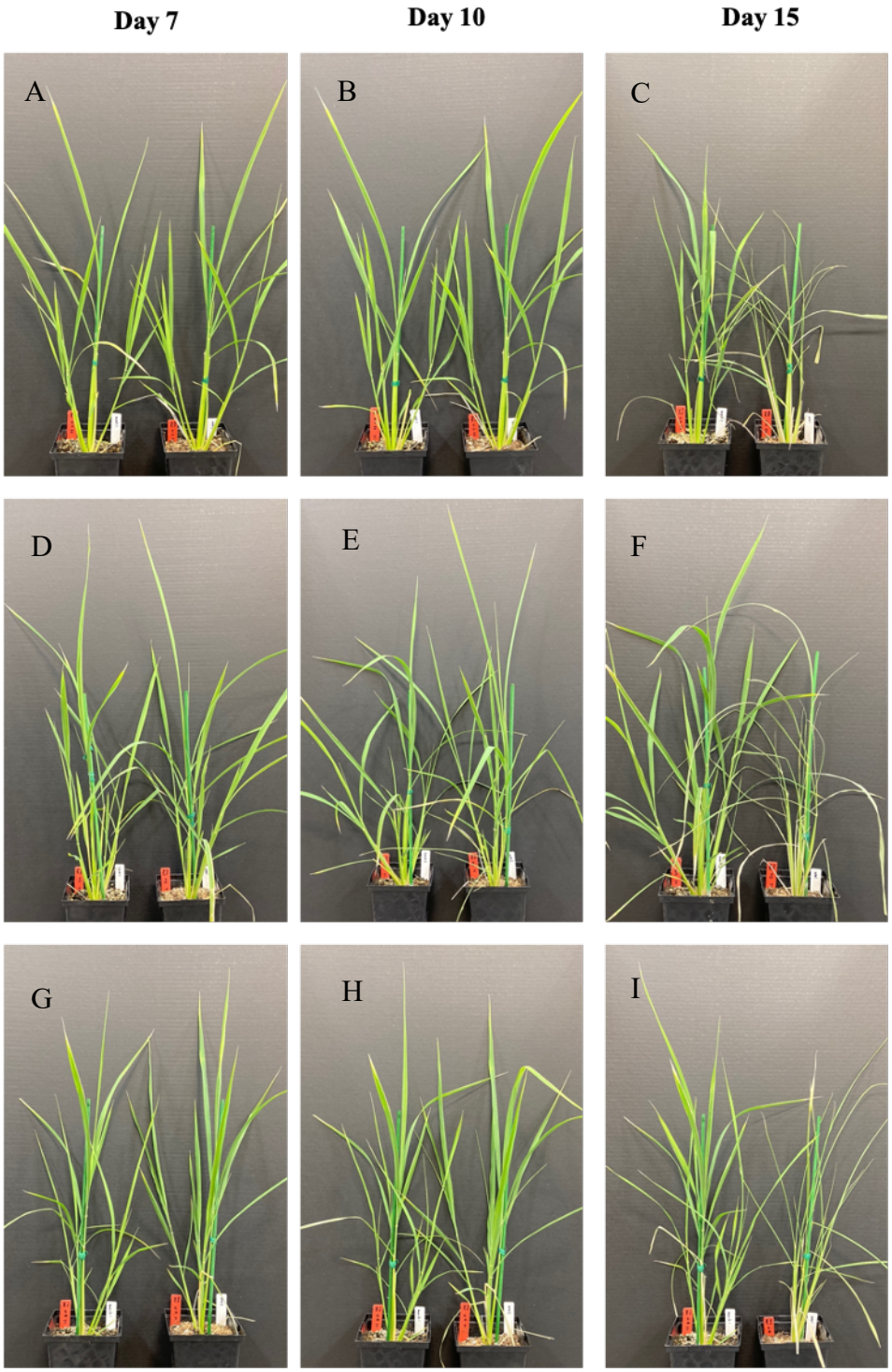

Figure 12 Whole plant images of mock (left) and drought (right) treated rice after 7-, 10-, and 15 days of water cessation. Mock control group were submerged in 6 cm deep deionized water. Transgenic rice SD9-2 event 7 (A-C), Neg event 2 (D-F), and Neg event 4 (G-I). Significant leaf-rolling was observed in drought-stress treated rice after 15 days.

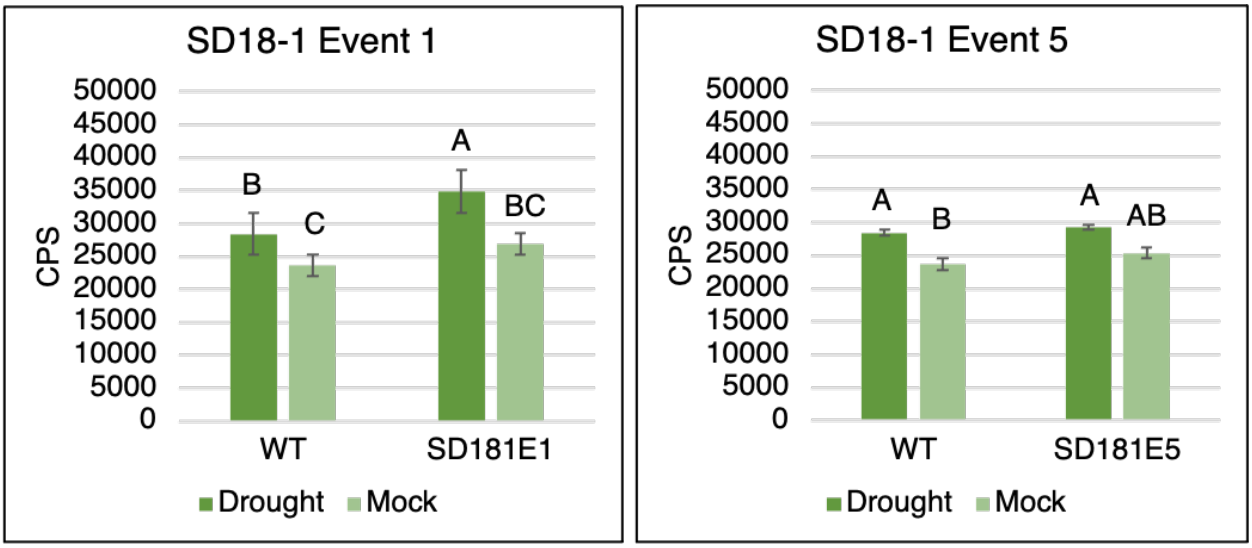

Figure 13 Green fluorescence values in counts per second (CPS) between mock and drought-treated SD18-1 transgenic rice events versus the WT control. Green fluorescence values were measured at 502 nm under a fixed excitation wavelength of 465 nm after 15 days of water-cessation. Mock control consisted of plant pots submerged in 6 cm deep de-ionized (DI) water. Values are the mean ± standard error (SE). n = 3 transgenic plants per event per mock control and drought-stress treatment group, each plant consisted of independent measurements of the 3 youngest leaves from the main tiller. Different letters above error bars represent significant differences in green fluorescence values determined by mixed-model analysis of variance (Fisher's LSD $P<0.05$).

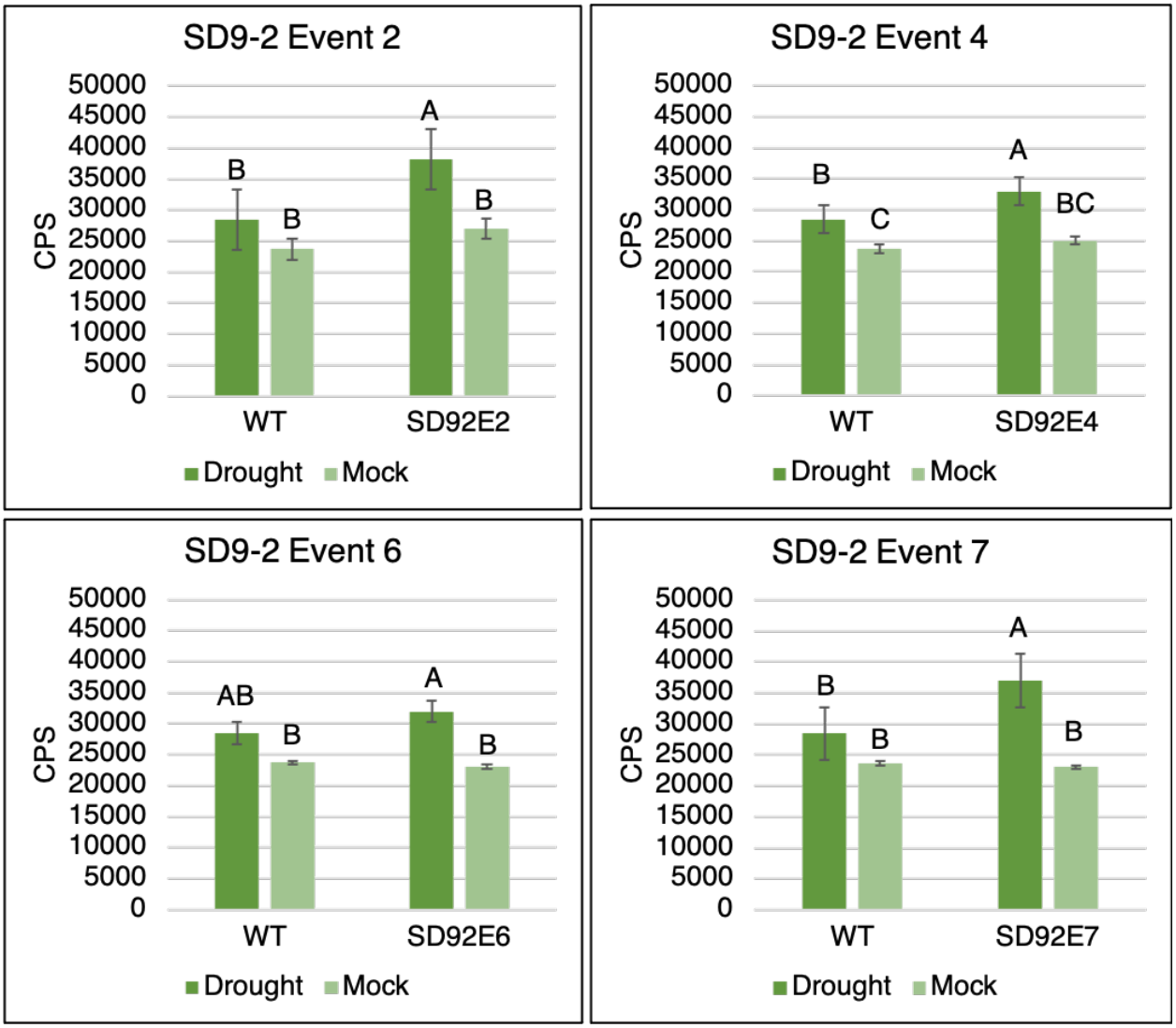

Figure 14 Green fluorescence values in counts per second (CPS) between mock and drought-treated SD9-2 transgenic rice events versus the WT control. Green fluorescence values were measured at 502 nm under a fixed excitation wavelength of 465 nm after 15 days of water-cessation. Mock control consisted of plant pots submerged in 6 cm deep de-ionized (DI) water. Values are the mean ± standard error (SE). n = 3 transgenic plants per event per mock control and drought-stress treatment group, each plant consisted of independent measurements of the 3 youngest leaves from the main tiller. Different letters above error bars represent significant differences in green fluorescence values determined by mixed-model analysis of variance (Fisher's LSD $P<0.05$).

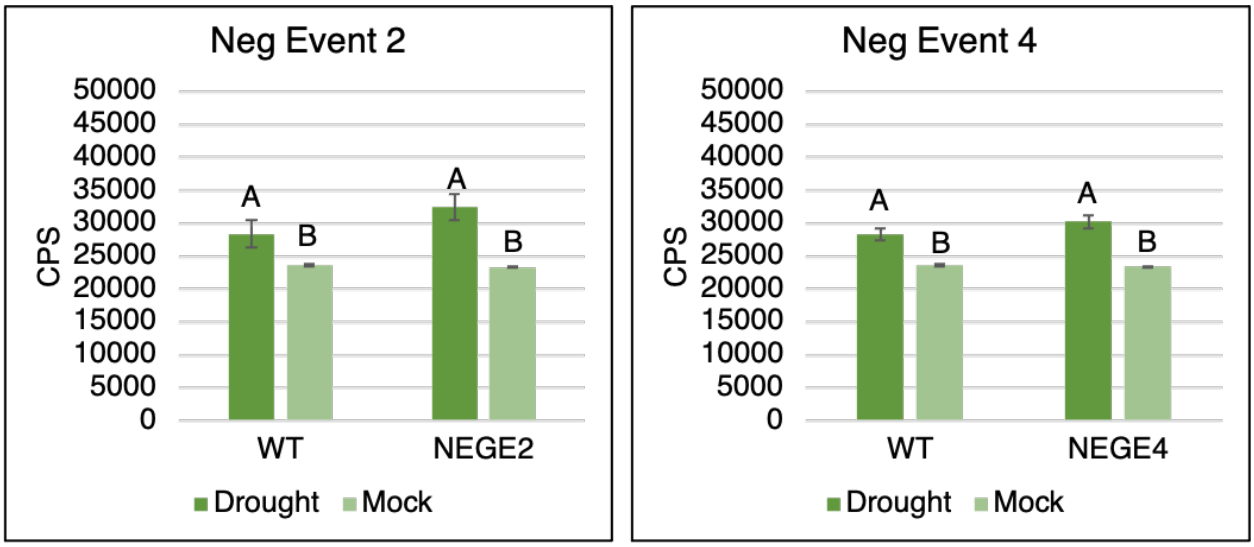

Figure 15 Green fluorescence values in counts per second (CPS) between mock and drought-treated Neg transgenic rice events versus the WT control. Green fluorescence values were measured at 502 nm under a fixed excitation wavelength of 465 nm after 15 days of water-cessation. Mock control consisted of plant pots submerged in 6 cm deep de-ionized (DI) water. Values are the mean ± standard error (SE). n = 3 transgenic plants per event per mock control and drought-stress treatment group, each plant consisted of independent measurements of the 3 youngest leaves from the main tiller. Different letters above error bars represent significant differences in green fluorescence values determined by mixed-model analysis of variance (Fisher's LSD $P<0.05$).

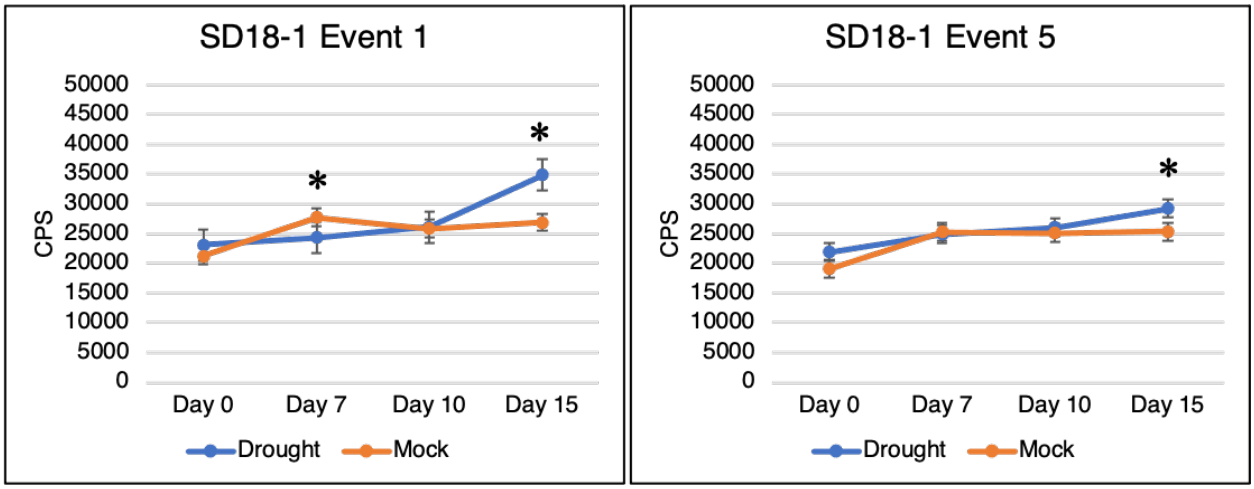

Figure 16 Green fluorescence values (CPS) between mock and drought-treated transgenic SD18-1 rice at various time points of drought-stress treatment. Green fluorescence values were measured at 502 nm under a fixed excitation wavelength of 465 nm. Values are the mean ± standard error (SE). n = 3 transgenic plants per event per mock control and drought-stress treatment group for each time point, each plant consisted of independent measurements of the 3 youngest leaves from the main tiller. Day 0 was the last day the plants under drought-stress treatment submerged in 6 cm deep water. Mock control consisted of plant pots submerged in 6 cm deep de-ionized (DI) water. Asterisks represent significant differences in green fluorescence between mock and drought-stress treated rice for each time point, determined by mixed-model analysis of variance ($P<0.05$).

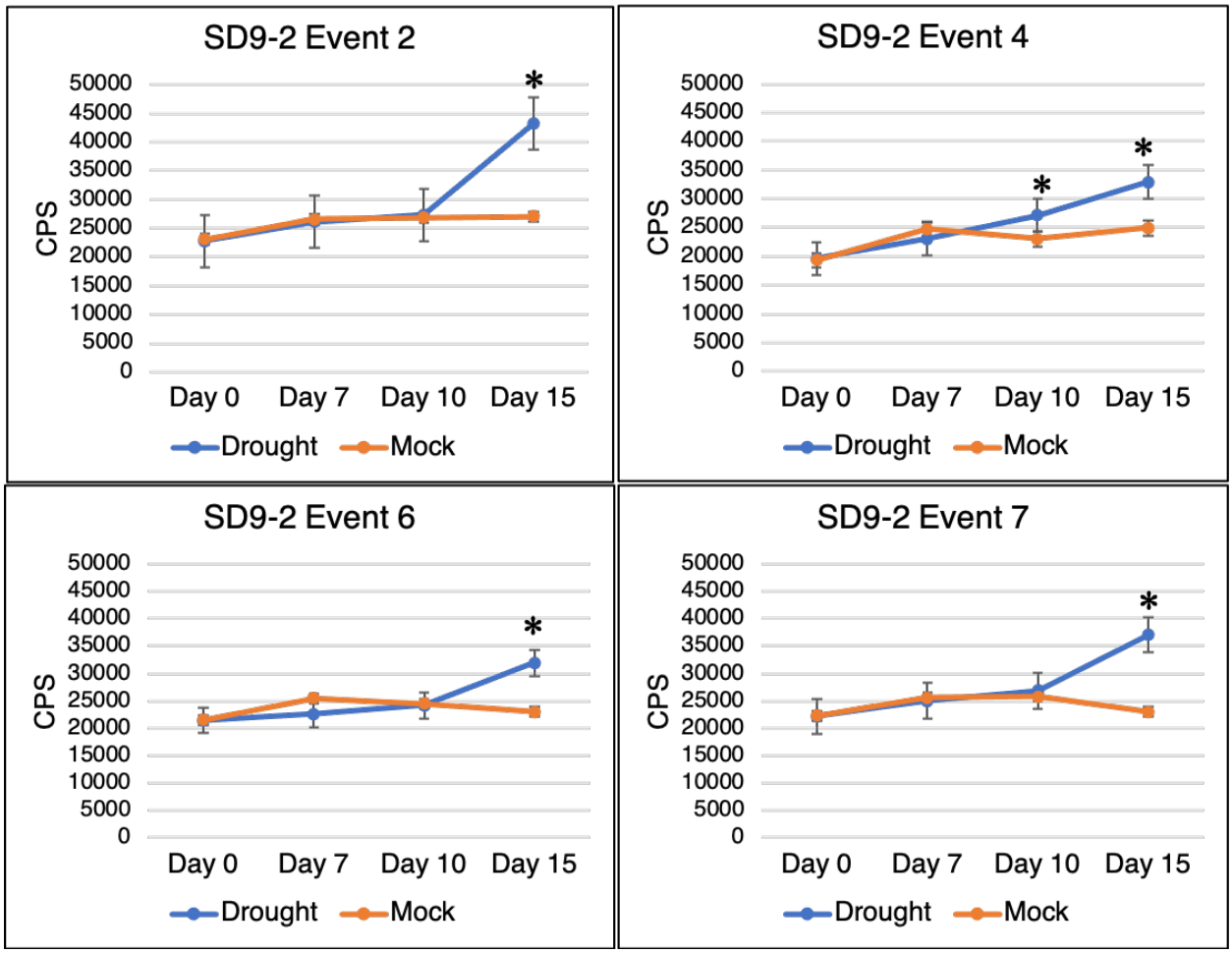

Figure 17 Green fluorescence values (CPS) between mock and drought-treated transgenic SD9-2 rice at various time points of drought-stress treatment. Green fluorescence values were measured at 502 nm under a fixed excitation wavelength of 465 nm. Values are the mean ± standard error (SE). n = 3 transgenic plants per event per mock control and drought-stress treatment group for each time point, each plant consisted of independent measurements of the 3 youngest leaves from the main tiller. Day 0 was the last day the plants under drought-stress treatment submerged in 6 cm deep water. Mock control consisted of plant pots submerged in 6 cm deep de-ionized (DI) water. Asterisks represent significant differences in green fluorescence between mock and drought-stress treated rice for each time point, determined by mixed-model analysis of variance ($P<0.05$).

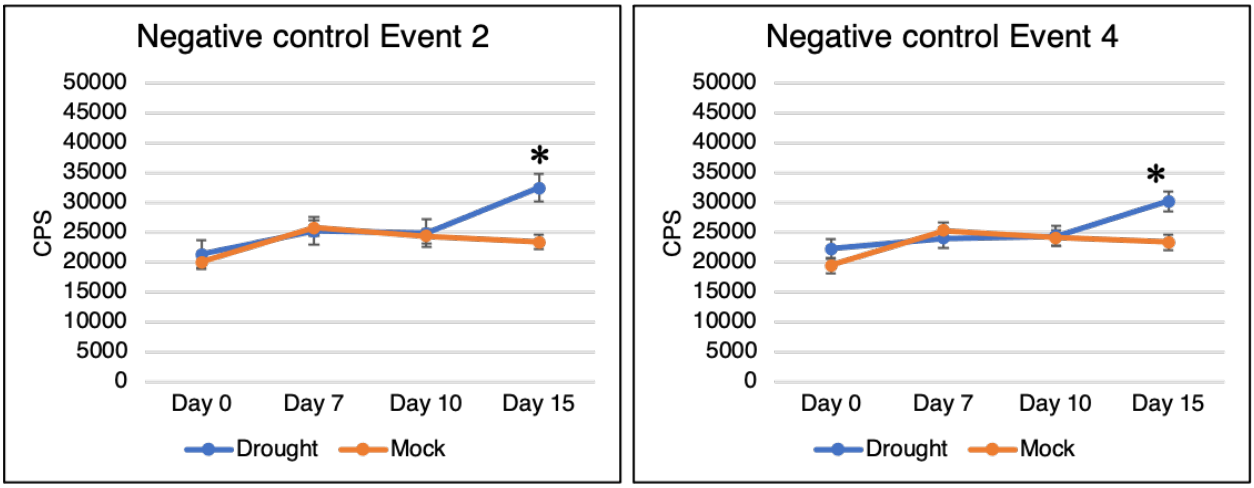

Figure 18 Green fluorescence values (CPS) between mock and drought-treated transgenic Neg rice at various time points of drought-stress treatment. Green fluorescence values were measured at 502 nm under a fixed excitation wavelength of 465 nm. Values are the mean ± standard error (SE). n = 3 transgenic plants per event per mock control and drought-stress treatment group for each time point, each plant consisted of independent measurements of the 3 youngest leaves from the main tiller. Day 0 was the last day the plants under drought-stress treatment submerged in 6 cm deep water. Mock control consisted of plant pots submerged in 6 cm deep de-ionized (DI) water. Asterisks represent significant differences in green fluorescence between mock and drought-stress treated rice for each time point, determined by mixed-model analysis of variance ($P<0.05$).

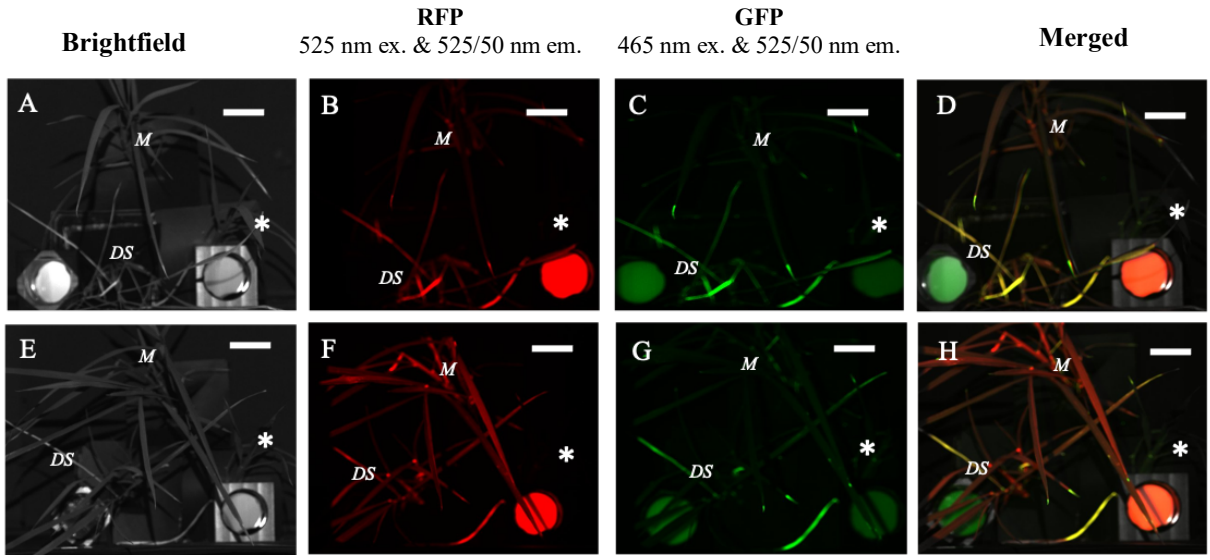

Figure 19 Fluorescence inducing laser projector images of transgenic rice (T1) harboring the SD18-1 construct event 1 (A-D) and event 5 (E-H)) taken after 15 days of drought-stress treatment. The same WT was used for all images and is denoted by a white asterisk; mock control denoted by M and drought-stress treated transgenic rice identified by DS. The transgenic rice samples had high red fluorescence intensity as observed in the RFP column. Transgenic rice under drought-stress had higher green fluorescence intensity than the mock and WT controls as observed in the GFP column. Laser power for both the 465 nm and 525 nm lasers was 1.4 W power. Images were acquired using a camera exposure time of 300 ms from a distance of 3 meters. Scale bars represent 5 cm. The round components are fluorescence standards (left: blue wavelength standard USFS-200-020; right: orange wavelength standard USFS-336-020).

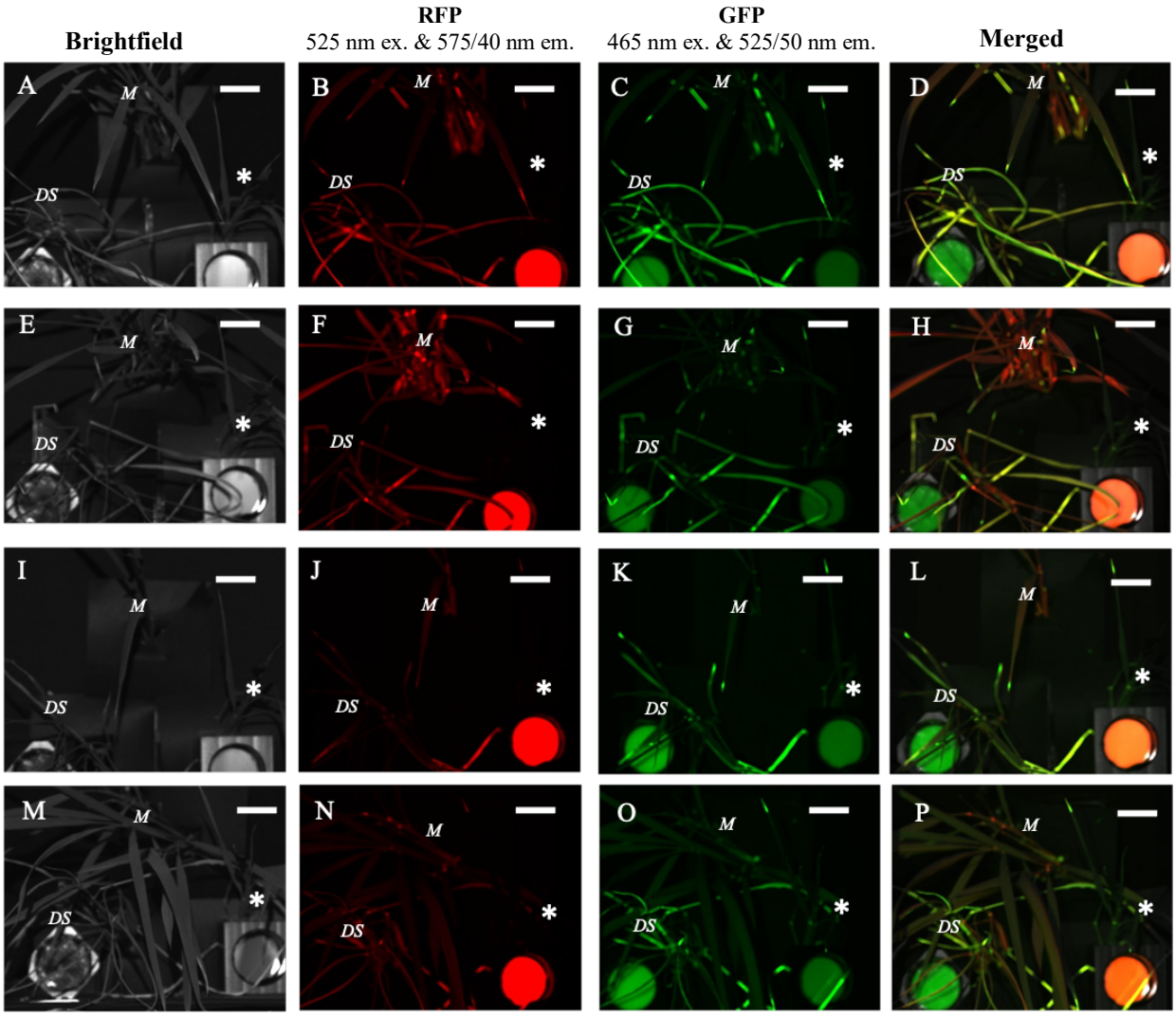

Figure 20 Fluorescence inducing laser projector images of transgenic rice harboring the SD9-2 construct(event 2 (A-D), event 4 (E-H), event 6 (I-L), and event 7 (M-P)) taken after 15 days of drought-stress treatment. The same WT was used for all images and is denoted by a white asterisk; mock control denoted by M and drought-stress treated transgenic rice identified by DS. The transgenic rice samples had high red fluorescence intensity as observed in the RFP column. Transgenic rice under drought-stress had higher green fluorescence intensity than the mock and WT controls as observed in the GFP column. Laser power for both the 465 nm and 525 nm lasers was 1.4 W power. Images were acquired using a camera exposure time of 300 ms from a distance of 3 meters. Scale bars represent 5 cm. The round components are fluorescence standards (left: blue wavelength standard USFS-200-020; right: orange wavelength standard USFS-336-020).

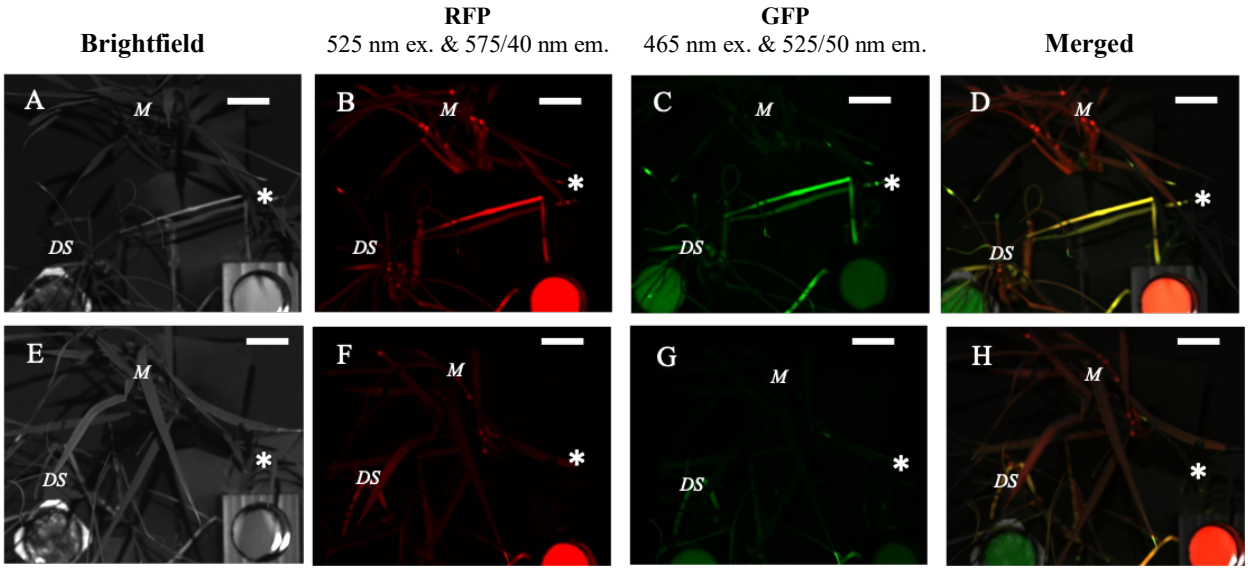

Figure 21 Fluorescence inducing laser projector images of transgenic rice harboring the Neg construct (event 2 (A-D) and event 4 (E-H)) taken after 15 days of drought-stress treatment. The same WT was used for all images and is denoted by a white asterisk; mock control denoted by M and drought-stress treated transgenic rice identified by DS. The transgenic rice samples had high red fluorescence intensity as observed in the RFP column. Transgenic rice under drought-stress had similar green fluorescence intensity with the mock and WT controls as observed in the GFP column. Laser power for both the 465 nm and 525 nm lasers was 1.4 W power. Images were acquired using a camera exposure time of 300 ms from a distance of 3 meters. Scale bars represent 5 cm. The round components are fluorescence standards (left: blue wavelength standard USFS-200-020; right: orange wavelength standard USFS-336-020).

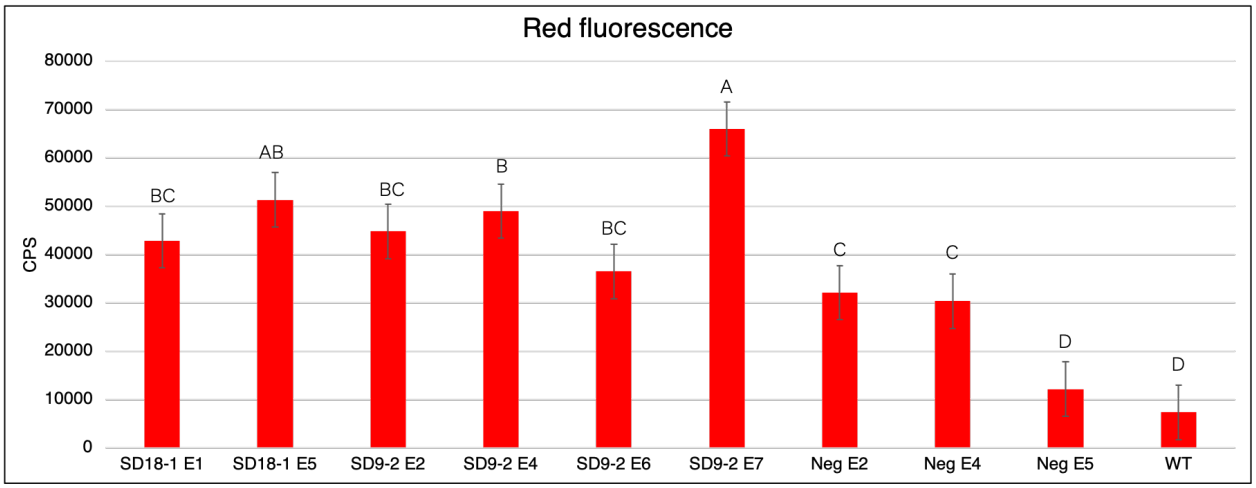

Figure 22 Red fluorescence values in counts per second (CPS) of each of the SD18-1, SD9-2, and Neg transgenic events tested for the salt-stress experiment. Red fluorescence intensity values were measured at 572 nm under a fixed excitation wavelength of 540 nm before salt-stress treatment. Values are the mean ± standard error (SE) (n = 6 transgenic plants per event, each plant consisted of independent measurements of the 3 youngest leaves from the main tiller). From the 6 transgenic plants of each transgenic event, three transgenic plants were randomly assigned to either the salt-stress treatment and mock control groups (Table 3). Different letters above error bars represent significant differences among red fluorescence means determined by mixed-model analysis of variance (Fisher's LSD $P<0.05$). Event 5 of the transgenic rice harboring the Neg construct (Neg E5), having similar letter grouping with the wild-type (WT), was not included in subsequent analyses.

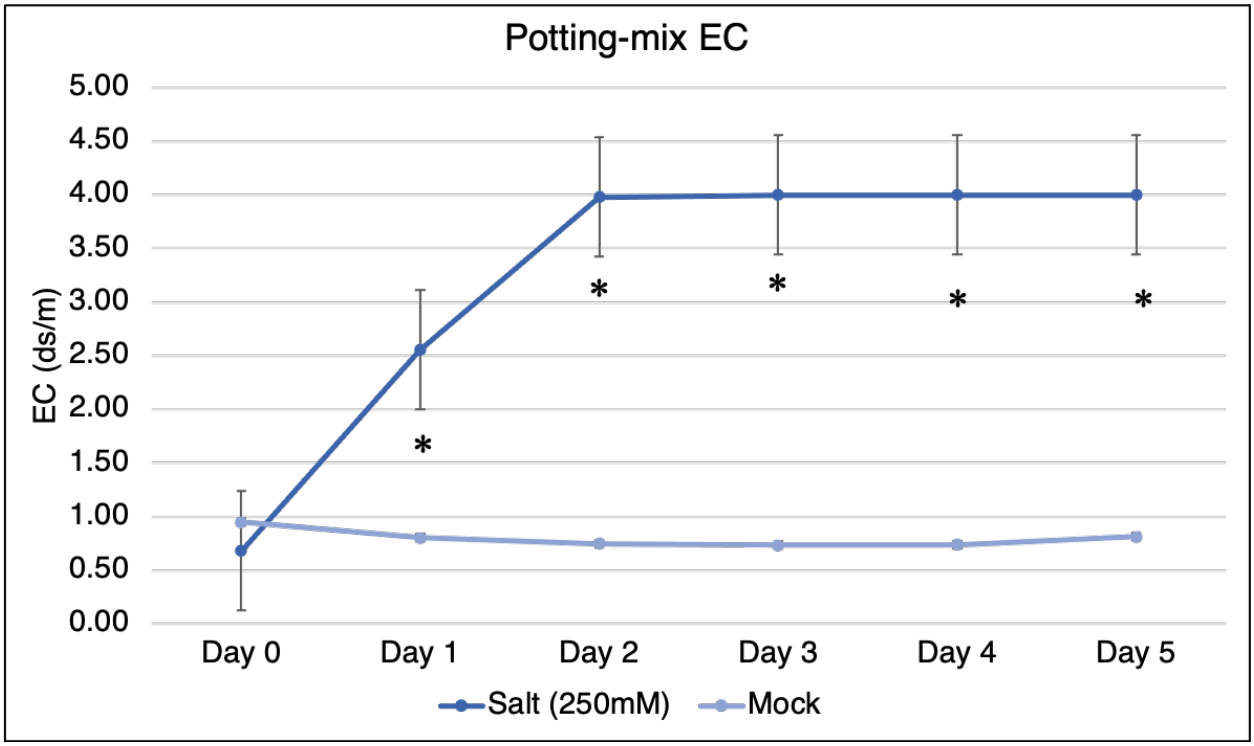

Figure 23 Potting-mix electrical conductivity (EC) between mock control and salt-stress treated pots at various time intervals. Potting-mix EC (dS/m) was measured daily until leaf-tip burning was observed (day 5). Values are the mean ± standard error (SE). Potting-mix EC measurement was performed in 11 cm deep square pot using a soil EC meter. Three independent pot measurements per transgenic event (SD18-1 events 1 and 5; SD9-2 events 2, 4, 6, and 7; Neg events 2 and 4) and WT control were performed. n = 27 total potting-mix EC measurement per mock control and salt-stress treatment per time point. Starting on day 0, EC was measured before applying 250 mL of 250 mM NaCl solution directly into the potting mix. After adding the salt solution into the potting mix for each day, the pots of plants under salt-stress treatment remained submerged in the salt solution collected in the containment tray of the said pots. The salt solution in the containment trays from the previous day's application was removed before applying the fresh salt solution directly into the potting mix. The last day of applying the salt solution is on day 4. Starting on day one until day 5, daily EC measurements are values obtained one day after applying the salt solution. Mock control consisted of plant pots submerged in 6 cm deep de-ionized (DI) water. The asterisks represent a significant difference between mock and salt-stress treatment means for each time point, according to mixed model analysis of variance ($P<0.05$).

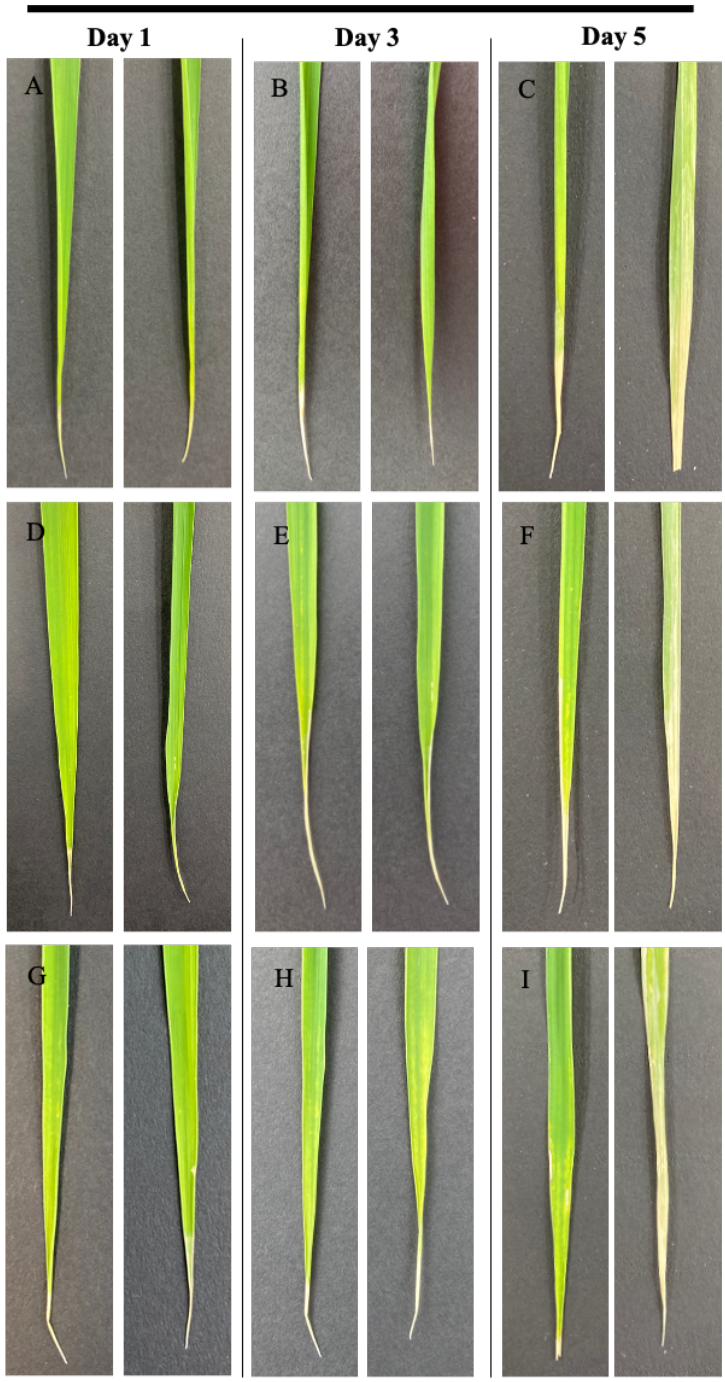

Figure 24 Representative leaf images of mock (left) and salt-stress (right) treated rice after 1-, 3-, and 5 days of stress imposition. Salt-stress treatment consisted of applying 250 mM NaCl solution to each pot daily. Mock control had pots submerged in 6 cm deep de-ionized water. Wild-type (WT; A-C) and transgenic rice SD18-1 event 1 (D-F), and SD18-1 event 5 (G-I). Significant leaf-tip burning was observed in salt-stress treated rice after 5 days.

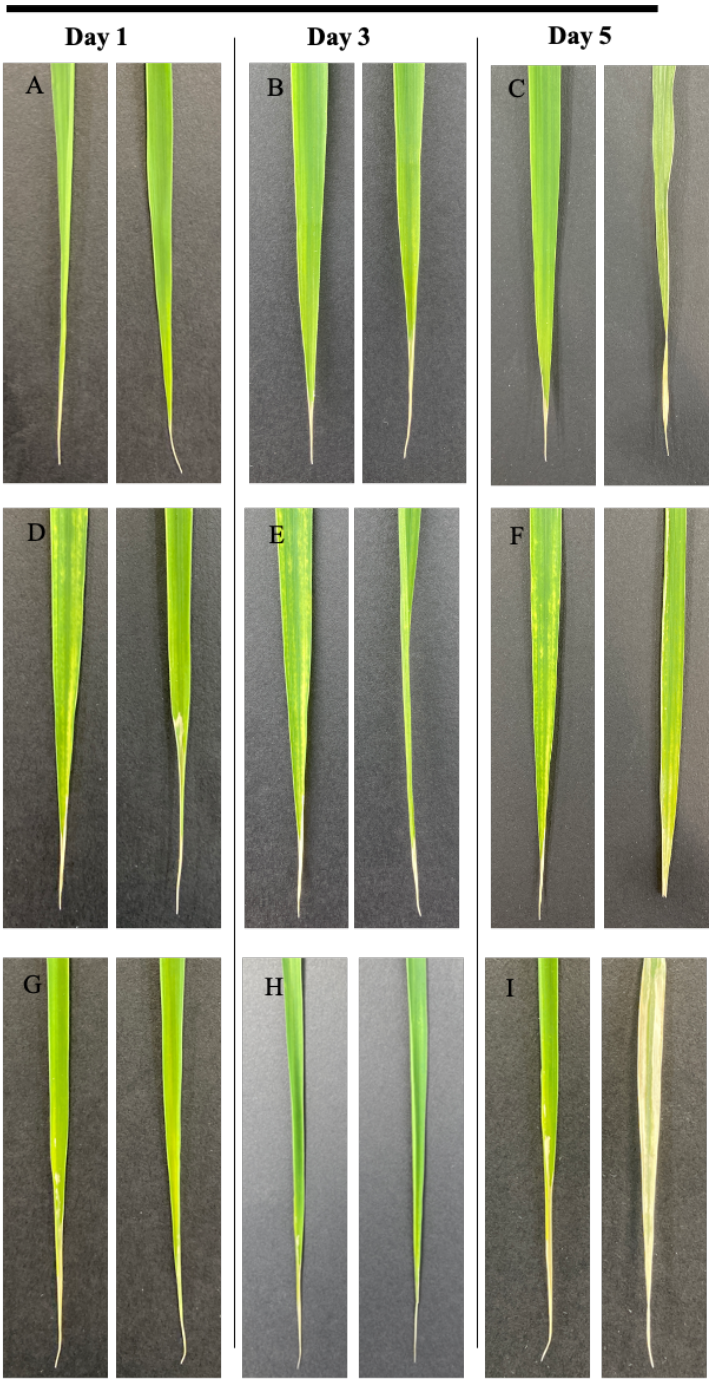

Figure 25 Third-leaf images of mock (left) and salt-stress (right) treated rice after 1-, 3-, and 5 days of stress imposition. Salt-stress treatment consisted of applying 250 mM NaCl solution to each pot daily. Mock control had pots submerged in 6 cm deep de-ionized water. Transgenic rice SD9-2 event 2 (A-C), SD9-2 event 4 (D-F), and SD9-2 event 6 (G-I). Significant leaf-tip burning was observed in salt-stress treated after 5 days.

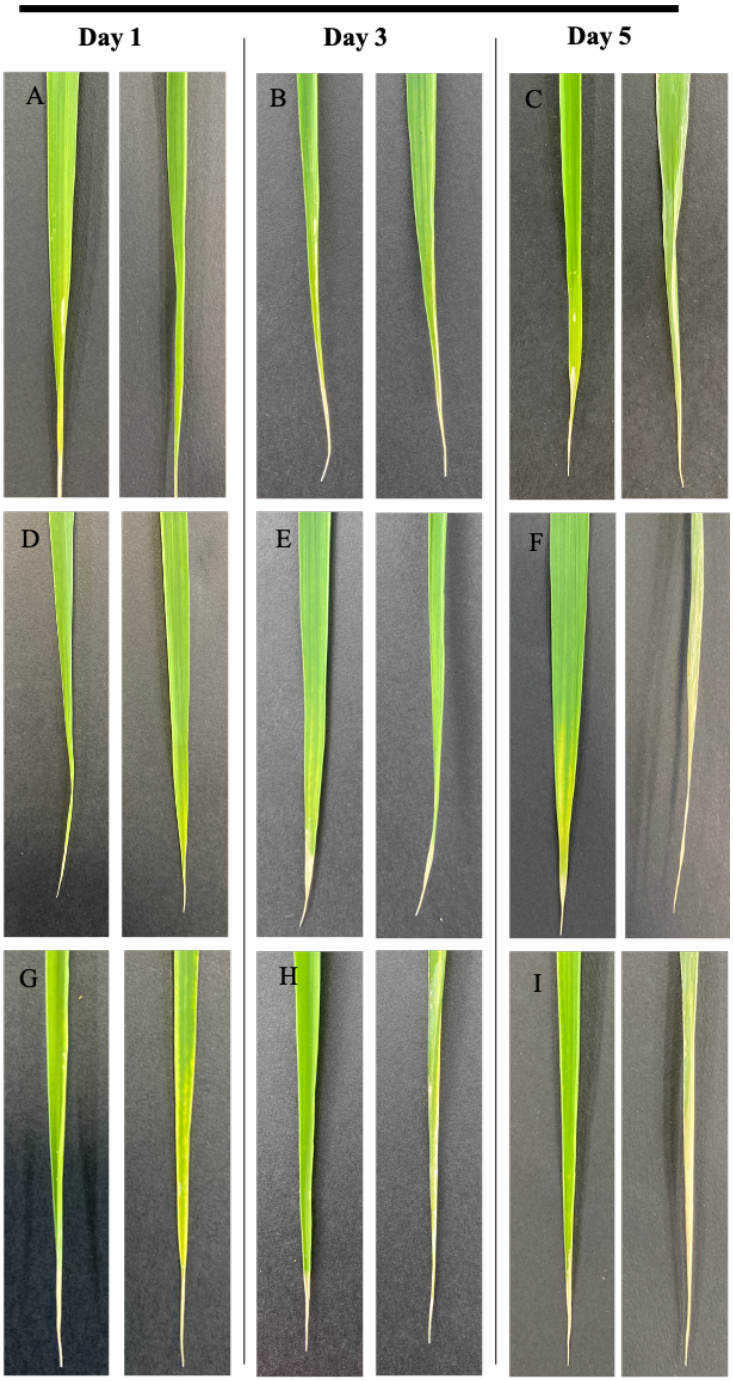

Figure 26 Third-leaf images of mock (left) and salt-stress (right) treated rice after 1-, 3-, and 5 days. Salt-stress treatment consisted of applying 250 mM NaCl solution to each pot daily. Mock control had pots submerged in 6 cm deep de-ionized water. Transgenic rice SD9-2 event 7 (A-C), Neg event 2 (D-F), and Neg event 4 (G-I). Significant leaf-tip burning was observed in salt-stress treated rice after 5 days.

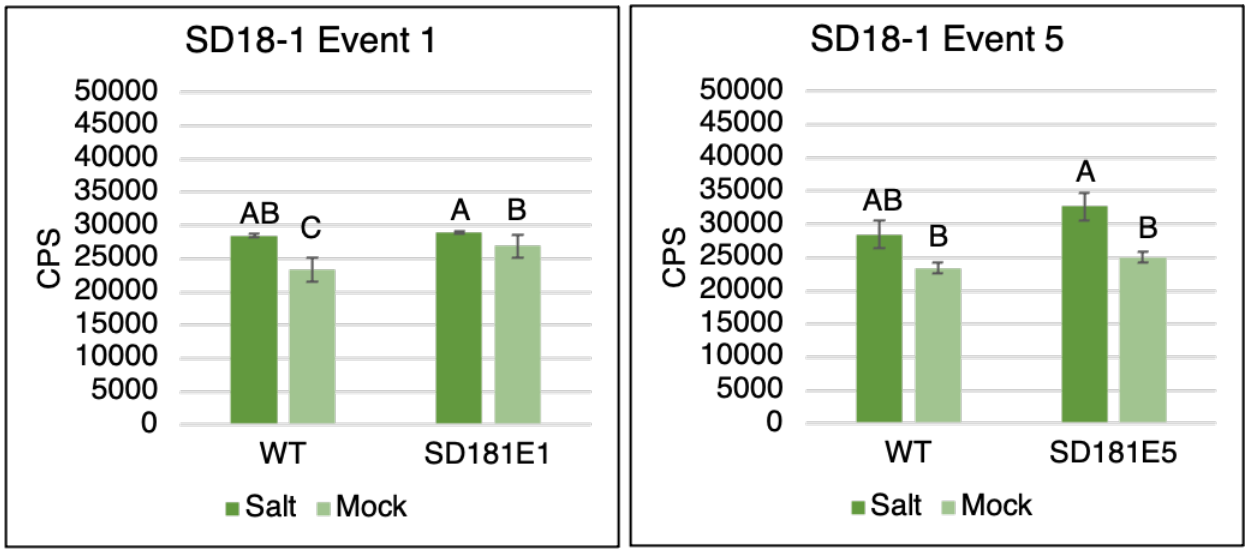

Figure 27 Green fluorescence values in counts per second (CPS) between mock and salt-treated SD18-1 transgenic rice events versus the WT control after 5 days of imposing salt-stress. Green fluorescence values were measured at 502 nm under a fixed excitation wavelength of 465 nm. Green fluorescence measurement was done after 5 days of daily application of 250 mM NaCl solution directly into the potting mix. Mock control consisted of plant pots submerged in 6 cm deep de-ionized (DI) water. Values are the mean ± standard error (SE). n = 3 transgenic plants per event per mock control and salt-stress treatment group, each plant consisted of independent measurements of the 3 youngest leaves from the main tiller. Different letters above error bars represent significant differences in green fluorescence values determined by mixed-model analysis of variance (Fisher's LSD $P<0.05$).

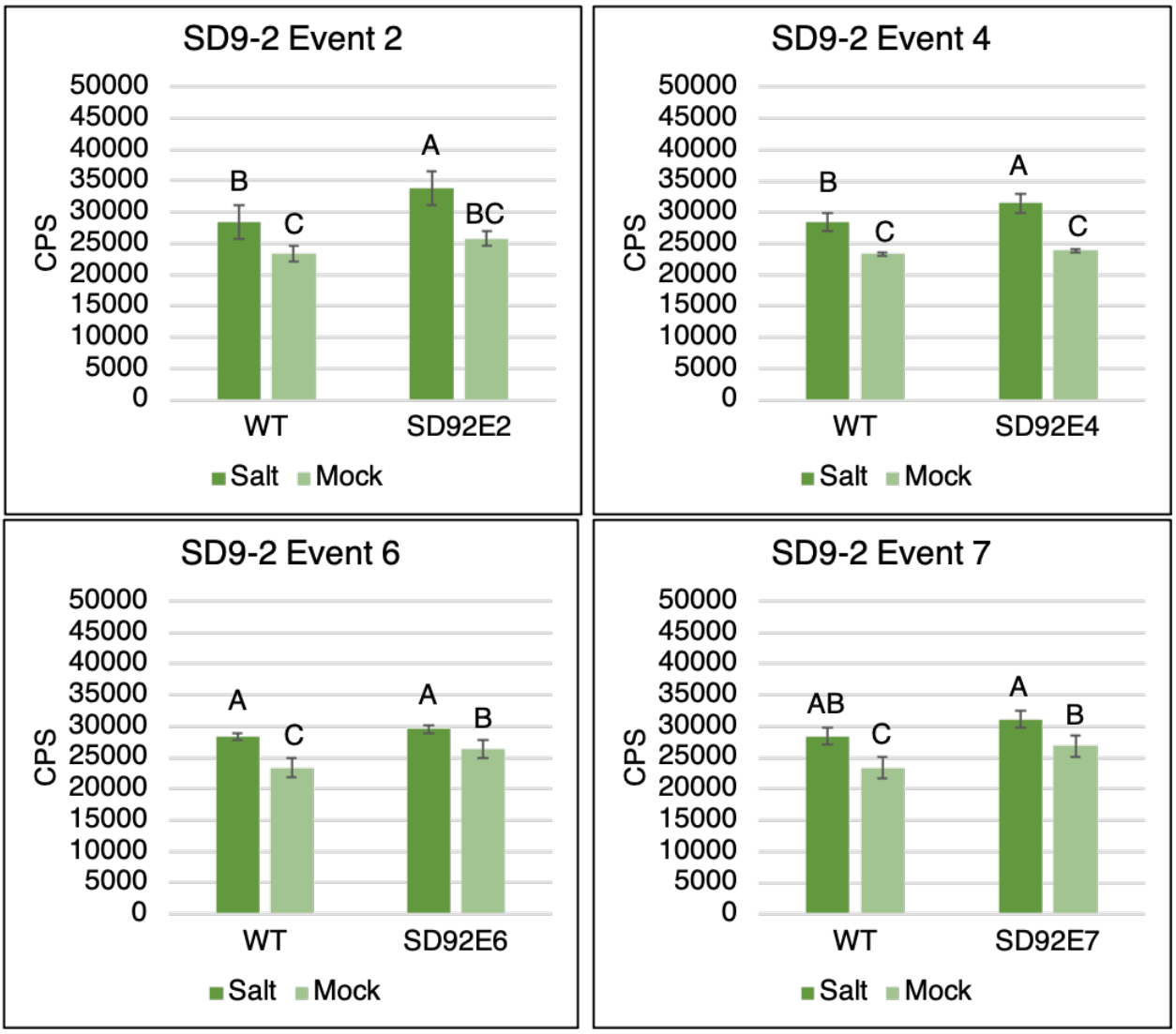

Figure 28 Green fluorescence values in counts per second (CPS) between mock and salt-treated SD9-2 transgenic rice events versus the WT control after 5 days of imposing salt-stress. Green fluorescence values were measured at 502 nm under a fixed excitation wavelength of 465 nm. Green fluorescence measurement was done after 5 days of daily application of 250 mM NaCl solution directly into the potting mix. Mock control consisted of plant pots submerged in 6 cm deep de-ionized (DI) water. Values are the mean ± standard error (SE). n = 3 transgenic plants per event per mock control and salt-stress treatment group, each plant consisted of independent measurements of the 3 youngest leaves from the main tiller. Different letters above error bars represent significant differences in green fluorescence values determined by mixed-model analysis of variance (Fisher's LSD $P<0.05$).

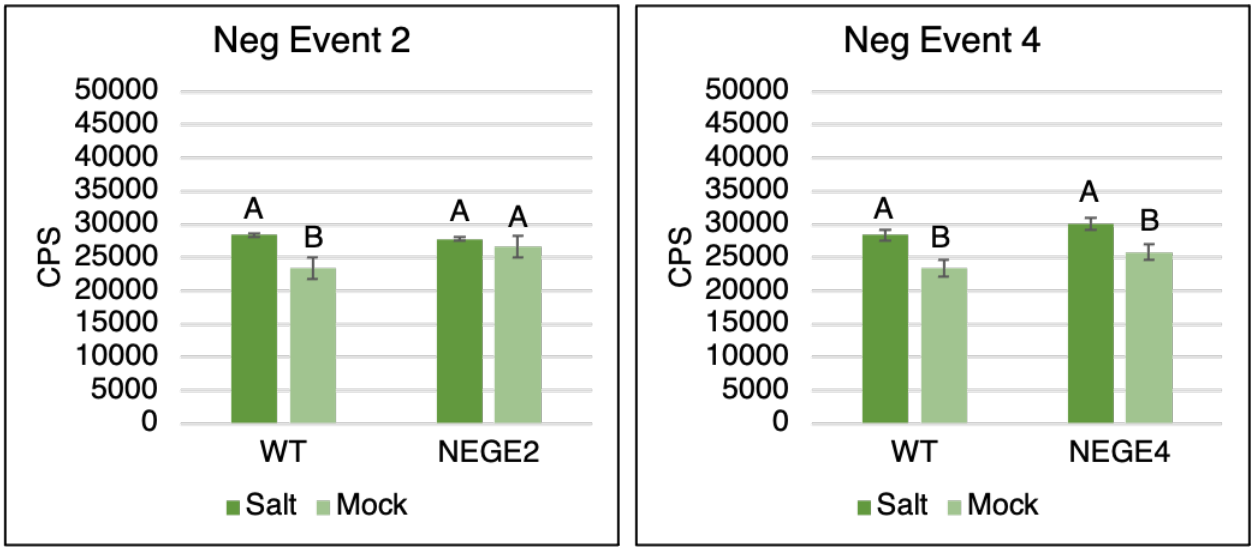

Figure 29 Green fluorescence values in counts per second (CPS) between mock and salt-treated Neg transgenic rice events versus the WT control after 5 days of imposing salt-stress. Green fluorescence values were measured at 502 nm under a fixed excitation wavelength of 465 nm. Green fluorescence measurement was done after 5 days of daily application of 250 mM NaCl solution directly into the potting mix. Mock control consisted of plant pots submerged in 6 cm deep de-ionized (DI) water. Values are the mean ± standard error (SE). n = 3 transgenic plants per event per mock control and salt-stress treatment group, each plant consisted of independent measurements of the 3 youngest leaves from the main tiller. Different letters above error bars represent significant differences in green fluorescence values determined by mixed-model analysis of variance (Fisher's LSD $P<0.05$).

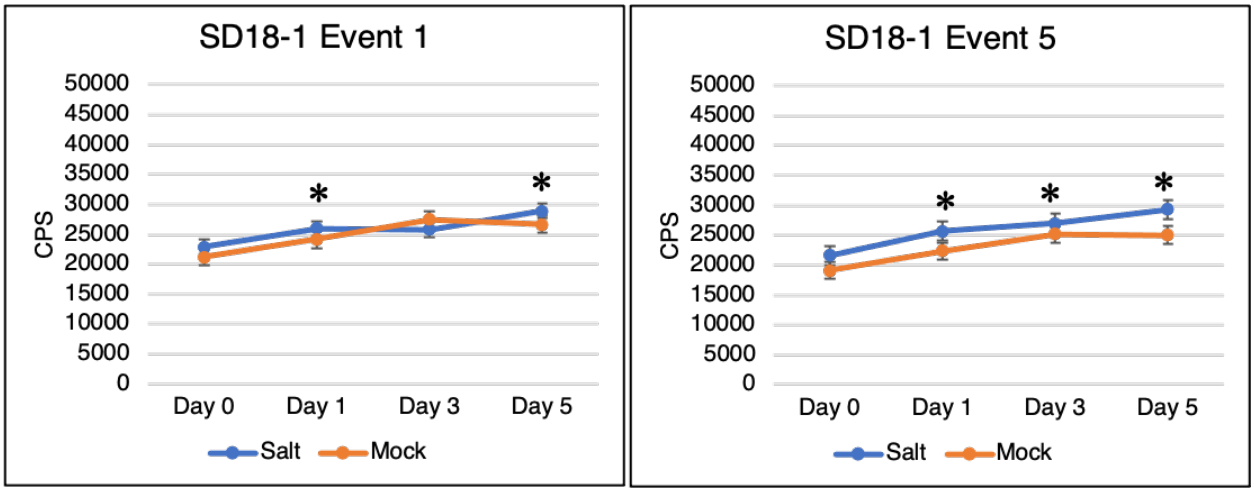

Figure 30 Green fluorescence values (CPS) between mock and salt-treated transgenic SD18-1 rice at various time points of salt-stress treatment. Green fluorescence values were measured at 502 nm under a fixed excitation wavelength of 465 nm. Green fluorescence measurements were values obtained before (day 0) and after 1-, 3-, and 5- days of applying the salt solution. Values are the mean ± standard error (SE). n = 3 transgenic plants per event per mock control and salt-stress treatment group for each time point, each plant consisted of independent measurements of the 3 youngest leaves from the main tiller. On day 0, green fluorescence was measured before applying 250 mL of 250 mM NaCl solution directly into the potting mix per plant. Salt solution application into the potting mix was done for five straight days. After adding the salt solution into the potting mix for each day, the pots of plants under salt-stress treatment remained submerged in the salt solution collected in the containment tray of the said pots. On the next day, the salt solution in the containment trays from the previous day's application was removed before applying fresh 250 mM salt solution directly into the potting mix per plant. Mock control consisted of plant pots submerged in 6 cm deep de-ionized (DI) water. Asterisks represent significant differences in green fluorescence between mock and drought-stress treated rice for each time point, determined by mixed-model analysis of variance (P<0.05).

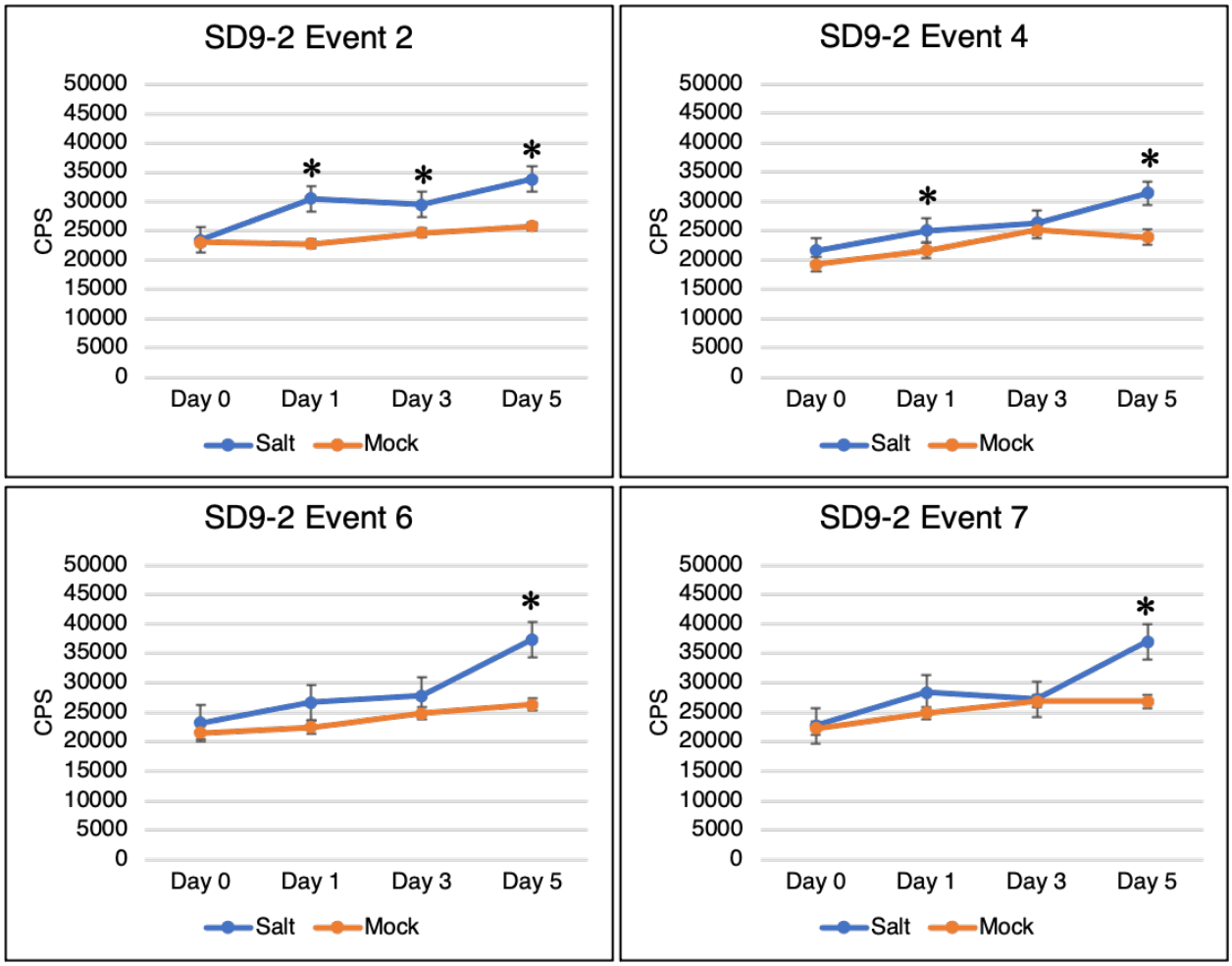

Figure 31 Green fluorescence values (CPS) between mock and salt-treated transgenic SD9-2 rice at various time points of salt-stress treatment. Green fluorescence values were measured at 502 nm under a fixed excitation wavelength of 465 nm. Green fluorescence measurements were values obtained before (day 0) and after 1-, 3-, and 5- days of applying the salt solution. Values are the mean ± standard error (SE). n = 3 transgenic plants per event per mock control and salt-stress treatment group for each time point, each plant consisted of independent measurements of the 3 youngest leaves from the main tiller. On day 0, green fluorescence was measured before applying 250 mL of 250 mM NaCl solution directly into the potting mix per plant. Salt solution application into the potting mix was done for five straight days. After adding the salt solution into the potting mix for each day, the pots of plants under salt-stress treatment remained submerged in the salt solution collected in the containment tray of the said pots. On the next day, the salt solution in the containment trays from the previous day's application was removed before applying fresh 250 mM salt solution directly into the potting mix per plant. Mock control consisted of plant pots submerged in 6 cm deep de-ionized (DI) water. Asterisks represent significant differences in green fluorescence between mock and drought-stress treated rice for each time point, determined by mixed-model analysis of variance (P<0.05).

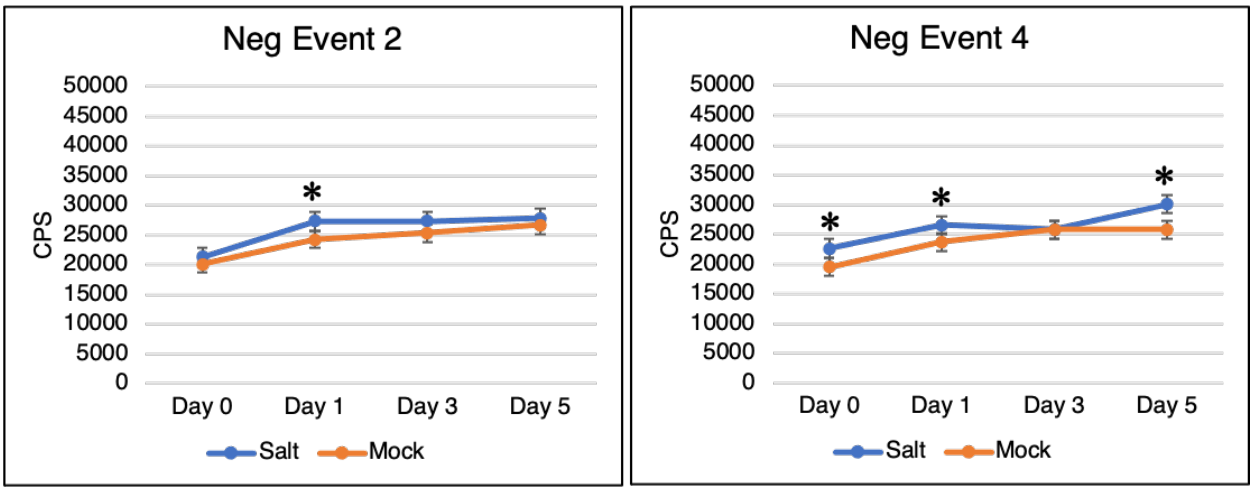

Figure 32 Green fluorescence values (CPS) between mock and salt-treated transgenic Neg rice at various time points of salt-stress treatment. Green fluorescence values were measured at 502 nm under a fixed excitation wavelength of 465 nm. Green fluorescence measurements were values obtained before (day 0) and after 1-, 3-, and 5- days of applying the salt solution. Values are the mean ± standard error (SE). n = 3 transgenic plants per event per mock control and salt-stress treatment group for each time point, each plant consisted of independent measurements of the 3 youngest leaves from the main tiller. On day 0, green fluorescence was measured before applying 250 mL of 250 mM NaCl solution directly into the potting mix per plant. Salt solution application into the potting mix was done for five straight days. After adding the salt solution into the potting mix for each day, the pots of plants under salt-stress treatment remained submerged in the salt solution collected in the containment tray of the said pots. On the next day, the salt solution in the containment trays from the previous day's application was removed before applying fresh 250 mM salt solution directly into the potting mix per plant. Mock control consisted of plant pots submerged in 6 cm deep de-ionized (DI) water. Asterisks represent significant differences in green fluorescence between mock and drought-stress treated rice for each time point, determined by mixed-model analysis of variance ($P<0.05$).

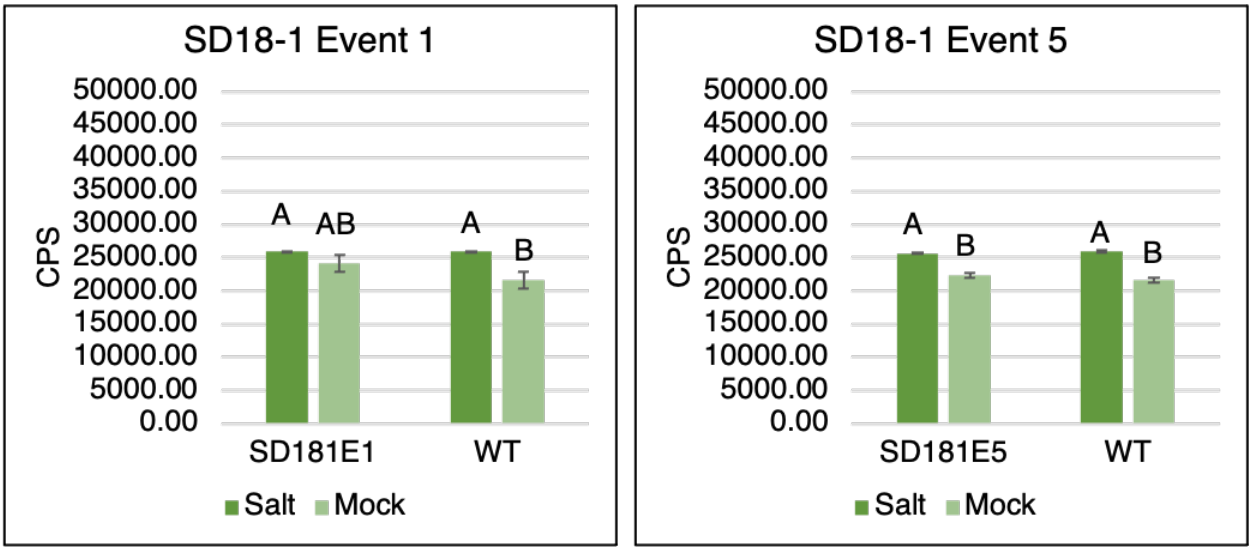

Figure 33 Green fluorescence values in counts per second (CPS) between mock and salt-treated SD18-1 transgenic rice events versus the WT control after one day of imposing salt-stress. Green fluorescence values were measured at 502 nm under a fixed excitation wavelength of 465 nm. Green fluorescence measurement was done after 1 day of applying 250 mM NaCl solution directly into the potting mix. Mock control consisted of plant pots submerged in 6 cm deep de-ionized (DI) water. Values are the mean ± standard error (SE). n = 3 transgenic plants per event per mock control and salt-stress treatment group, each plant consisted of independent measurements of the 3 youngest leaves from the main tiller. Different letters above error bars represent significant differences in green fluorescence values determined by mixed-model analysis of variance (Fisher's LSD $P<0.05$).

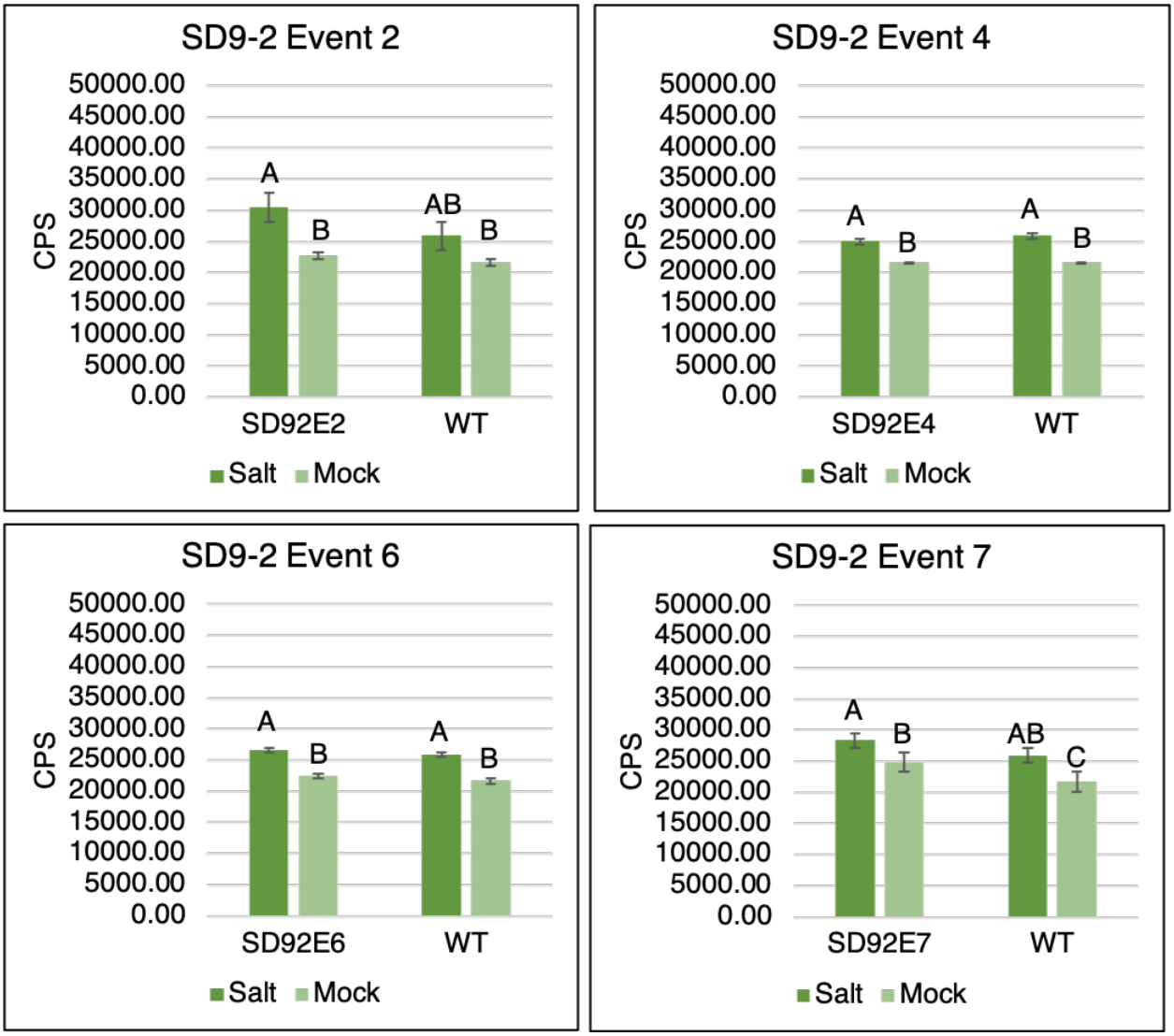

Figure 34 Green fluorescence values in counts per second (CPS) between mock and salt-treated SD9-2 transgenic rice events versus the WT control after one day of imposing salt-stress. Green fluorescence values were measured at 502 nm under a fixed excitation wavelength of 465 nm. Green fluorescence measurement was done after 1 day of applying 250 mM NaCl solution directly into the potting mix. Mock control consisted of plant pots submerged in 6 cm deep de-ionized (DI) water. Values are the mean ± standard error (SE). n = 3 transgenic plants per event per mock control and salt-stress treatment group, each plant consisted of independent measurements of the 3 youngest leaves from the main tiller. Different letters above error bars represent significant differences in green fluorescence values determined by mixed-model analysis of variance (Fisher's LSD $P<0.05$).

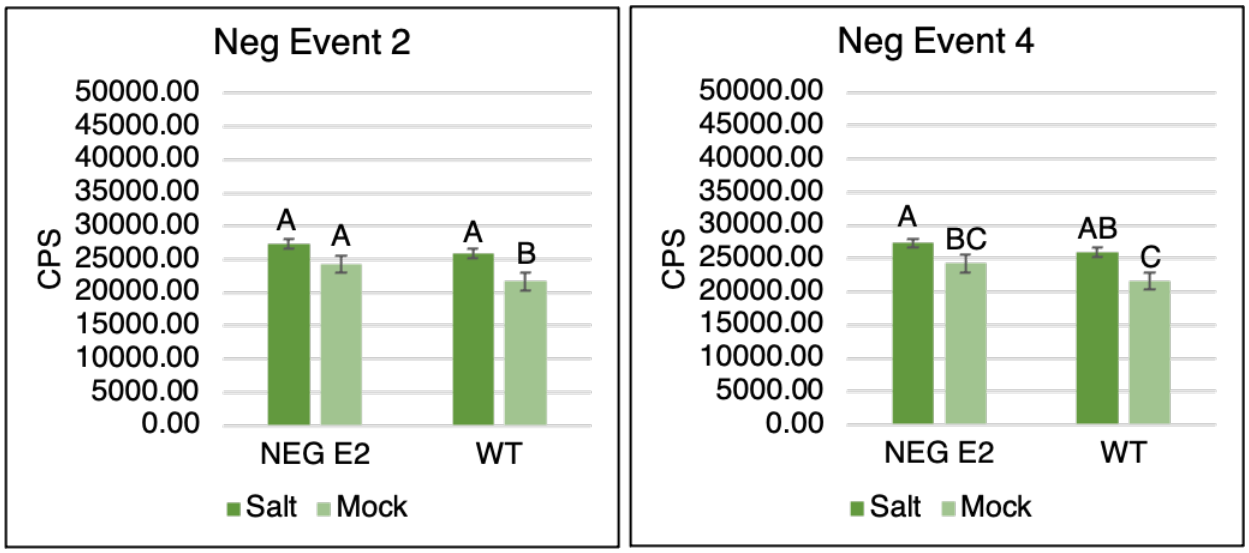

Figure 35 Green fluorescence values in counts per second (CPS) between mock and salt-treated Neg transgenic rice events versus the WT control after one day of imposing salt-stress. Green fluorescence values were measured at 502 nm under a fixed excitation wavelength of 465 nm. Green fluorescence measurement was done after 1 day of applying 250 mM NaCl solution directly into the potting mix. Mock control consisted of plant pots submerged in 6 cm deep de-ionized (DI) water. Values are the mean ± standard error (SE). n = 3 transgenic plants per event per mock control and salt-stress treatment group, each plant consisted of independent measurements of the 3 youngest leaves from the main tiller. Different letters above error bars represent significant differences in green fluorescence values determined by mixed-model analysis of variance (Fisher's LSD $P<0.05$).

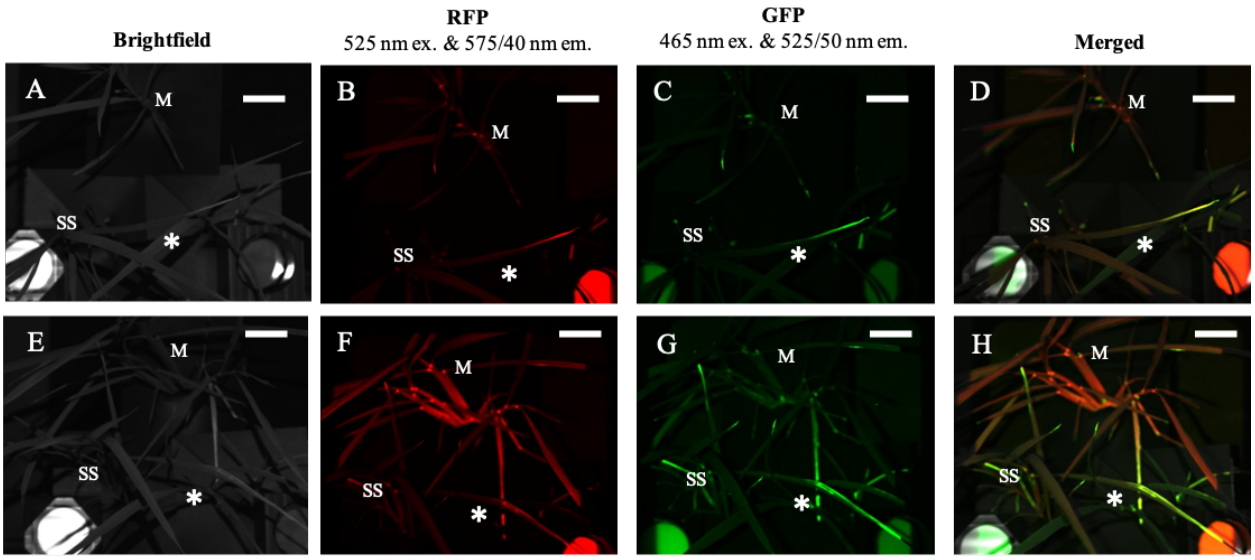

Figure 36 Fluorescence inducing laser projector images of transgenic rice (T1) harboring the SD18-1 construct (event 1 (A-D) and event 5 (E-H)) taken after 5 days of salt-stress treatment. The same WT was used for all images and is denoted by a white asterisk; mock control denoted by M and salt-stress treated transgenic rice identified by SS. The transgenic rice samples had high red fluorescence intensity as observed in the RFP column. Transgenic rice under salt-stress had similar green fluorescence intensity with the mock and WT controls as observed in the GFP column. Laser power for both the 465 nm and 525 nm lasers was 1.4 W power. Images were acquired using a camera exposure time of 300 ms from a distance of 3 meters. Scale bars represent 5 cm. The round components are fluorescence standards (left: blue wavelength standard USFS-200-020; right: orange wavelength standard USFS-336-020).

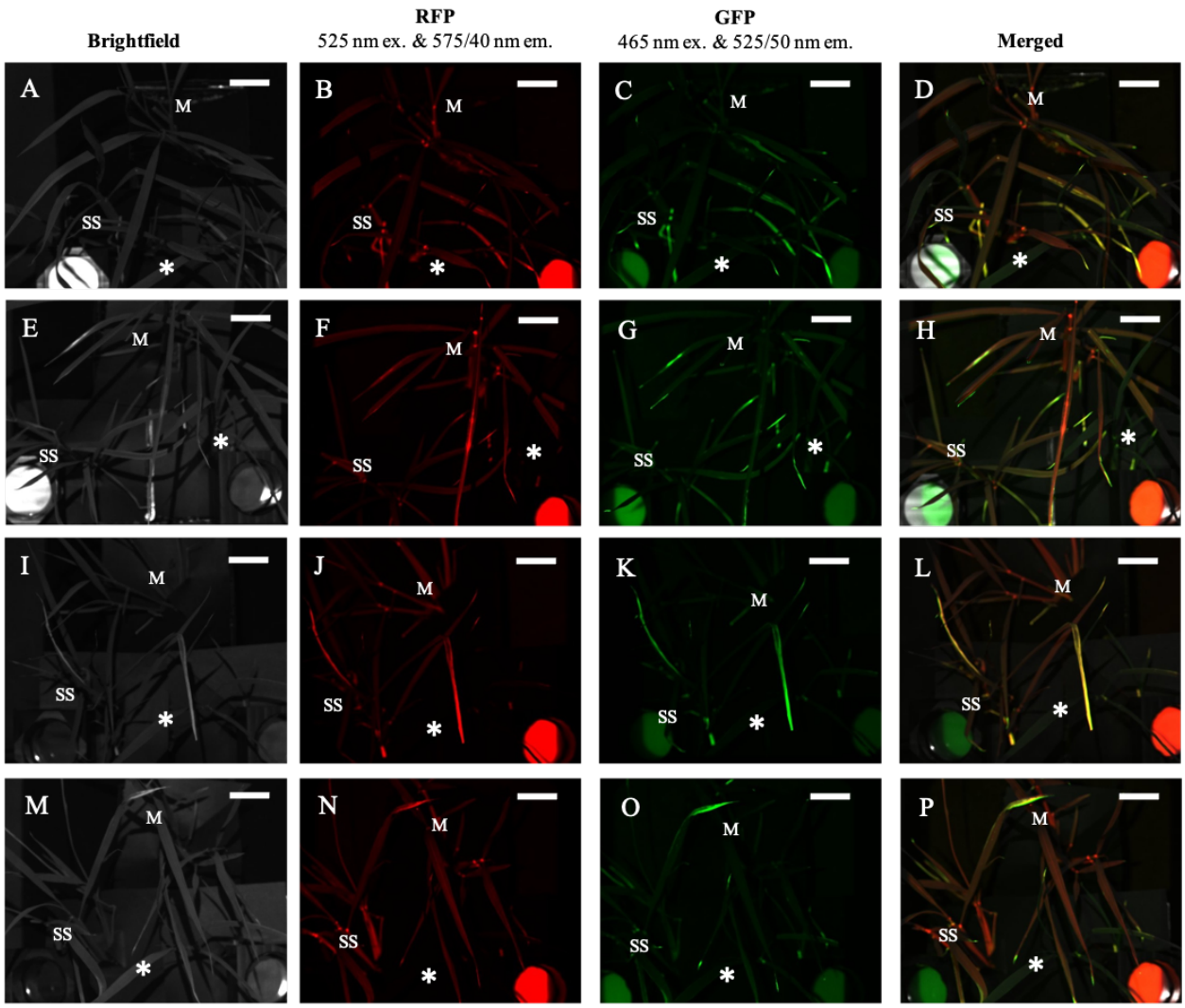

Figure 37 Fluorescence inducing laser projector images of transgenic rice harboring the SD9-2 construct(event 2 (A-D), event 4 (E-H), event 6 (I-L), and event 7 (M-P)) taken after 5 days of salt-stress treatment. The same WT was used for all images and is denoted by a white asterisk; mock control denoted by M and salt-stress treated transgenic rice identified by SS. The transgenic rice samples had high red fluorescence intensity as observed in the RFP column. Transgenic rice under salt-stress had similar green fluorescence intensity with the mock and WT controls as observed in the GFP column. Laser power for both the 465 nm and 525 nm lasers was 1.4 W power. Images were acquired using a camera exposure time of 300 ms from a distance of 3 meters. Scale bars represent 5 cm. The round components are fluorescence standards (left: blue wavelength standard USFS-200-020; right: orange wavelength standard USFS-336-020).

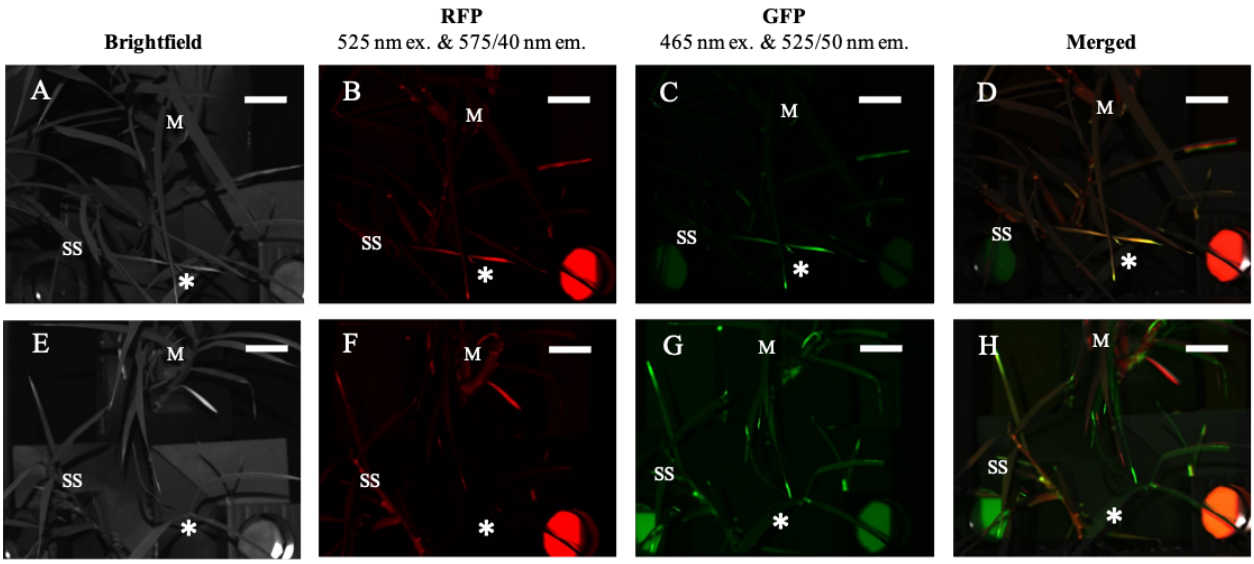

Figure 38 Fluorescence inducing laser projector images of transgenic rice harboring the Neg construct (event 2 (A-D) and event 4 (E-H)) taken after 5 days of salt-stress treatment. The same WT was used for all images and is denoted by a white asterisk; mock control denoted by M and salt-stress treated transgenic rice identified by SS. The transgenic rice samples had high red fluorescence intensity as observed in the RFP column. Transgenic rice under salt-stress had similar green fluorescence intensity with the mock and WT controls as observed in the GFP column. Laser power for both the 465 nm and 525 nm lasers was 1.4 W power. Images were acquired using a camera exposure time of 300 ms from a distance of 3 meters. Scale bars represent 5 cm. The round components are fluorescence standards (left: blue wavelength standard USFS-200-020; right: orange wavelength standard USFS-336-020).

Vita

Paolo M. Tagaloguin was born on December 3, 1993. He earned his bachelor's degree in Mindanao State University, General Santos City, Philippines. He spent five years in the same university as an instructor in Biology before coming to the US for studying a master's degree in Plant Sciences at the Stewart Laboratory.